QATAR UNIVERSITY

COLLEGE OF ENGINEERING

PILOT-SCALE INVESTIGATION OF OSMOTIC CONCENTRATION FOR REDUCING WASTEWATER INJECTION VOLUMES IN QATARI GAS FIELDS

BY

REM ABRAHIM JALAB

A Thesis submitted to

the College of Engineering

in Partial Fulfillment of the Requirements for the Degree of

Masters of Science in Environmental Engineering

June 2020

COMMITTEE PAGE

The members of the Committee approve the Thesis of
Rem Abrahim Jalab defended on 20/04/2020.

_____
Dr. Mustafa S. Nasser
Thesis Supervisor

_____
Prof. Reyad Shawabkeh
External Examiner

_____
Prof. Fares AlMomani
Internal Examiner

_____
Dr. Mustafa S. Nasser
Committee Chair

Approved:

_____

Khalid Kamal Naji, Dean, College of Engineering

ABSTRACT

JALAB, REM, A., Masters: June: [2020], Masters of Science in Environmental Engineering.

Title: Pilot-Scale Investigation of Osmotic Concentration for Reducing Wastewater Injection Volumes in Qatari Gas Fields.

Supervisor of Thesis: Mustafa, S., Nasser.

In the past 10 years, forward osmosis (FO) has been capturing the attention as a low-energy membrane technology for wastewater reclamation. FO relies on the osmosis phenomenon from osmotic pressure difference across semi-permeable membrane. The permeate water is drawn by the effect of high saline draw solution (DS) turning diluted with permeate transfer and leaving the wastewater feed solution (FS) concentrated. Through permeation, net driving force diminishes from the reduced salinity of DS that can be recovered via high-energy consumption step. However, the energy benefit of FO technology emerges when DS recovery step is obviated and FO is applied for osmotic concentration (OC). In fact, FO as an OC process is best suited for volume reduction of wastewater from oil and gas wells' drilling to be injected into underground wells. In literature, the OC implementations for volume reduction are still at bench-scale and the investigation at larger scale is among the breakthroughs in FO technology.

In this study, an OC pilot-plant was constructed for volume reduction of FS mimicking the conditions of produced and process water (PPW) stream from gas operations in Qatar. This study is an outcome of National Priorities Research Program (NPRP) project funded by

Qatar National Research Fund (QNRF) and is in collaboration with industry represented by ConocoPhillips company. This study examines the concentration of 2000 $mg.L^{-1}$ FS using salt rich solution of 40000 $mg.L^{-1}$ as DS representing seawater through two different hollow fiber (HF) membranes. To perform a comparative analysis for the two membranes, maximum achieved FS recovery rate by OC pilot plant and role of changing the flowrates and temperature on performance of OC were investigated. The results revealed that the two tested membranes succeeded in concentrating the FS by 90% at produced water flux ranging from 1.66 to 6.54 LMH. Higher DS flowrate and temperature induced higher water permeation and FS recovery rate. Above all, the operational stability of OC pilot plant was demonstrated through 48 hours of continuous operation where 75% of feed water was recovered at an average water flux ranging from 1.47 to 6.00 LMH using both HF membranes.

DEDICATION

This thesis is dedicated to my husband, parents who have been supporting me continuously to pursuit my academic ambition by completing master's study, and for my supervisor who has assisted, encouraged and guided me sincerely to complete my research study.

ACKNOWLEDGMENTS

I would like first to express my gratitude to my master's thesis supervisor Dr. Mustafa S. Nasser who gave me the opportunity to work on such an important research project and believed in my outstanding academic performance to accomplish it efficiently. His proficient mentorship and research experience along with his useful engagement in my research and thesis learning process supported me to complete my master's degree.

I would like also to thank the experts I worked with, Eng. Abdelrahman Awad from Gas Processing Center (Qatar University), Dr. Samer Adham and Eng. Joel Minier-Matar from Global Water Sustainability Center (ConocoPhillips, Qatar) for their appreciated assistance and guidance through the project phases. The project was funded by Qatar National Research Fund (QNRF) under the National Priorities Research Program (NPRP). I would also acknowledge the contribution of Prof. Simon Judd from Cranfield Water Science Institute (Cranfield University, UK) for his contribution as a consultant through all the project phases. In addition, I thank the lab technician of Gas Processing Center Mr. Dan Cortes and undergraduate students (Abdullah Omar, Tasneem Hussein and Arafat Mohammed) from Qatar University for their valued help in the experimental work.

Finally, I must express my deepest gratitude to my husband, parents and my other family members for their continuous patience and encouragement through the challenging graduate study education. This achievement would not have been successfully completed without their greatest support.

TABLE OF CONTENTS

LIST OF TABLES

LIST OF FIGURES

Chapter 1 : Introduction

1.1. Research overview

The current global growth of population along with the advances in technologies have raised the water and energy consumption per capita. Besides, the exploitation of natural water resources for sustenance and industrial processes has boosted the water depletion problems. In spite of that, the diminished water resources have stimulated the need for the reclamation and reuse of wastewater. Forward osmosis (FO) stands out as an emerging osmotically driven membrane separation treatment technology to help in resolving the worldwide water challenges including scarcity and depletion of water resources [1]. Fundamentally, FO is featured by the minimal energy consumption and fouling due to the exploitation of natural osmosis phenomenon for the water transport across a semi-permeable membrane [2–4]. Through the membrane, the fresh water (permeate) is produced as a result of water movement from low osmotic pressure feed solution (FS) to high osmotic pressure solution with high electrolyte concentration known as draw solution (DS). Obviously, the osmotic pressure gradient across the membrane acts as a driving force which allows DS to draw permeate from FS [5]. Consequently, the water permeation makes the low salinity FS more concentrated at less volume and dilutes the saline DS with increasing its volume. For the net water transport across the membrane, FO process relying on natural osmosis consumes less energy when compared with processes demanding hydraulic pressure application such as reverse osmosis (RO).

During water permeation using FO operation, the osmotic concentration of DS decreases leading to diminish the net osmotic driving force. Therefore, the DS recovery by separating the transferred permeate is required for osmotic driving force replenishment and reuse of

DS. Accordingly, FO technology is described by being two-steps process comprising both stages of membrane separation and DS re-concentration as in *Figure 1-1*. Normally, reverse osmosis [6], nanofiltration [7] or membrane distillation [8] are the most practically integrated with FO as the recovery step of the DS. Despite the low energy consumption by FO membrane separation stage, DS recovery demands intensive energy and renders the implementation of FO technology technically challenging. For instance, it has been calculated that the recovery of permeate and draw solution during osmotically- driven FO operation incurs 65- 140% higher costs than conventional pressure-driven RO for wastewater reclamation from agricultural or mining activities [9,10].

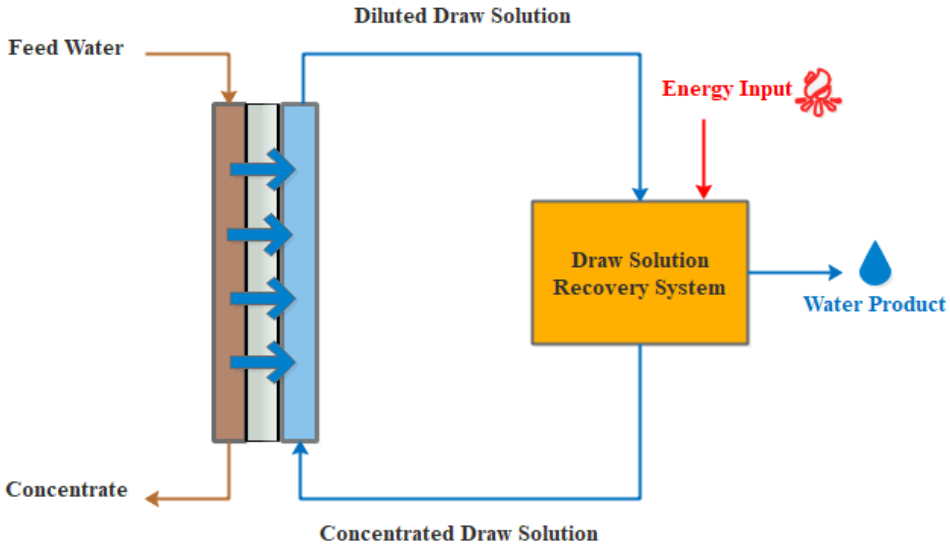

Figure 1-1: FO process scheme.

Nevertheless, FO can beat the pressure- driven processes in terms of costs when FO implementation is prioritized to applications where DS regeneration is not compulsory [3]. Therefore, osmotic dilution (OD) is an application of the low energy FO process where the

process's diluted DS is directly reused without the regeneration [11]. Few studies have performed OD mode of FO using concentrated fertilizer as DS for the utilization of diluted fertilizer DS in fertigation purpose where it gets injected to the irrigation systems [12–14]. Moreover, DS recovery can be eliminated in osmotic concentration (OC) applications when the quality of permeate water product is not a concern and the aim is having the concentrated feed.

Several advantageous features of FO made it a distinctive technology raising the research interests in the recent years. The high solute rejection [15], irreversible fouling [16], low fouling propensity [17] and low energy consumption are all key attributes of FO. However, FO process is still encountering some critical operational problems in the areas of concentration polarization inside and around the membrane, reverse solute flux and fouling [18]. In fact, concentration polarization incidence is related to the difference in concentration between FS and DS across the membrane. FO-based processes experience both external and internal concentration polarization (ECP, ICP) through an asymmetric FO membrane, where ICP exists in porous support layer and ECP occurs at the surface of active layer of the membrane [19]. Concentration polarization crucially diminishes the osmotic pressure gradient across the membrane's active layer and then decreases the water flux. Furthermore, the flux decline is assigned to the reverse solute flux (RSF) which is the diffusion of salts from DS side through the membrane to FS side. Cath et al. [15] and Lay et al. [17] have mentioned that RSF can jeopardize the process performance and intensify the fouling.

Although osmosis was first recognized as a feasible separation process technology around 80 years ago [20] and was demonstrated technically for juice concentration over 50 years

ago [21], the practical demonstration of FO has taken place since the past 10-12 years with full-scale implementation only within the past 3-5 years. The growth in FO research publications exceeds the 20% based on Scopus released papers within years from 2005 to 2019, but rare applications for real life full-scale operation have been demonstrated.

Hydration Technology Innovations company (HTI) in 2002 demonstrated the first commercial project based on FO technology in USA for potable water supply[22]. Additionally, the company involved its FO technology for oil and gas (O&G) exploration and production (E&P) wastewater (WW) minimization in 2009 [23]. Furthermore, two industrial FO plants were constructed earlier by Modern water in Gibraltar and Oman in 2008 and 2009 respectively. Afterward, FO technology remained under improvements with current existence of six membrane manufacturers including Aquaporin (Denmark), Porifera (USA), Trevi (USA), Toyobo (Japan), Fluid Technology Solutions (previously named HTI) (USA) and Modern Water (UK). Mainly, the manufactured membranes are composed of thin film of Polyamide, cellulose triacetate (CTA) and hollow fiber (HF)[24]. Various reported studies have included expanded investigations of FO for seawater desalination sector [25–30] and wastewater reclamation [31–33]. Therefore, different scales of FO are considered for sea/brackish water (SW/BW) desalination, and both domestic and industrial wastewater (WW) treatment, including landfill leachate, produced water (PW), food and beverage wastewater. However, the focus of most researches is directed to the key process aspects covering; DS chemistry and its recovery [7,34–38], membrane fouling [39–41] and membrane fabrication developments [42,43]. Moreover, the attained findings of examined studies have linked the DS type and its recovery method to the required quality of the water product; declaring that FO treated water cannot be

tolerated for potable water uses. Overall, the FO technical performance is restricted to feed water type, chosen DS and quality of water product [24].

Nowadays, the implementation of FO technology in the field of wastewater treatment is of substantial increase. For instance, complex wastewater streams especially from textile industries [44], municipal utilization [45], nuclear operations [18] and wells drilling [46] are fed to FO process characterized by its endurance to the high fouling tendency associated with these wastewater streams. In process of wastewater treatment, FO is utilized as a pretreatment step which reduces fouling and provides smooth operation to another subsequent water production process at lowered treatment costs [18].

Despite the fact of FO technology being a high energy demanding process when operated as standalone process with downstream DS recovery step, it is claimed that the technology can be energetically favored when desalination of high salinity water stream is conjugated with wastewater stream [25,47–51]. The wastewater can be treated with saline seawater as the DS, subsequently, a downstream RO process can desalinate the diluted seawater at a reduced hydraulic pressure and so the operating costs [5,52]. Moreover, FO can replace the RO in the hybrid system (MBR-RO) for reclaiming a secondary or tertiary membrane bioreactor (MBR) treated effluent [5]. Another alternative to MBR-RO is the FO integrated within MBR as an innovative osmotic membrane bioreactor (OMBR) application for minimizing the fouling and the costs through wastewater treatment [53].

At present, FO is extensively being examined for the reclamation of impaired water from O&G operations as a novel application for the technology after its confirmed convenient performance by several studies [23,54–56]. Typically, the wastewater associated with the O&G production from conventional and unconventional wells is mainly the produced and

process water (PPW) generated from injected fluid during hydraulic fracturing actions and water utilized for O&G processing or cooling purposes [57]. Current practices for managing the high quantity of produced water from the wells exploration were through deep well injection and reuse for future wells development operations [58]. However, the rising stringent regulations on PPW disposal aiming to preserve economically fruitful operation with protection of mankind and environment are enforcing the industrial sector to desalinate and reuse O&G wastewater [54]. Particularly, FO was designated as a promising desalination technology for O&G wastewater in terms of economics as presented in the life cycle cost of Coday et al. [59] along with its better environmental impacts.

FO is a robust technology for O&G PPW treatment being eligible for the rejection of contaminants and dissolved constituents in produced water along with tolerating its high total dissolved solids (TDS) content reaching more than 150,000 ppm [54,55,60–62]. Through several demonstrated studies, FO has been employed for desalination and reuse of PPW for internal uses during E&P operation and as base fluid for hydraulic fracturing, or for external uses where advanced treatment providing better water quality is required [54]. Nevertheless, FO operating as an osmotic concentration (OC) process is best suited for volume reduction of wastewater stream from oil and gas wells' drilling activities [23,48]. OC is considered as the most energetically favored application for the technology, as obviated DS recovery step renders OC a close to zero energy consumption application. The investigation of Hickenbottom et al. [55] for OC at bench- scale level demonstrated an effective role in volume reduction of drilling mud and fracturing wastewater by 80%.

1.2. Research Contribution

In literature, there are many studies concerned with enhancing the FO technology performance by finding solutions to the problems of concentration polarization and fouling through improving the fabrication of FO membranes [63]. Furthermore, other studies are targeting the discovery of novel DS that can be recovered at low energy utilization, thus reducing the costs of stand-alone FO process [35]. However, limited studies have exploited the FO as low-energy consuming process in applications requiring no need for DS regeneration. In the field of wastewater treatment from O&G industries, few research studies have implemented FO as an osmotic dilution process without recovering the diluted DS, but utilizing it again in well's drilling processes [64]. Besides, FO as an osmotic concentration (OC) process was demonstrated at bench-scale in two research projects for the volume reduction of O&G wastewater [55,65]. In spite of the promising outcomes, osmotic concentration for the purpose of wastewater volume reduction have not been investigated at larger scale. Therefore, this research study provides a comprehensive review of all executed FO-based projects for the reclamation of O&G wastewater and highlights their concluded results with gap analysis. This study also presents the novel implementation of osmotic concentration application -based on FO process principles- at pilot-scale and demonstrates the performance for the volume reduction of feed water. For the first time, the operation of OC process to achieve various targeted recovery rates of feed water has been examined through this study. Additionally, the operation for reaching feed water recovery of 90% has been evaluated in which no present study has succeeded in achieving that. The effectiveness of the process during recovery of feed on the water flux and reverse solute flux trends has been demonstrated. This research study on the

constructed OC pilot plant does not only investigate the success in recovering various rates of feed water, but also explores the effect of changing the operating conditions. The effect of variable DS flowrate and temperature have been examined on the recovery, water flux and reverse solute flux alteration.

Moreover, the tested pilot-scale OC application is a scale up to the successfully implemented bench-scale OC system in Qatar as a proof of osmotic concentration concept for feed water volume reduction [65]. The bench-scale system proved OC feasibility in volume reduction of PPW blend from Qatari's gas processing facilities. In Qatar, an onshore well of 2.5b m^3 capacity is allocated for injecting the oil and gas process and produced water (PPW). However, the expansion in oil and gas explorations are restricted by the finite capacity of PPW wastewater injection well. Currently, for ensuring long-term sustainability of injection well, the Qatari government has imposed stringent regulations for 50% cut in the liquid discharge form O&G facilities [66]. Therefore, the investigated pilot-scale OC system tackles this challenge by providing a low-energy consumption solution for reducing the volume of discharged PPW. Furthermore, by using brine discharged from thermal desalination plants as DS, the problem of managing the brine discharge is resolved since FO dilutes the brine to seawater salinity at close to zero energy consumption and allows the direct discharge to the sea. Subsequently, the OC technology displays dual benefit of O&G wastewater volume reduction at dramatic cut of energy utilization with reduced environmental impacts associated with the saline brine.

Lastly, the impact of successful implementation of the OC application will provide suitable management approaches for O&G wastewater and make the process widespread in volume

reduction applications of industrial effluents carrying lower salinity than used DS of high salinity similar to the desalination brine or seawater.

1.3. Research objectives

The current research study seeks to achieve the following main objectives:

i- Conducting technoeconomic analysis of the novel wastewater treatment by MBR-FO process. This objective can be done through life cycle cost analysis (LCCA) and evaluating its net present value (NPV) comparing to classical MBR-RO treatment process.

ii- Assessing the technical viability of FO technology for osmotic concentration through the construction and commissioning of pilot-scale plant.

iii- Testing the performance of two hollow fiber (HF) FO membranes in the constructed pilot osmotic concentration plant. The commercial membrane manufactured by TOYOBO and pre-commercial membrane developed by Nanyang Technological University (NTU), working with different operating mechanisms and configurations will be used.

iv- Evaluating the eligibility of pilot osmotic concentration plant with each chosen HF membrane module to reduce the volume and recover up to 90% of feed water. This can be achieved by observing the performance on the trends of water flux and reverse solute flux.

v- Examining the integrity and operational stability of the constructed pilot-scale osmotic concentration plant. Each HF membrane will be tested for 48 hours of continuous operation aiming to recover 75% of feed water.

vi- Determining the effect of operating conditions including changing DS flowrate at constant FS flowrate and operating at different temperatures. The effect can be analyzed on the obtained recovery rates, water flux and reverse solute flux trends.

In addition to that, observing the temperature effect on the intrinsic properties of both HF membranes.

1.4. Thesis structure

The structure of the present thesis seeking the pilot-scale investigation of FO technology as an osmotic concentration (OC) process for volume reduction of feed water begins from the deeply conducted literature review in *chapter 2*. Through the literature review, the operating principles, features, challenges and applications of FO process are comprehensively described. The chapter focuses on FO for wastewater reclamation and recovery applications and demonstrates the worldwide pilot-scale FO plants. Furthermore, the limited implementations of FO as an osmotic concentration process in the field of oil and gas industries are pointed out. Above all, the chapter brings to light the existing gap in performance validation of the OC at larger scales and real life conditions.

Chapter 3 contains the materials required for the technoeconomic analysis, construction of osmotic concentration pilot-plant and execution of experiments. In addition, it demonstrated the pursued methodology for approaching the defined objectives.

Following that, *chapter 4* presents the results of the conducted economic study for the FO-based wastewater reclamation process. Besides, an exhaustive comparison of the performed whole life cycle cost analysis is established between novel FO-based and widespread RO-based processes.

Chapter 5 illustrates the outcomes of the experimental work executed on the pilot-plant. The illustrated results are consequences of the experiments aiming to test two different hollow fiber FO membranes, operate for various feed water recovery and change the operating conditions.

Lastly, *Chapter 6* provides a comprehensive conclusion of all the approached findings by this research study. In additions, it suggests future recommendation for enhancing the process performance and reveals the future research prospects of interest for OC process.

1.5. Thesis outcomes (publications)

1- A.M. Awad, **R. Jalab**, J. Minier-Matar, S. Adham, M.S. Nasser, S. Judd, "The status of forward osmosis technology implementation", *Desalination*. 461 (2019) 10–21 (*Desalination* Journal IF= **7.01**)

2- **R. Jalab**, A.M. Awad, M.S. Nasser, J. Minier-Matar, S. Adham, S.J. Judd, "An empirical determination of the whole-life cost of FO-based open-loop wastewater reclamation technologies", *Water Research,* 163 (2019) 114879. (*Water Research* Journal IF= **8.55**)

3- J. Minier-Matar, A.M. Awad, M. Al-Maas, **R. Jalab**, S. Judd, MS. Nasser, S. Adham (2019) "Osmotic Concentration for Reducing Wastewater Volumes from Gas Processing Facilities in Qatar". Paper presented at ICSEWEN19, December 2-5, 2019 in Doha, Qatar.

4- A.M. Awad, **R. Jalab**, MS. Nasser, J. Minier-Matar, S. Adham, (2020) "Pilot-Scale Osmotic Concentration for Reducing Injected Wastewater Volume in Qatar". Paper presented at MTC March 16-20, 2020, Phoenix, Arizona, United States.

5- **R. Jalab**, A.M. Awad, M.S. Nasser, J. Minier-Matar, S. Adham, (2020)." Pilot-Scale Testing of Two Hollow Fiber Forward Osmosis Membranes in Osmotic Concentration Process", *Desalination Journal, Under Preparation.*

6- **R. Jalab**, A.M. Awad, M.S. Nasser, J. Minier-Matar, S. Adham, (2020)." Pilot-Scale Evaluation of Osmotic Concentration for Reducing Wastewater Volumes from Qatari's Gas Processing Facilities Using Hollow Fiber Forward Osmosis Membranes", *Desalination Journal, Under Preparation.*

7- A.M. Awad, **R. Jalab**, M.S. Nasser, J. Minier-Matar, S. Adham, (2020)."

Optimization of Operating Conditions for Osmotic Concentration Process Using Hollow Fiber Forward Osmosis Membrane", *Desalination Journal, Under Preparation.*

Chapter 2 : Literature Review

2.1. Osmotic based membrane processes

Osmosis is the physical phenomenon represented by the natural transport of the water through a membrane of selective permeability from the low concentration solution side to the side of higher solution's concentration. The passage of water across the permeability selective membrane results from the osmotic pressure difference ($\Delta\Pi$) caused by salt concentration gradient. Despite the earlier studies that examined the water passage through natural materials, more interests had been directed towards developing synthetic polymeric materials since 1960s for evaluating the phenomenon. In addition, due to advancement in membrane separation processes covering diverse areas, osmosis has been capturing the attention to be implemented in engineered applications.

Forward osmosis (FO) is currently the engineered name for osmosis and is an emerging water purification technology exploiting the naturally occurring osmosis, the diffusion of a solvent - normally water - through a semi-permeable membrane barrier from a low to high electrolyte (or salt) solution concentration. Permeate is transferred by the action of the highly concentrated stream named "draw solution (DS). In contrast to the familiar and formerly known reverse osmosis (RO) process performed in the water treatment field, FO has been executed to take advantage of osmosis using osmotic pressure gradient across both sides of membrane and eliminate the hydraulic pressure applied in the RO. Thus, FO concentrates the low salinity side and dilutes the highly saline side. The osmotic pressure of a typical diluted solution is described by Van't Hoff equation as [15]:

$$\Pi = nC_sRT \qquad (2\text{-}1)$$

where n represents the number of moles of solutes in the solution, C_s: is for the solute concentration, R is the universal gas constant and T is the absolute temperature.

If a hydraulic pressure (P) of a specific magnitude is applied to the highly concentrated solution turning out the hydraulic pressure difference (ΔP) to be equal to the osmotic pressure difference (ΔΠ), there will be no water transport in the solutions across the membrane. Alternatively, applying hydraulic pressure to the high salinity side in an amount greater than the osmotic pressure (P > ΔΠ) will allow water to transfer to the diluted side as demonstrated by RO process. Adding to the described conditions for FO and RO processes, another process named pressure retarded osmosis (PRO) combines FO and RO conditions and occurs when hydraulic pressure (lower than ΔΠ) is applied to the reverse side of the osmotic pressure differential similar to RO, causing the water to flow towards the high salinity solution like what happens in FO.

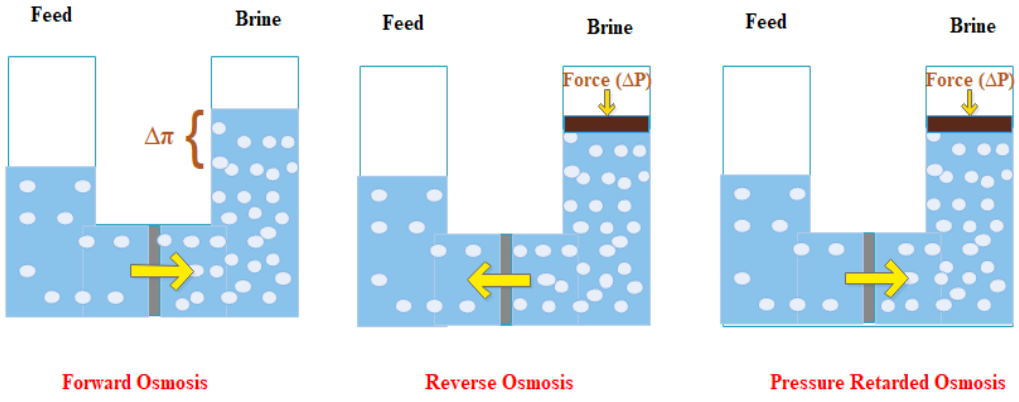

Figure 2-1: FO, RO and PRO process conditions.

The water flux in osmosis driven membrane processes demonstrated by the water transport across the membrane can be described by the following equation [67]:

$$J_w = A(\sigma \Delta \Pi - \Delta P) \quad (2\text{-}2)$$

where J_w: is the water flux (water flows through a surface area), A is the coefficient indicating the water permeability, σ: is the membrane reflection coefficient (usually it is assumed as unity).

It should be noted that Fick's law of diffusion governs the solute transport across the membrane due to its concentration gradient as per this general equation [68]:

$$J_s = B(C_{DS} - C_{FS}) \quad (2\text{-}3)$$

The solute flux J_s equals to the multiplication of the solute permeability coefficient (B) with the difference between molar concentration in draw solution (C_{DS}) and feed solution(C_{FS}).

Above all, osmotic-driven membrane processes are known by dual diffusion of salts- draw solutes are reversely diffused, whereas, feed solutes experience forward diffusion- which negatively affects the quality of product water and enhances fouling.

Lu et al., [69] have conducted a study explaining the measurement of bidirectional flux of ions by analyzing the total concentration of feed ions in draw solution and draw solution ions in feed after specified time period using the volume of feed and draw solution. Hence, forward and reverse solute fluxes$J_S^{Forward}$, $J_S^{Reverse}$ are found as per the following equations:

$$J_s^{Forward} = \frac{C_D(V_D^i + J_w A_m t)}{A_m\, t} \quad (2\text{-}4)$$

$$J_s^{Reverse} = \frac{C_F(V_F^i - J_w A_m t)}{A_m\, t} \quad (2\text{-}5)$$

where $C_D$is feed ions concentration in the draw solution after time t, V_D^i is the initial draw solution volume, $C_F$is the concentration of draw solutes ions in feed solution after time t, V_F^i is the initial feed solution volume, $J_w$is the average water flux and $A_m$is the membrane area.

2.2. Overview on forward osmosis technology

The FO technology is a new emerging membrane process gaining the popularity as low cost process compared to other pressure driven membrane processes. FO process comprises the membrane separation with additional DS recovery step (*Figure 2-2*) providing the separation between DS and permeated water with DS reuse permit, usually purification with reverse osmosis (RO) is implemented. The intense energy requirements for the DS recovery step keeps the FO as technically challenging high-energy process.

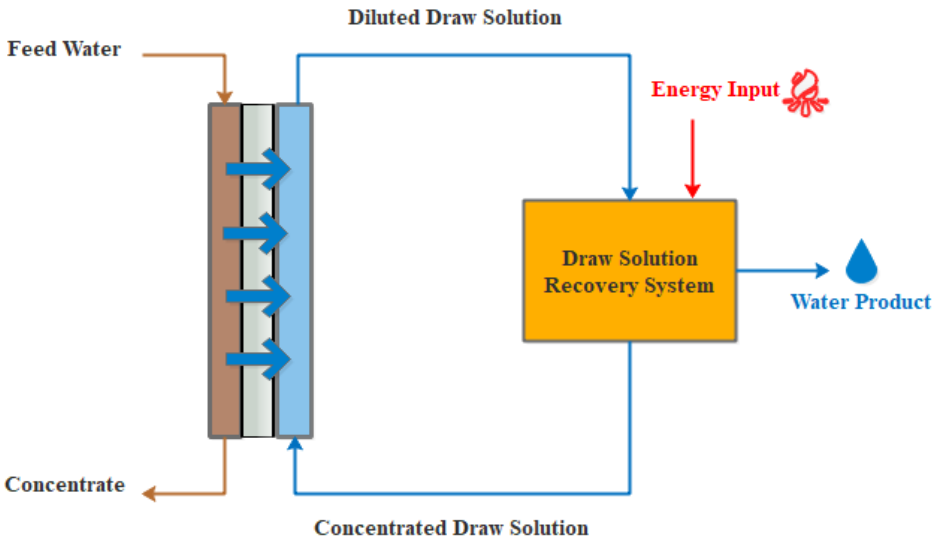

Figure 2-2: FO process scheme.

Despite FO being dependent on spontaneous solutions flow, the process has further advantages involving: (1) good product quality, (2) low energy consumption due to reduced hydraulic pressure requirement, (3) high driving force obtained using appropriate DS, (4) high achievable recovery with high solute rejection, (5) low fouling propensity, facilitating simple physical cleaning mechanisms of the membrane and eliminating extensive pretreatment.

In the beginning, FO appeared to be new promising low-cost process for water purification for a diverse set of applications as food concentration, wastewater reclamation, wastewater concentration, water reuse and seawater desalination. Thus, FO was investigated as a practical commercial process for water desalination in the 1930's where it was first recognized [20]. Then after 30 years, the FO concept was considered for the food concentrating where the primary technical employment of the process goes back to 1966 for fruit juice production [70]. Because FO was advantageous in keeping the original taste

and color of the food due to capability of concentrating at low temperature and pressure [71], FO consideration was expanded to industrial processing of tomato, orange, beetroot juices and many others [72–74]. Recently, the concerns towards FO utilization for wastewater treatment purposes have been increasing significantly [31,33,75].

Besides the prolonged discovery of FO concept from over 90 years and the intensive researches published starting from 2005 [15] examining membrane developments and potential applications with the limitations and challenges [27] , the full-scale demonstration has started to take place in the last 5 years [5]. Although the growth in FO research reached around 2,339 published papers that are available in the literature from 2005 to 2019 (*Figure 2-3*), the real-life applications at full scale are rarely performed compared to the tested bench scale experiments.

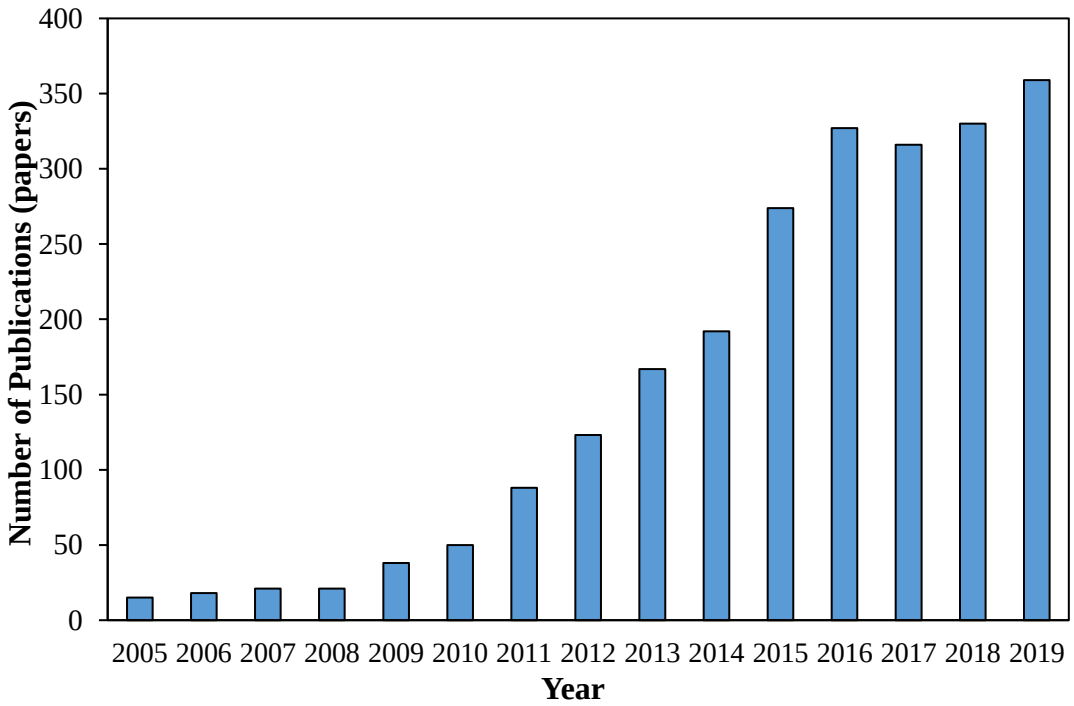

Figure 2-3: FO publication growth (based on SCOPUS database).

In fact, sea/brackish water desalination, domestic and industrial wastewater treatment applications for FO have been examined at different scales [26]. The implementation of FO as stand-alone process is limited due to the energy intensive step for regenerating the draw solution. Contradictory reports exist regarding the energy benefit of FO-based desalination over the classical single-stage RO process. Theoretical [34,76] and experimental [77,78] investigations for FO combined with RO or nanofiltration (NF) as DS recovery step have presented the energy consumed was estimated to be higher than the consumption of the conventional RO process; however, other reported studies [22,50] have concluded the reverse. Therefore, in present-day applications, the issue is getting resolved by employing FO for osmotic dilution (OD) or osmotic concentration (OC) as a new low-energy consumption FO alternative. Comparing this FO application with the conventional two steps FO process, OD/OC processes involve only the first separation step by FO membrane and the DS regeneration step is eliminated. OD targets the direct utilization of the diluted DS after the low salinity feed water is transferred to it. Indeed, OD is being implemented for seawater desalination applications using wastewater to be reused for simultaneous cost reduction [11,79]. On the other hand, when the applications rely on using the concentrate stream originated from the feed with transferred water from DS side during membrane separation stage, osmotic concentration (OC) term is used. For instance, OC is advantageous for the applications addressing the volume reduction of industrial wastewater including the processed water or the produced water generated from the oil extractions that to be injected to deep wells [55,65,80].

2.2.1. Draw solutions

FO operational performance is robustly linked to the chosen draw solution (DS), as an efficient DS helps in creating high osmotic pressure difference; leading to successful operation [5]. Indeed, there are around 500 inorganic components options that can be utilized as DS and recovered by heating, RO, NF, membrane distillation (MD) and precipitation by $Ca(OH)_2$ [28]. Some organic draw solute like ethanol, glucose and fructose can be used, however, the efficiency of separation is not assured because of the low osmotic driving force generated [28]. Further development of organic DS is worthy due to their advantageous biodegradability and rejection during re-concentration stage. A study by Lutchmiah et al. [31] revealed the extremely tested draw solutes in literature for various published FO applications. According to the surveyed applications, investigated FO experiments utilized synthetic sodium chloride solution comparable to brine the most (*Figure 2-4*). *Table 2-1* presents some promising DS of different categories along with their features and regeneration method.

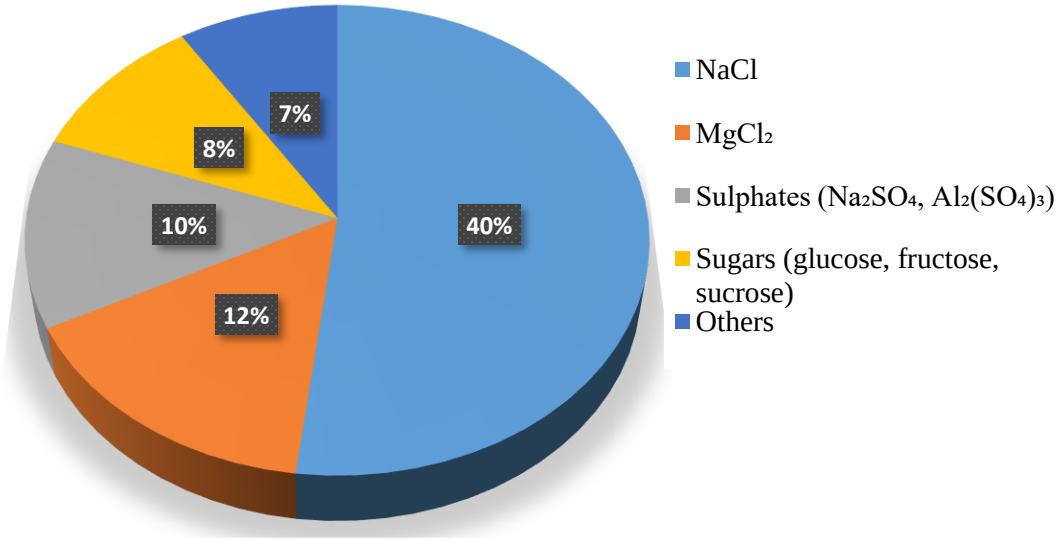

Figure 2-4: Most examined draw solutes in literature for FO applications [31].

Also, better draw solutes electrolytes are characterized by having high Van't Hoff factor, diffusion coefficient, low viscosity [7] and high solubility avoiding scaling in RO or distillation recovery steps [28]. Some draw solutes reagents outperform others by providing higher osmotic pressure and leading to higher water flux due to nature of the governing relationship between the osmotic pressure (Π) and electrolyte concentration on mass basis (*Figure 2-5*).

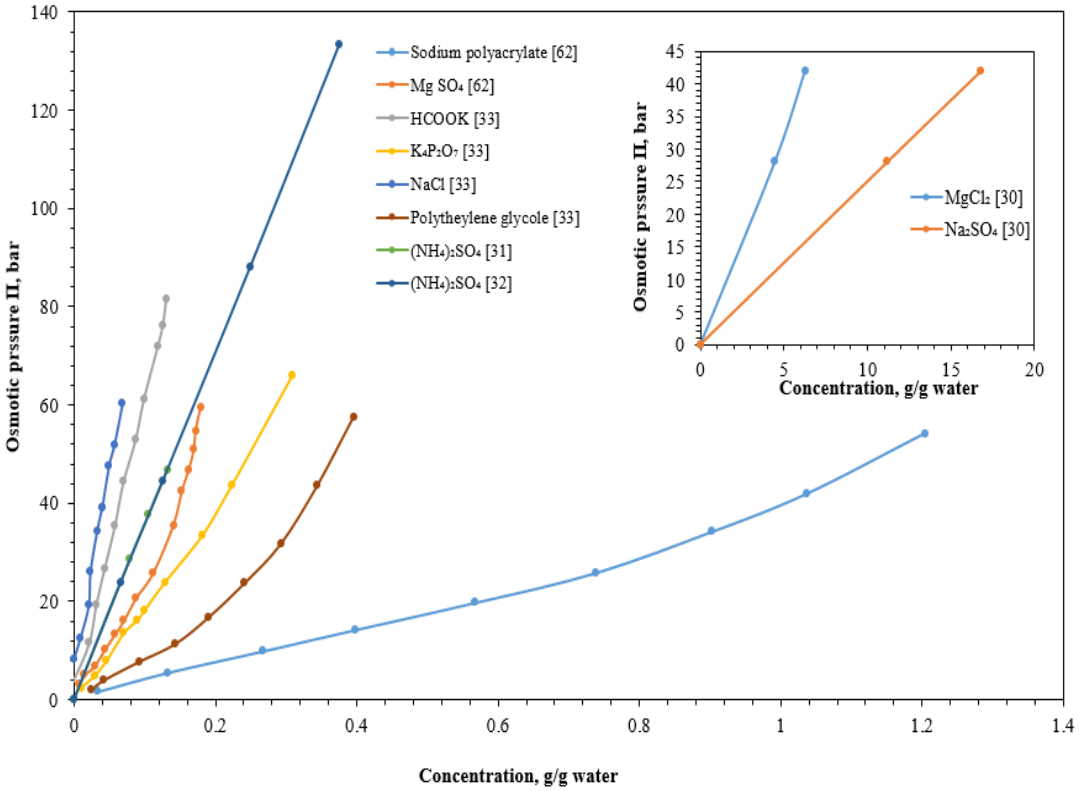

Figure 2-5: Osmotic pressure with DS concentration for different DS electrolytes [12,14,81,82].

Table 2-1: Promising draw solutions for FO applications.

DS	Recovery Method	Features	Reference
Inorganics			
NaCl			
$MgCl_2$	RO, NF	Stock availability and low	[81]
Na_2SO_4		cost	
Thermolytic			

Table 2-1: Promising draw solutions for FO applications.

DS	Recovery Method	Features	Reference
NH_3-CO_2 (NH_4HCO_3)	Heating to 60 °C	High water solubility and recovery at low temperature	[83–85]
SO_2	Stripping using heated gas	The recovery step is inexpensive	
Organics			
Alcohols	Distillation	Require difficult separation	[86]
Sugars	Not necessary	Eliminate the energy intensive recovery stage	[87]
Organic ionic salts (e.g., $Mg(CH_3COO)_2$)	RO, Biodegradability in OMBR	Considered a carbon source	[88]
Proteins (Albumin)	Solidification by heating and denaturation	High water solubility	[89]
Polymer-based			
Polyethyleneglycol	UF, NF	Easy recovery	[90]
Magnetic nanoparticles	Magnetic field	Absence of reverse solutes flux	[91]

Table 2-1: Promising draw solutions for FO applications.

DS	Recovery Method	Features	References
Polyacrylic acid	NF	High osmotic driving force provided from surface group dissociation	[92]
Hydrogel	Pressurizing or heating for de-swelling	Release of good water without the degradation of products	[93]
Fertilizers-Based $NaNO_3$ / KNO3 / NH_4NO_3 KH_2PO_4 $(NH_4)_2SO_4$ / NH_4Cl	No recovery- Direct utilization of diluted fertilizers in fertigation application	Rich in soil nutrients	[94]

2.2.2. FO commercialization history

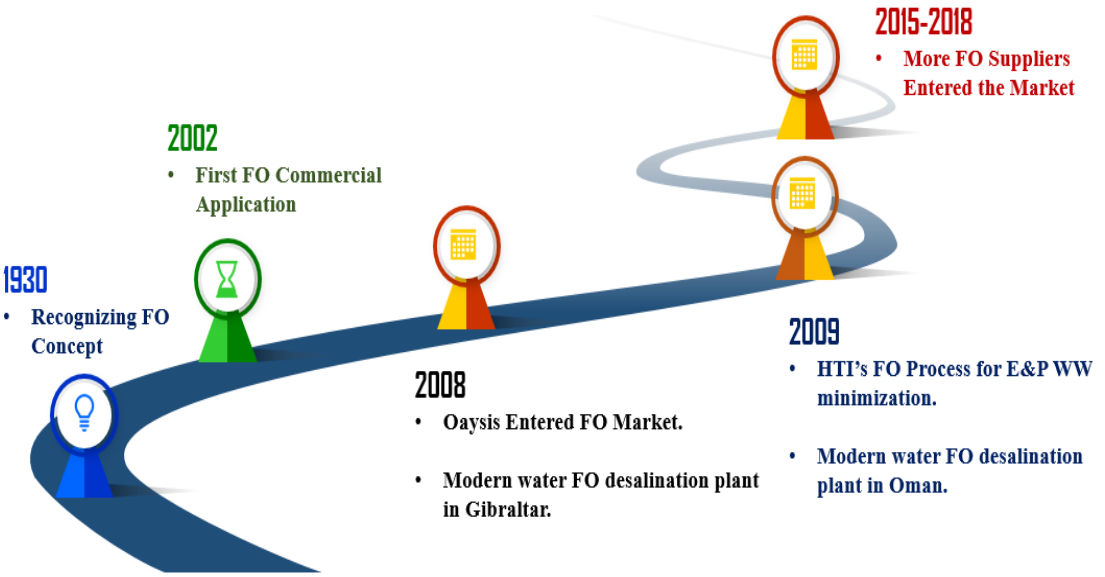

Figure 2-6: FO commercialization history.

The earliest commercial development of FO technology was by Hydration Technology Innovations (HTI) in 2002 (*Figure 2-6*). HTI was the leader in FO membrane manufacturing where the process was commercialized for emergency energy drink supply for the US military. The sugary drink was produced from contaminated water through a pouch of selective-permeability membrane containing sugar solution inside it [22]. Their food and beverage concentration projects confirmed the good quality of products and convenient energy costs. Thus, HTI development allowed the access to water recovery and waste reduction field for NASA and other commercial ventures [95]. In addition to that, HTI was the first company applying FO for Exploration and Production (E&P) for wastewater minimization which succeeded in reclaiming 75% of the pit water to be the base fluid used in hydraulic fracture [23].

Oasys was the second company entering the FO market in 2008 with developed thin film polyamide membrane. In the year of 2013, the company was able to present full FO desalination process incorporated with thermal recovery step for ammonium carbonate (NH_3-CO_2) DS [96]. Following Oasys, two worldwide projects at industrial scale in real environment were operated by Modern Water after several laboratory tests in University of Surrey. The first implementation was in 2008 in Gibraltar for drinking water supply and the regeneration of osmotic agent or DS was through RO. The FO-RO process utilized the permeate of adjacent seawater RO (SWRO) plant and produces potable water with total dissolved solids less than 200 ppm. Consequently, the success achieved from first implementation's results stimulated the design of a 200 m^3/d desalination plant to be deployed in Oman in 2009. Modern Water desired to compare between performance of existent SWRO plant with 25% feed recovery and their newly developed FO technology. Above all the challenges in the tough ambient operating conditions, FO has been running effectively and achieved 35% of feed recovery and 60% saving in energy consumed compared to the SWRO plant [22].

2.2.3. FO membranes manufacturer

Following the preceding inventors of the FO process developed, new global FO membrane developers entered the FO market. However, the current global FO membrane suppliers are Aquaporin, Porifera, Trevi, Toyobo, Fluid Technology Solutions and Modern Water [5].

With an experience estimated by 130 years in the market of fibers and membrane development, the Japanese based company named "Toyobo" demonstrated their hollow fiber (HF) membrane type after being utilized in the world's largest desalination plant in

1989 located in Saudi Arabia. Moreover, the company preserved the improvement of the membrane fibers to enhance the performance and suit new emerging technology. The FO membrane developed by Toyobo is described by the high packing density of the fibers stacked in a pressure vessel, the increased water permeability and ions rejection. Because of the useful features of the FO membrane, the membrane was adopted at a power plant in Denmark in 2018 [97].

Porifera was established in 2009 for FO membrane development, they provide flat sheets FO stacked in diverse configurations to fit broad applications area. The membrane elements are predominant in co-current and counter-current modes performance, high flux and low head loss with the scalability from laboratory experiments to industrial applications for maximum of 0.6 g/L reverse solute flux [98].

Trevi Systems is famous by its demonstrated cellulose triacetate (CTA) FO membrane since 2010 and awarded for the low energy consumption desalination processing. Trevi was engaged in 6 projects at pilot scale in USA (2013-2018) and Gulf region (2015). Trevi throughout the executed projects aimed to validate energy savings, low fouling potential and the good water quality of their FO technology. The scope of their FO process application included working for RO brine desalination, wastewater treatment and examining the preferable pretreatment for the FO system. Trevi is still active in the field of FO membrane testing and development. Currently, the company latest massive project is about constructing FO plant from the 4^{th} generation in Hawaii. The plant will be commissioned in 2020 for the generation of 500 m^3/d from the potable water with 60% recovery of feed water. Despite delivering the potable water to the population, the product water can be used by commercial customers for algae growth. Undoubtedly, the energy

required for the system will be used from renewable resources and no carbon dioxide (CO_2) will be emitted during the operation [99].

In 2017, Aquaporin launched the first forward osmosis membrane after several testing experiments of The Aquaporin Inside™ Forward Osmosis Technology at laboratories of NASA Ames in 2011 and on the space station in 2015-2016. The Aquaporin developed membrane consists of hollow fiber elements with aquaporin proteins coat, there are 0.6, 2.3, 13.8 m^2 membrane elements suitable for lab scale, pilot testing and industrial applications respectively. The membrane is characterized by minimal reverse diffusion of solutes in DS and high rejection rates due to 100% water selective aquaporin proteins [100].

2.2.4. Pilot-scale FO implemented projects

Despite the increasing number of published researches about developing the promising FO process since 2005, less than 2.5% of the articles address large-scale plants commissioning and implementation. Most of the study areas in literature are addressing DS options and characterization, membrane type and performance (fouling potential), the FO process effectiveness in water recovery and pollutants rejection for several bench scales studies.

On the other hand, around 17 pilot testing projects were implemented at different locations for diverse targets, which have been categorized for seawater (SW) /brackish water (BW) desalination, wastewater (WW) reclamation and treatment of oil and gas (O&G) effluent.

Table 2-2: Surveyed FO pilot-scale projects.

Project	Location	Feed	DS	Process Scheme	FO Membrane	Trial Period	Capacity (m^3/day)	Ref
Desalination								
1	Oman	Seawater	NaCl	FO - RO	HF	8 years	100	[101]
2	Australia	Brackish water	NaCl	FO - RO	SWo-TFC	7 days	-	[102]
3	Australia	Brackish water	$(NH_4)_2SO_4$	FDFO	SWo-CTA	3 days	-	[12]
Wastewater Treatment								
4	Spain	MBR effluent	$MgSO_4$	FO - NF	FS-TFC	1.4 years	4.3	[9]

Table 2-2: Surveyed FO pilot-scale projects.

Project	Location	Feed	DS	Process Scheme	FO Membrane	Trial Period	Capacity (m^3/day)	Ref
5	USA	MBR effluent	NaCl	FO - RO	SWo-CTA	55 days	4.4	[103]
6	USA	Domestic WW	NaCl	UF - OMBR	PTF-CTA	249 days	-	[104]
7	Singapore	Domestic Sewage	NaCl/ $MgSO_4$	OMBR	FS-CTA	8.3 days	13	[105]
8	Australia	Municipal effluent	Nutrient solution	FDFO - PAO	SWo-TFC	-	72	[13]
9	Australia	Coal mine WW	$(NH_4)_2SO_4$	FDFO	SWo-CTA	180 days	15	[14]
10	Korea	Power-plant WW	Seawater	OD (FO-RO)	FS-TFC	150 days	21.8	[106]

Table 2-2: Surveyed FO pilot-scale projects.

Project	Location	Feed	DS	Process Scheme	FO Membrane	Trial Period	Capacity (m^3/day)	Ref
11	USA	Secondary and tertiary effluent	Brine	OD (FO-RO)	FS-CTA	13 days	-	[47]
O&G Effluent Treatment								
12	USA	PW	NaCl	FO	SWo-CTA	-	926	[23]
13	USA	PW	NaCl	FO – RO	SWo-CTA	7 days	-	[28]
14	USA	PW	NaCl	FO - RO	SWo-CTA	28 days	8.6	[107]
15	USA	PW	NH_3/CO_2	FO - distillation	SWo-TFC	4.1 days	21.8	[60]
16	USA	O&G drilling wastewater	NaCl	FO-RO	SWo-CTA	-	-	[64]
17	USA	O&G drilling wastewater	NaCl	FO-RO	SWo	7 days	-	[64]

HF: hollow fiber, FS: flat sheet, SWo: spiral wound, PTF: plate and frame, TFC: Thin film composite, CTA: cellulose triacetate. FDFO: fertilizer drawn forward osmosis, NF: nanofiltration, UF: ultrafiltration, OMBR: osmotic membrane bioreactor, PAO: pressure assisted osmosis, OD: osmotic dilution.

2.2.5. Challenges

The commercial implementation of FO technology remains in confront with some challenges that need to be resolved for being truly competitive and attractive water treatment process. The frequent operational challenges with FO are the internal and external concentration polarization, high bidirectional solute flux, fouling and costly draw solution re-concentration step as they were mentioned in a recently published review addressing FO trends in desalination and wastewater treatment [108].

2.2.5.1. Concentration polarization

The concentration polarization (CP) is inevitable phenomenon in FO process and is mainly initiated from the concentration difference across asymmetric FO membrane. In addition, according to many investigated studies, the low flux trend is attributed to this phenomenon inhibiting the permeate flow [109,110]. Internal and external concentration polarization (ECP, ICP) are encountered during FO operations in porous support layer and active layer respectively (*Figure 2-7*). Then, each type of concentration polarization is divided into two categories of concentrative and dilutive.

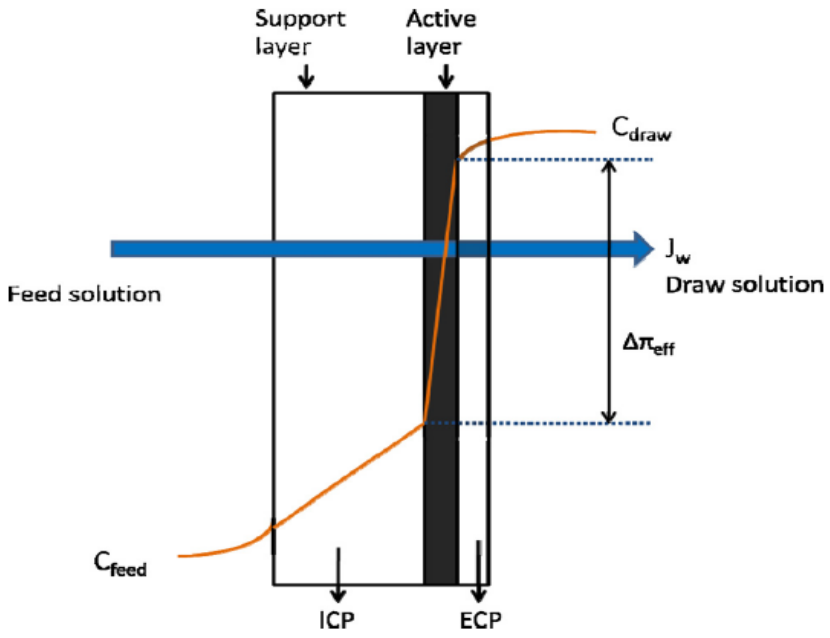

Figure 2-7: ECP and ICP across asymmetric FO membrane [18].

According to the review of McCutcheon and Elimelech [111] which examined the influence of concentration polarization on FO flux, the concentrative ECP happens when the solute is left concentrated at active layer surface after permeation of water. Thus, sufficient driving force should defeat it in order for water to permeate. The dilutive ECP is when permeated water pulls the draw solution solutes away from membrane surface. Moreover, the effect of internal concentration polarization is said to be concentrative when feed is sited facing the porous layer and feed solutes find difficulty in penetrating the structure of this layer reaching the active layer. Whereas, dilutive ICP is similar to ECP in terms of feed facing the active layer and the permeated water to porous layer dilutes the draw solution. Therefore, approaches for improving membrane's properties and disturbing the concentration polarization should be explored to mitigate this factor limiting the FO performance [108].

2.2.5.2. Reverse solute diffusion

The diffusion of DS solutes to the feed side originated from concentration gradient across the membrane is designated by reverse solute flux (RSF); thereby cross membrane movement of DS solutes results in salinity buildup on feed side [112]. Comparing RSF with fouling, RSF resolution has gained a lower attention relying on accomplished studies in the literature. However, RSF also reduces the driving force (low flux), accelerates fouling and causes gradual loss in the DS [113]. The detrimental impacts of RSF will display the FO process as infeasible technology due to substantial increased operating costs. Deep realization of RSF impacts has uncovered its influencing factors such as membrane parameters (porosity and tortuosity)[111] and DS features (ion charge, viscosity and solutes diffusivity) [114] which were included in a mathematical model prepared by Lu et al. [69]. Therefore, control strategies for RSF is of prior importance for efficient FO performance. It should be understood that indirect control approaches for raised salinity on feed side would not mitigate RSF. Thus, direct RSF control by picking up novel DS that is less permeable similar to stimuli-responsive polymers -as an example- helps in energy efficient separation due to having large hydrodynamic diameter [115]. Moreover, some strategies may be performed during operation by coupling the FO separation with electrodialysis [116]. Besides, membrane surface modification or fabrication have been presented as promising RSF reduction techniques. Throughout many investigation studies, RSF was brought down by innovative supporting materials developed [117], substrates fabricated [118] and surface modification with alternative functionalized groups coated on the surface [119]. A new study was among the earliest examinations conducted addressing FO membrane modification and has preceded in 35% diminishing of the flux decline

resulted from the bidirectional solute diffusion mitigation by coating the surface with zwitterion functionalized carbon nanotubes.

2.2.5.3. Fouling

Although FO fouling has minimal detrimental effects on performance of the process due to less acute cake layer formed on membrane surface if compared with RO [61] (*Figure 2-8*), the fouling in FO remains a challenge that reduces the water permeability and plugs the membrane pores [120]. Also, the companion effects of fouling may be the membrane deformation and salt rejection hindering [121]. Therefore, understanding the fouling mechanisms, reasons along with mitigation procedure and cleaning aspects is required for superior FO operation. Among the possible reasons for fouling as Lee et al. [61] declared is the reverse diffusion of DS salt to feed side which accelerates the cake formation. Moreover, higher water permeation drag leads to reinforces the foulants adhesion to membrane surface as evaluated by the research of Boo et al. [120].

Also, the study of Mi and Elimelech addressed the effect of chemical and physical interactions during organic fouling using three model foulants: bovine serum albumin, sodium alginate and humic acid [122]. The intermolecular adhesion forces were correlated to organic fouling and the extent of fouling was determined by foulant-foulant interaction. The strong intermolecular interactions, calcium binding and hydrodynamic shear force are the leading factors to deposition and cake formation. The investigation results disclosed that alginate formed cake layer under all tested conditions due to calcium binding and bovine serum albumin had weak intermolecular forces that permit the cake formation at optimum conditions only. Distinct studies have been performed for the elucidation of fouling mechanisms of FO and its reduction. Accordingly, fouling can be alleviated by feed

pretreatment, antifouling membrane fabrication and operation at ideal conditions [123–125].

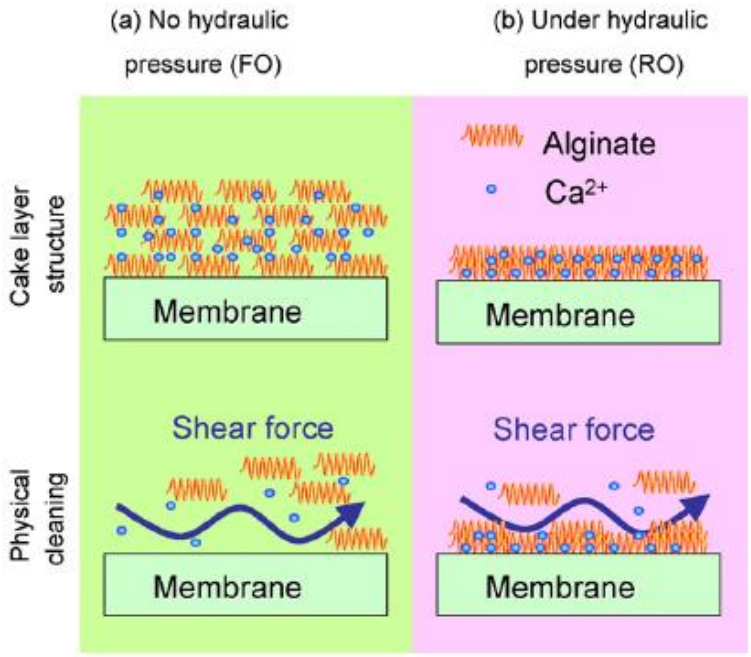

Figure 2-8: Schematic illustration of fouling on membrane surface with and without the physical cleaning for (a) no application of hydraulic pressure, (b) application of hydraulic pressure [62].

Nowadays, among the fouling mitigation approaches is the increased focus brought toward the fabrication of anti-fouling FO membranes by modification of polyamide (PA) layer with hydrophilic substrates [126,127]. For instance, a recent study by Bao et al. [16] has investigated the fouling mechanism through different fabricated TFC-FO membranes where the polyamide (PA) layer was polymerized with varied structures of hydrophilic polyethersulfone (PES) with different additives for domestic wastewater concentration.

Experimental outcomes have indicated that sponge-like shape substrate with polyvinyl pyrrolidone (PVP) additive facilitates a thick cake layer formation when compared with FO fabricated with polyethylene glycol (PEG) additive which endows the FO membrane a higher fouling resistance. Moreover, some control strategies including the enhancement of hydrodynamic mixing by increasing cross-flow velocity, spacers placement and pulse flow generation had successfully removed the loos fouling layer on membrane surface in an osmotic dilution process [120].

2.2.5.4. Costs associated with DS recovery step

It is widely recognized that the DS recovery represents the greatest challenge to the technical and economic feasibility of the FO process [38,75]. Thus, selecting a suitable draw solution that can be readily re-concentrated at low competitive cost is highly desired [38]. Nevertheless, OD is the novel FO application earning the researchers' interests by targeting the direct utilization of diluted DS, thereby minimal energy requirements and elimination of DS re-concentration stage [120].

Moreover, Chekli et al. [75] in their review have emphasized on operating the FO as a pretreatment step to improve the overall efficiency for challenging feed waters desalination. In fact, around 60% of desalination applications and 13% of wastewater treatment applications are employing FO in hybrid systems. For instance, Yangali-Quintanilla et al. [50] demonstrated around 50% reduction in energy consumption of FO hybridized with low pressure reverse osmosis (LPRO) for seawater desalination compared to conventional seawater RO (SWRO). Besides, energy consumption savings and monitored fouling in FO-LPRO have allowed 56% and 21% reduction in operating expenditure (OPEX) and capital expenditure (CAPEX) respectively [128]. In addition, FO

coupling with pressure-retarded osmosis (PRO) hybrid desalination system presents decreased specific energy consumption rather than SWRO.

In contrast, Limited attention has been paid to the whole-life costs of the various FO-based process options for wastewater reclamation. However, several studies reported that the conjunction of wastewater recovery with desalination is energetically favored based on conducted life cycle cost analysis (LCCA) [47,48,51,128]. Simultaneous wastewater recovery/seawater desalination (*Figure 2-9*) through hybrid FO-RO comes at 12% reduced cost compared to SWRO [129].

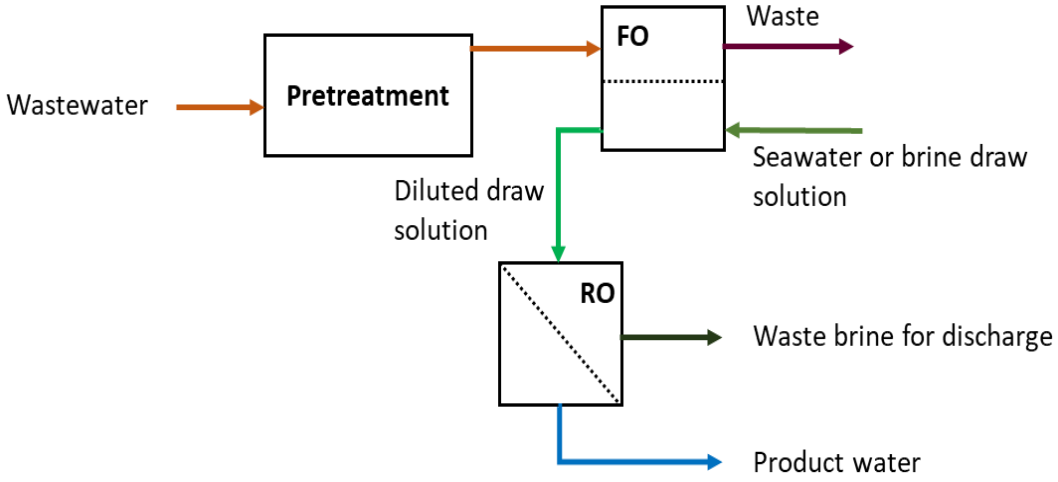

Figure 2-9: Open-loop wastewater reclamation and seawater desalination.

2.3. Forward osmosis and wastewater treatment

The current growth in population and industry's development have led to drinking water resources diminishing. The treatment of wastewater from industrial sectors for direct potable reuse may relieve the stress on drinking water resources as well as, it allows the recirculation of the treated water to be used again in the industrial processes. Several alternatives comprising microfiltration (MF), ultrafiltration (UF), nanofiltration (NF) and reverse osmosis (RO) managed to treat the wastewater successfully, FO was examined as an additional low-cost alternative with the potential to treat complex water due to low fouling propensity and high product water quality.

Recently, the interests for applying FO in the wastewater treatment field has been rising considerably. The research of Lutchmiah et al., 2014 reported that around 7% of conducted studies for investigating FO performance were aiming to treat high-strength water [31]. It should be noted that the increasing implementation of FO for treating wastewater is due to its superior attributes that encouraged the researchers to involve it in the examinations. Indeed, FO membranes are not only susceptible for the rejection of the salt, but also remove the pathogens and a set of contaminants along with the reliability in performance [64]. Furthermore, FO can handle the complex feeds as it beats MF/UF/NF/RO if compared with them in terms of fouling resistance which relies on membrane's active layer design [61,62,130].

The first industrial application for wastewater treatment through forward osmosis-based process was operated by university of Rhode Island and published in 1977 [131]. The aim of the study was determining the feasibility of FO in concentrating a dilute wastewater stream having heavy metal traces. During testing a bench scale setup, the RO cellulose

membranes were adopted and a flux of 4.51 L/m^2.h (LMH) which is lower than expected (10-17 LMH) was observed. As a consequence to the inconclusive findings, the authors suggested replacing the used membranes with developed ones tailored for FO process [131]. Following that, other studies reported applying FO for treating landfill leachate [132] and wastewater to be reusable for direct potable during long term missions in space [133,134].

Nowadays, more research efforts on FO applications for wastewater treatment have been directed towards the treatment of municipal wastewater and produced water from the oil and gas operations [25,32,57,64,75,135–138]. Considering the easiness of FO fouling reversibility via physical cleaning for most of the cases, the motivation towards applying the process for complex feed solutions without inclusive pretreatment is increasing. Nevertheless, looking at most of the wastewater treatment applications, FO operates as a step for effective pretreatment before a fundamental desalination process [15].

2.3.1. FO process configurations for wastewater treatment

Over the past 20 years, a number of pilot and full-scale demonstration studies reported that the widely accepted state-of-the-art involves the adoption of the membrane bioreactor (MBR) for fouling suppression and as pretreatment for the wastewater before entering RO [139–145]. The MBR-RO process (*Figure 2-10*) is an established option for small-scale industrial applications, and has been implemented at full-scale for around 20 years [146]. Therefore, in addition to the operation of the standard FO process, FO may be employed either downstream of the MBR, i.e. as a synergistic process combined with RO desalination step (*Figure 2-11*) or integrated with the MBR as an osmotic membrane bioreactor (OMBR, *Figure 2-12*). The OMBR technology offers and advantages over the MBR-RO

by combining desalination and biological treatment in a single stage. While studies are investigating the FO attributes, none of the researches has conducted LCCA for wastewater treatment options with FO included, compared to traditional MBR-RO.

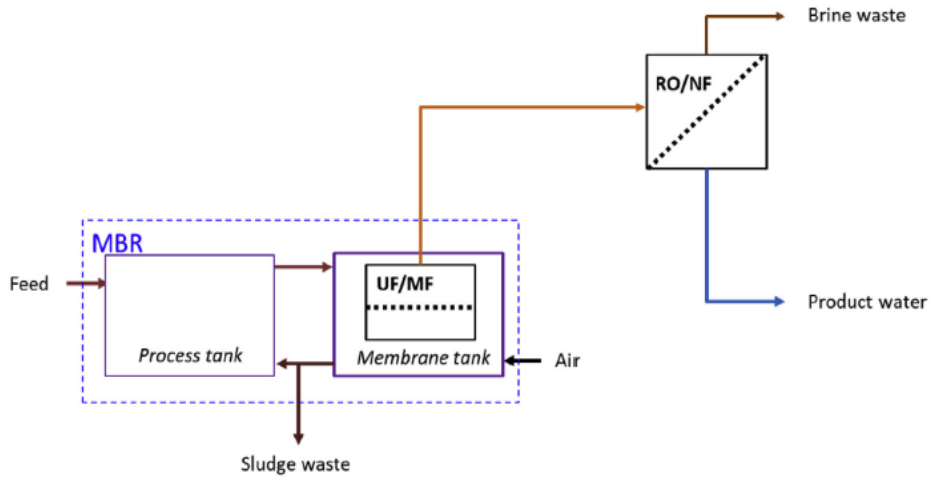

Figure 2-10: MBR-RO process scheme.

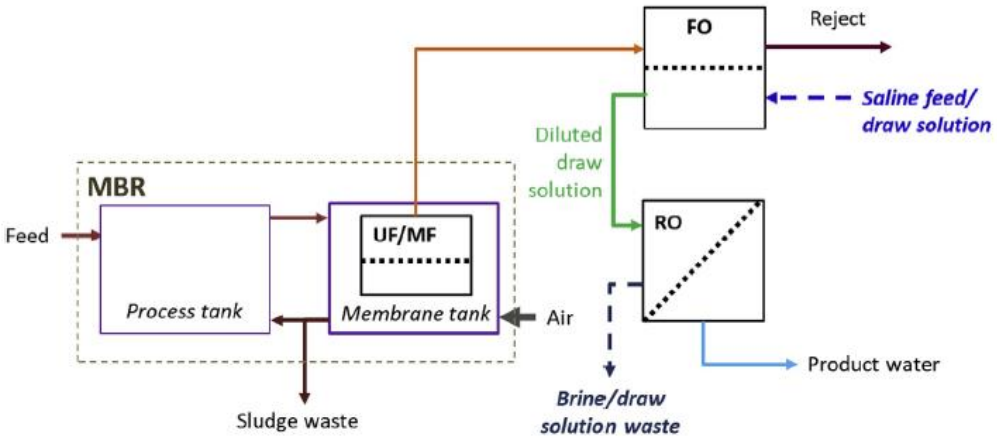

Figure 2-11: MBR-FO process scheme.

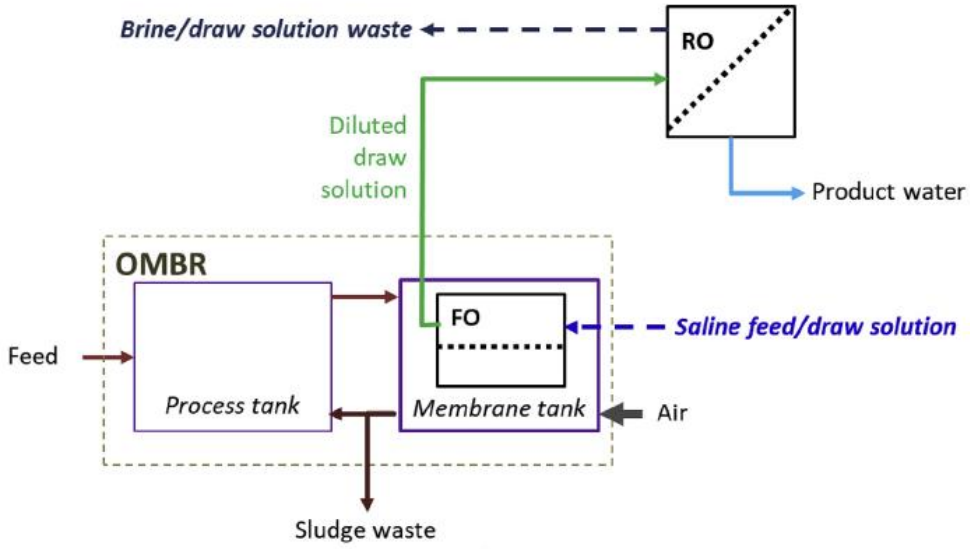

Figure 2-12: OMBR-RO process scheme.

Several FO pilot projects have been structured to reclaim industrial and municipal wastewater obtained from membrane bioreactor (MBR) effluent, sewage and power plants [47,103] (*Table 2-2: Surveyed FO pilot-scale projects.*). The wastewater fed to the implemented FO processes was characterized by its low salinity and high susceptibility to cause fouling due to high total organic carbon (TOC) content. Furthermore, three projects were performed for achieving the fertilizer drawn forward osmosis (FDFO) process (*Figure 2-13*) and injecting the diluted fertilizer or brine to an irrigation system [13,14,147]. It was mentioned that one pilot was built for treating 3 m^3/h municipal wastewater by the utilization of six flat sheets FO membranes obtained from Porifera, while another one was for treating 15 m^3/h of mine-impaired groundwater utilizing two 8040 CTA FO membrane from HTI.

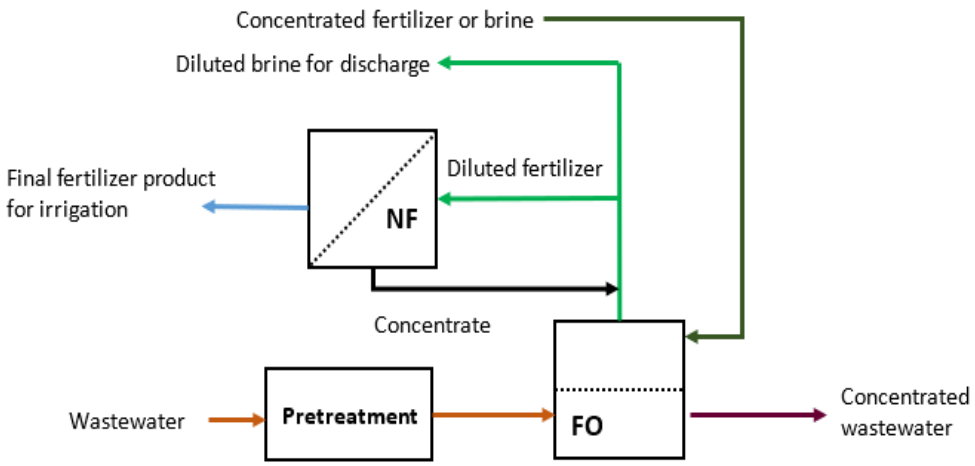

Figure 2-13: FDFO process scheme.

Cath et al., 2010 and Choi et al., 2017 investigated osmotic dilution (OD) process (*Figure 2-14*) performance at pilot scale for combined wastewater treatment and seawater desalination [47,106]. In both studies, the OD was combined with SWRO for further desalination of diluted seawater diluted after FO process and reduction of its osmotic pressure. The process is advantageous in reducing the energy needed for pressurizing the concentrated water downstream in the RO step. Coal-fired plants' wastewater was fed to 21.8 m^3/d pilot plant operated for 5 months to evaluate the flux achieved, fouling reversibility, and efficiency of the process from amount of consumed energy for assessing the reliability of implementing such dual barrier process for water supplying applications [106]. Moreover, Cath et al., 2010 compared between short-term and long-term OD process demonstrated by bench and pilot scale performance respectively for secondary and tertiary treated effluents reclamation and sweater desalination [47]. The research revealed that enhanced fouling in the long-term process run could be minimized with manipulating the DS concentration and feed quality through pretreatment.

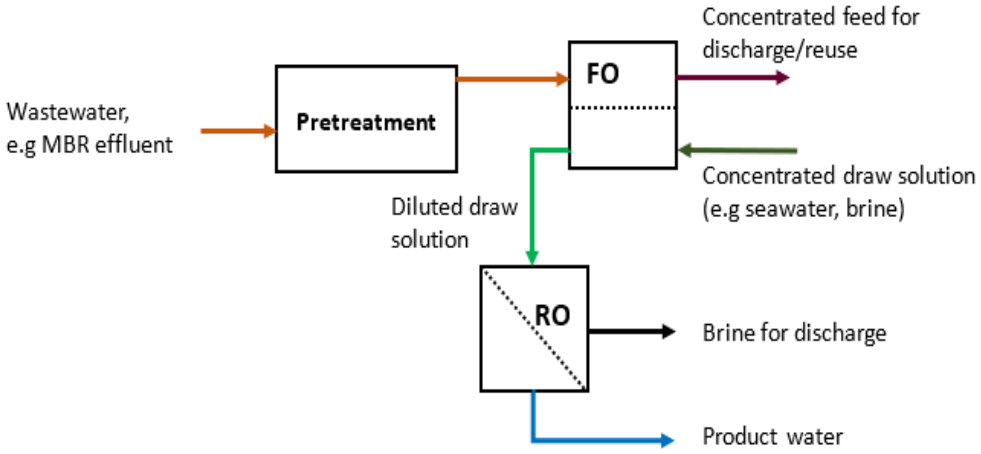

Figure 2-14: Osmotic dilution process scheme.

Besides the above- mentioned processes, two executed OMBR pilot scale projects were operated for wastewater reclamation [105,148]. In OMBR process, wastewater is firstly treated with activated sludge then sent to FO membrane to obtain permeate with the action of DS (*Figure 2-12*). The innovative OMBR process beats the conventional membrane bioreactor (MBR) by the reduced operating costs resulted from the elimination of hydraulic pumps used for microfiltration/ultrafiltration (MF/UF) in MBR and relying on osmotic pressure difference. Besides, the FO membrane potentials in OMBR facilitates the rejection of trace organic compounds, ions [149,150] and achievement of high water flux [151]. The pilot project of Qin et al. [105] for domestic sewage treatment with OMBR confirmed the fouling reversibility with air scouring and enhanced permeate quality compared to MBR (*Table 2-3*).

Table 2-3: MBR and OMBR permeate quality comparison [105].

Parameter	MBR Permeate ($mg.L^{-1}$)	OMBR Permeate ($mg.L^{-1}$)
TOC ($mg.L^{-1}$)	5.7-7.1	< 0.5-1.6
Ammonium ($mg.L^{-1}$as N)	0.09-1.6	< 0.01-0.1
Nitrate ($mg.L^{-1}$)	11.2-14.3	3.4-6.8
PO_4 ($mg.L^{-1}$)	14-21	0.08-0.14

On the other hand, OMBR performance is challenged with accumulation of TDS, nutrients and dissolved compounds inside the bioreactor. The accumulation of salinity and other compounds harmfully affects the microbial activity and lowers the separation driving force. Therefore, a new application of OMBR with UF and FO submerged inside the bioreactor (UFO-MBR) was introduced as a novel alternative for the resolution of salinity buildup and operated for 120 days at pilot scale level [104]. In addition to UFO-MBR operation, an OMBR was operated under the same conditions for performance comparison. The UF membrane helped in considerable fouling reduction and preserving constant driving force and stable flux of 4.8 LMH for the entire operational duration.

2.4. Wastewater associated with conventional and unconventional oil and gas operations

Increasing the energy demand along with petroleum-based products have driven the increase in oil and gas consumption globally. Investments for expanding the production are on the rise to include discovery of unconventional oil and gas infrastructures supplementing the conventional resources. Therefore, both conventional and unconventional resources represented by oil fields and trapped oil in low permeability rocks formations respectively contribute to the oil and gas production.

The production from unconventional reservoirs discovery is enabled by means of hydraulic fracturing (fracking) and horizontal drilling. Extraction operations in unconventional resources are initiated by horizontal drilling to distance of 2 km at several kilometers underground [152]. Following that, massive quantity of water estimated by 2-20 million gallons [152] is injected at a pressure of 700-1400 bar [153] adequate for fracturing the rocks. In addition, the fracturing fluid is referred to the injected mixture of water with sands and chemical additives. Basically, the injection of several millions of gallons of high-water content slurry at high pressure for fracturing the subsurface in the well and enhancing the oil recovery generates the wastewater as form of flowback water and the produced water [56]. The flowback water (FBW) is the portion of fracturing fluid returned to the surface after being injected to the well until the oil production stabilizes, while the remaining amount of fluid turns to be produced water (PW) by undergoing a change to natural formation water and being co-produced with hydrocarbons when extracted. FBW and PW can be distinguished from their chemical composition; FBW composition is mostly the slurry fluid, while produced water has an identical composition to the structure of the well in which it has extracted from [154].

In the conventional petroleum industry operations water is required for all operational segments in upstream and downstream facilities. The upstream facilities during oil extraction operations has to handle mainly the water extracted with the produced hydrocarbons from the reservoirs along with process water obtained from oil processing. However, in downstream operations, water is mainly utilized to process the extracted oil after the oil production stage, as well as it is required for cooling purposes. The supplied water sources can be seawater, surface water, groundwater and potable water that can provide the process water and cooling water. Therefore, major wastewater resources from conventional and unconventional resources are the produced and process water, and it is important to manage the use and reuse of this wastewater to maintain cost-effective operations.

2.4.1. Produced water (PW)

Produced water (PW) is a complex industrial waste produced as the main by-product during exploration and drilling of oil and gas wells. This water is always a companion to oil and gas when are brought to surface. As well, the produced water may be generated from naturally preserved water within the surface formation or the formerly injected water during fracking of unconventional wells [155]. In addition, the flowback water generated as a result of lowering the pressure after cracking the subsurface from the unconventional fields is considered as produced water too [155]. The flowback production diminishes after several weeks from the fracking operations. It worth noting that around 70% of the total wastewater yield from wells is designated for produced water flowing with gas and oil [64].

2.4.2. Produced water volume

Oil to water ratio relies on the geological structure of the origin surface and it was estimated that 3-4 barrels of produced water are obtained with the extraction of 1oil barrel (42 US gallons) [156]. In the United States, 9.5 barrels of water come with extraction of 1 oil barrel as reported by Veil et al., 2004 [157]. Throughout the whole lifetime of the well, produced water is recovered with the oil and its quantity significantly increases with the age of the well [58]. For old wells, more than 95% of the production represents the captured produced water [158]. Moreover, the quantity produced varies according to the location and type of injected water during hydraulic fracturing works. For instance, onshore and offshore exploration activities of conventional and unconventional wells in U.S. have resulted in generating 20 billion barrels of produced water [153]. Overall, the produced water yield varies over time [159] and possesses a growing trend that is projected to approach 340 billion barrels annually produced worldwide in 2020 [57] compared to the obtained 77 billion barrels/year in 1999 [160] (Figure 2-15).

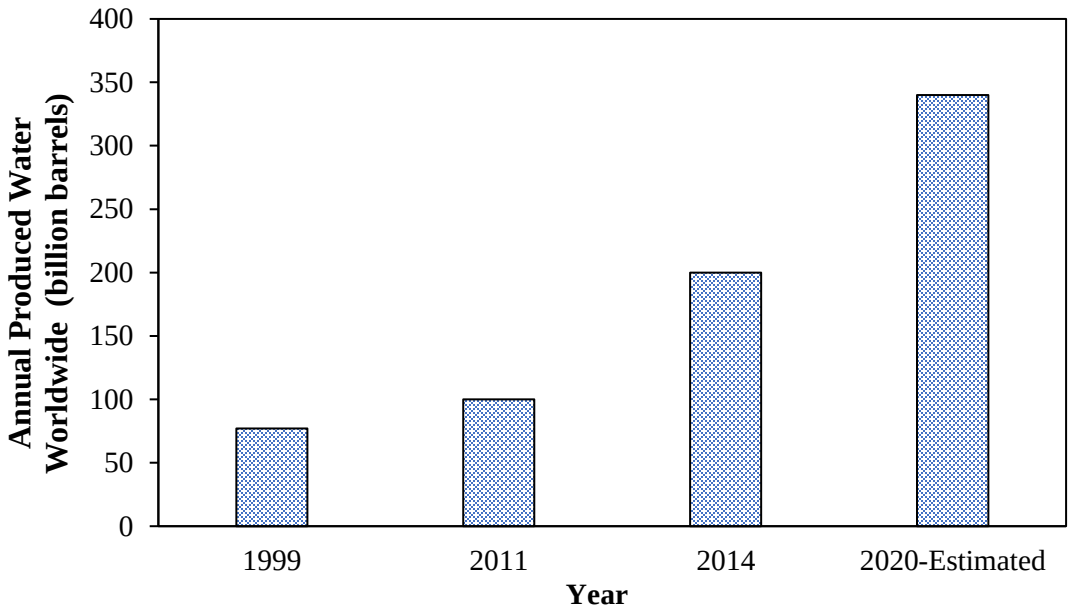

Figure 2-15: Worldwide annual quantity of produced water [57,160].

2.4.3. Produced water characteristics

The physical and chemical characteristics of produced water have a spatially and temporally changing attitude similar to the produced water quantity. Also, the characteristics are very subjected to the type of geological formation, chemical additives during fracturing activities and hydrocarbon produced [64,153,158]. In that case, the characteristics of oily produced water from oil wells differ from the water which accompanies the gas extraction [158,161]. Gas fields' produced water is a combination of condensed and formation water from rocks, as fracking activities for gas fields do not utilize water injection. Besides, the volume of PW from gas filed is smaller and of higher acidity when compared with the greater volume and low acidity of PW from oil field [162]. In fact, produced water is classified as brackish or very saline groundwater with high concentrations of total dissolved solids (TDS), organic, inorganic components, salts,

bacteria, heavy metals and naturally formed radioactive materials leached out from the earth subsurface [155,158,163,164]. Moreover, the oil and grease are prime constituents of the oily produced water in which their concentrations ranges between (40-2000 ppm) [158]. The analysis of produced water from different resources demonstrates the variation in salinity level as shown in (*Table 2-4*). Generally, produced water is characterized by having a higher salinity than seawater and conventional oil wells can produce wastewater with salinity more than 100,000 $mg.L^{-1}$ [57].

Table 2-4: Salinity of produced water from various resources.

Location	TDS ($mg.L^{-1}$)	Produced Water Resource	Reference
Western USA	1,000-400,000	Oil Field	[165]
Qatar	247,000	Oil Field	[166,167]
Qatar-North Field	5,200	Gas Field	[168]
Pennsylvania-Marcellus region	106,390-345,000	Gas Field	[169]
Australia-Surat Basin	1,200-4,300	Unconventional Gas Field	[170]
South Africa	5,125	Unconventional Gas Field	[158]
Walsenburg-USA	588-722	Unconventional Gas Field	[171]

The most abundant ions in produced water are the sodium and chloride similar to seawater. Moreover, produced water additional existing ions are calcium, potassium, magnesium, strontium, cadmium, barium, bromide, iron, zinc, arsenic and radon in which their concentrations vary with the well's formation. *Table 2-5* demonstrates the constituents of produced water from oil and gas fields. Oily PW is mainly described by the higher TOC and chemical oxygen demand (COD) along with sodium and chloride ions concentration compared to PW from gas fields. Indeed, the complexity of produced water nature is referred to available toxic organics and heavy metals that deteriorate the environment.

Table 2-5: PW constituents of produced water from oil and gas fields [172,173].

Parameter	Value	Parameter	Value
Produced water from oil field			
pH	4.3-10.0	Calcium ($mg.L^{-1}$)	13-25800
TSS ($mg.L^{-1}$)	1.2-1000	Magnesium ($mg.L^{-1}$)	8-6000
TOC ($mg.L^{-1}$)	0-1500	Copper ($mg.L^{-1}$)	<0.002-1.5
COD	1220	Iron ($mg.L^{-1}$)	<0.1-35
Sodium ($mg.L^{-1}$)	132-97000	Zinc ($mg.L^{-1}$)	0.01-35
Chloride ($mg.L^{-1}$)	80-200000	Mercury ($mg.L^{-1}$)	<0.001-0.002
Sulfate ($mg.L^{-1}$)	<2-1650	Phenol ($mg.L^{-1}$)	0.009-2.3
Cadmium ($mg.L^{-1}$)	<0.005-0.2	Strontium ($mg.L^{-1}$)	0.02-1000
Barium ($mg.L^{-1}$)	1.3-650	Lead ($mg.L^{-1}$)	0.002-8.8

Table 2-5: PW constituents of produced water from oil and gas fields [172,173].

Parameter	Value	Parameter	Value
Arsenic ($mg.L^{-1}$)	<0.005-0.3	Boron ($mg.L^{-1}$)	5-95
Produced water from natural gas field			
pH	4.4-7.0	Calcium ($mg.L^{-1}$)	25000
TSS ($mg.L^{-1}$)	14-800	Magnesium ($mg.L^{-1}$)	0.9-4300
TOC ($mg.L^{-1}$)	67-38000	Copper ($mg.L^{-1}$)	0.002
COD ($mg.L^{-1}$)	2600-120000	Iron ($mg.L^{-1}$)	1100
Sodium ($mg.L^{-1}$)	520-45000	Zinc ($mg.L^{-1}$)	0.022
Chloride ($mg.L^{-1}$)	1400-190000	Benzene ($mg.L^{-1}$)	1.8-6.9
Sulfate ($mg.L^{-1}$)	<0.1-47	Toluene ($mg.L^{-1}$)	0.857-3.37
Cadmium ($mg.L^{-1}$)	0.015	Strontium ($mg.L^{-1}$)	6200
Barium ($mg.L^{-1}$)	26	Bromide ($mg.L^{-1}$)	150-1149
Arsenic ($mg.L^{-1}$)	0.004-1	Boron ($mg.L^{-1}$)	56

2.4.4. Produced water management

Despite the resources potentials of the unconventional developed wells along with the gained economic benefits, the expansion in conventional and unconventional oil and gas (O&G) operations has triggered the concerns about environmental implications due to increase in the quantity of consumed water during drilling and hydraulic fracturing, concomitant wastewater stream produced and risks on groundwater quality [154,155,174,175]. Because water is the vital element for O&G operations; the competition on water resources has grown and raised the danger of their depletion. As a consequence

of the growth in exploration and production (E&P) practices, the demand for wastewater reuse and disposal to maximize water resources and minimize the waste volume is becoming serious [64].

Produced water from onshore operations is managed by several methods involving minimization by traditional evaporation approaches, followed by recycling and reuse for water that cannot be minimized. The surface discharge represents the cheapest disposal solution (*Table 2-6*), but it is limited by sequestration procedures to avoid ground contamination [153]. The recycle or reuse of produced water allows its utilization in the industrial and agricultural sectors. Moreover, the reuse of produced water can provide potable water supply for humanity after precise treatment in municipal wastewater treatment plants, though it appears to be insufficient for resolving the produced water issue [169,176]. Subsequently, the produced water which is invalid for minimization and recycling purposes is managed through deep wells injections for disposal or use for enhanced recovery [155,159]. In fact, the produced water management procedures are truly dependent on the characteristics of produced water, geological formation and capital investments costs. For instance, Pennsylvania's geology of the reservoirs is not suitable for accommodating the injected wastewater [56,153]. At advanced stages of fields' production, the disposal into deep well injections becomes favorable when increased quantities of PW is attained. Certainly, the disposal into injection wells is an economic preference when they are located near the production fields compared to recycle and reuse of PW in treatment plants [153].

Table 2-6: Estimated cost of PW disposal methods [177].

Disposal Method	Cost ($/bbl.)
Surface Discharge	0.01-0.08
Evaporation Pits	0.01-0.8
Well Injection	0.05- 2.65

2.4.5. Produced water treatment technologies

Over the past years, deep well injection was a widely practiced technique for disposing the flowback and produced water resulted from unconventional E&P operations after the treatment by settling the solids [58,176,178–181]. Despite the existence of 30,000 Class II injection wells in U.S. which are specified wells for injecting fluids from enhanced recovery purposes, or storing the wastewater [152], the restricted capacity of the wells limits the expansion in developing the O&G fields [169]. Furthermore, the long-term implications of the injection wells on the underground water, and the restricted capacity of injection wells limit the expansion in developing the O&G fields and encourage finding more promising management solutions.

Various standalone or hybrid physical and chemical technologies for treating the produced water and wastewater from O&G operations have been applied aiming for the separation of oil-water emulsions, desalination, removal of suspended particles and removal of hardness by softening and disinfection [182–184]. In the case of requiring high quality water source from the oily wastewater, advanced technologies including membranes-based

processes and advanced oxidation processes (AOPs) such as photo- Fenton processes and photocatalysis have presented their capabilities to meet the needs [153].

2.4.5.1. Implemented physical and chemical treatment technologies

Table 2-7: Features and limitations of some implemented physical and chemical produced water treatment technologies.

Technology	Features and limitations	Reference
Adsorption	• Good potential to reduce TOC and oil content. Minimal energy requirements • Long retention time and less efficiency at high concentration of feed wastewater.	[182,183]
Stripping	• Targets the volatile components. Cheap and practical treatment option. • High capital cost from large stripping columns.	[185]
Gas Flotation	• Achieves nearly 100% recovery of PW. • Problems with disposal of sludge generated.	[182]
Filtration by sand filters	• High removal efficiency (90%) with proper pretreatment. • Limited to removal of oil droplets with size bigger than 10 µm.	[177]

Table 2-7: Features and limitations of some implemented physical and chemical produced water treatment technologies.

Technology	Features and Limitations	Reference
Ion Exchange	• Effective for TDS removal from PW • Cost-ineffective when executed for large scales.	[186]
Coagulation	• Removal of suspended particles, dissolved matters including absorption of heavy metals. • Requires high coagulants dosage, high retention time and pH control.	[158]
Chemical Oxidation	• Removal of COD[1], BOD[2], organics and some inorganics depending on contact time, oxidant dose and type. • Cost of chemicals is considered high.	[182]
Biological Aerated Filters	• Oil removal efficiency of 80% and water recovery reaches 100%. • Requirement of upstream and downstream sedimentation for the utilization of entire filtration bed. The sedimentation sludge disposal acquires 40% of process' total cost.	[182]

[1]COD: Chemical oxygen demand, [2]BOD: Biological oxygen demand.

2.4.5.2. Membrane-based treatment technologies

Membrane filtration technologies are distinguished by their efficiency in isolating the components of O&G wastewater through the selective and porous membrane films. The most implemented membrane-based processes that proved their technical feasibility for O&G wastewater treatment are compared with each other in *Table 2-8*. Despite the effectively distinguished performance of membrane processes for desalination, produced water's organic compounds can be removed relying on processes' appointed type of driving force. For instance, the low-pressure membrane processes such as microfiltration (MF) and ultrafiltration (UF) guarantee the removal of suspended particles and macromolecules respectively [182]. Whereas, nanofiltration (NF) and reverse osmosis (RO) are two high-pressure driven processes, where the dissolved traces and ions are stripped off by RO and NF is eligible for particular removal of multivalent ions [182]. Additionally, it was demonstrated that sometimes membrane processes (e.g., UF) are coupled with biological treatment processes for removal of biodegradable organics from introduced saline PW [187–190].

Compared to the pressure driven processes, forward osmosis (FO) and pressure retarded osmosis (PRO) utilizing the natural osmotic pressure energy are capable of treating the oily produced water. A dual stage FO/PRO system was suggested by Altaee & Hilal [191] for hypersaline fracking wastewater treatment, the FO will treat the water and in the second stage PRO generates the power when osmotic energy is converted to mechanical energy by the application of hydraulic pressure to the draw solution. A recent review by Chang et al., 2019 [192] has presented that osmotically driven processes are currently being under investigation the most for treating the flowback and produced water, where it accounts for

23.3% of total studies on the membrane processes published in literature. Furthermore, thermal driven membrane processes like membrane distillation (MD) can be considered as a promising desalination technology for shale oil and gas produced water (SOGPW) with salinity up to 350,000 $mg.L^{-1}$; however, the high-energy requirements by MD restrict its applications. More membrane processes employing the electrical power are evaluated for high salinity produced water treatment [193,194]. Electrodialysis (ED) and electrodeionization (EDI) are two examples of the electrical membrane processes, where some projects showed how ED succeeded in treating PW with <5500 $mg.L^{-1}$ to drinking water standards [195]. An application of ED to reclaim SOGPW resulted in the removal of 35-90% existing TDS at laboratory scale examination [196]

Table 2-8: Comparison of most implemented membrane-based processes for produced water treatment.

Technology	Features	Obstacles	Life Span	Reference
UF/MF	High water recovery (80-100%) and tolerance of high TDS PW.	Feed pretreatment with chemicals, high fouling and energy utilization.	10 years	[183]
NF	Removal ability of divalent salts at high pressure leading to water softening, ability to remove metals from wastewater and poor efficiency for PW treatment.	High consumption of electrical energy, fouling which can be prevented by caustic inhibitors.	3-7 years	[170,183,186,197]
RO	Outstanding performance for PW treatment being properly pretreated and removal of monovalent salts at high pressure.	Extensive energy uses more than NF. Sensitivity to organics and inorganics, pretreatment is required.	3-7 years	[170,183,186]

Table 2-8: Comparison of most implemented membrane-based processes for produced water treatment.

Technology	Features	Obstacles	Life Span	Reference
FO	Good performance for treating the challenging feed waters including PW. Recognized by low fouling propensity and minimal energy consumption.	High-energy requirement for recovery of DS and bidirectional flow of salts.	8 years	[18,25,52]

2.5. FO applications for treatment of oil and gas industries wastewater

Forward osmosis as an engineered osmosis process has captured the attention as a promising option for treating complex water streams from O&G operations such as produced water, flowback water and process water, since it eliminates the operating obstacles associated with pressure-driven processes and rejects the contaminants by the removal of suspended solids and almost all dissolved ions. The main benefits of FO over the conventional membrane separation processes are the technical operation at very low hydraulic pressure and at ambient temperature. Therefore, no extensive pretreatment or sizable power utilization are required which helps in having the smallest carbon print among the other wastewater reclamation processes. Also, thin film composite (TFC) FO membranes showed the capability in retrieving fresh water and obtaining 11.8 $L/m^2.h$ water flux from oily solution prepared synthetically with concentration up to 200,000 ppm [25]. Consequently, the interests in employing FO for the reclamation and reuse of O&G industries' wastewater are rising.

2.5.1. Pilot-Scale Projects for O&G Wastewater Reclamation

Table 2-9: Pilot-scale projects for O&G wastewater treatment.

Project	Feed	Process Scheme	FO Membrane	Implementation Outcomes	Reference
A	PW of 70,000 $mg.L^{-1}$ TDS from gas fields in Pennsylvanian.	FO-MBC[1]	SWo[2]	62% of PW was recovered at an average flux of 2.6 LMH.	[60]
B	PW from Denver-Julesburg oil and gas basin.	FO-RO	SWo	99% removal of cations, anions with 92.9% rejection of boron.	[107]
C	PW from Haynesville shale gas field	FO-RO	SWo	85% of PW was recovered.	[64]

[1]MBC: Membrane brine concentrator, [2]SWo: Spiral wound membrane.

2.5.1.1. Project A

A pilot unit was constructed after several examinations of the desalination for the produced water from the gas extraction operations occurring in Pennsylvania in fully integrated FO membrane brine concentrator (MBC) process using NH_3/CO_2 DS [60]. The project tested the MBC process operated by Oasys water comprising pretreatment, FO-based separation,

and thermal recovery of the DS for treating 227 m^3 of frac-flowback water and PW of ~70,000 $mg.L^{-1}$ TDS. The produced water was treated by chemical softening, activated carbon, media filtration and cartridge filtration. The company's spiral wound FO membrane of polyamide thin film composite was tested in the pilot system and an average water flux of 2.6 LMH with 62% water recovery were achieved. The process's product water quality succeeded in complying with the state standard conditions having a TDS of 300 $mg.L^{-1}$. Although it was expected that the NH_3/CO_2 FO process would be less energy consumption technology compared to RO, however the situation is reversed due to the thermolytic re-concentration step for NH_3/CO_2 solution.

2.5.1.2. Project B

In the research of Maltos et al., 2018 [107], the impact of produced water on the effectiveness of the FO membrane was examined based on the built pilot plant receiving more than 10,000 L of produced water from Denver-Julesburg oil and gas basin. The pretreatment of produced water was conducted through FO-RO pilot system, and by using the spiral wound FO membrane type for the reproduction of the results of similar published bench scale operations [136,198]. The experiments investigated the ion exchange across the FO membrane along with assessing the hydrocarbons rejection in the produced water. In addition, the fouling was studied from analysis of Fourier transform infrared spectroscopy (FTIR) generated spectrum for active layers of the membrane after long exposure to the produced water. Consequently, the revealed results from the FO-RO system confirmed achieving 99% rejection of cations, anions and dissolved organic carbon (DOC) with 92.9% of boron rejection. However, the high organic matter content has led to intense fouling with membrane's characteristics modification.

2.5.1.3. Project C

For the purpose of O&G drilling wastewater reuse, a recent pilot plant project was constructed adopting the second generation of invented green machines in which 24 horizontally oriented spiral wound membrane are utilized and RO is combined to the FO system as a re-concentration step for the DS [64]. The second-generation green machine FO based system produces RO permeate applicable to wide range of uses rather than first generation machine producing reclaimed water suitable only as base fluid for future fracking activities. An 85% recovery of drilling wastewater in Haynesville shale gas field was attained at the expense of increasing its concentration from 3,500 $mg.L^{-1}$ to 16,000 $mg.L^{-1}$ using NaCl DS of 60,000 $mg.L^{-1}$ TDS concentration. Due to the increased concentration of feed wastewater and its high osmotic pressure, the osmotic driving force was dropped leading to slight flux decline.

2.5.2. Pilot-Scale Projects for Osmotic Concentration/ Osmotic Dilution of O&G Wastewater

The implementation of FO for osmotic concentration or osmotic dilution (OC / OD) is one of the good benefits of the process as depicted in the review of Coday et al., 2014 [64] for the treatment of O&G wastewater. The executed pilot projects are summarized in (*Table 2-10*).

Table 2-10: Pilot-scale OC/OD projects for O&G wastewater.

Project	Feed	DS (NaCl)	Water Recovery	Process Type	Reference
D	Reserve pit wastewater.	26% w/w	70%	Portable FO system	[23]
E	O&G wastewater.	26% w/w	70%	Green machine FO	[23]
F	Drilling wastewater.	26% w/w	50%	Optimized green machine	[64]

2.5.2.1. Project D

The feasibility of implementing FO was examined by several tests including the portable FO system developed in the research of Hutchings et al. [23] which was successful in treating 75% of reserve pit wastewater. The reclamation concept of the reserve pit or flowback wastewater with low TDS depends on using high salinity pure water mainly with NaCl or KCl to withdraw water molecules to draw solution side and diluting it while concentrating the feed wastewater. The system was operated in the osmotic dilution mode where the diluted brine was utilized as completion fluid during hydraulic fracture since NaCl and KCl help in providing the stability of the wells' clays. Besides, the FO system was scalable and portable to provide on-site treatment nearby the wells and limit the additional wastewater and reclaimed water trucking costs and it is called by the green machine relying on its concept [64].

The FO pilot unit for 8 gal/min capacity was built and tested reserve pit wastewater batches of 500 barrels to assess the performance of 20 cylindrical spiral wound FO membranes installed in one pressure vessel using 26% w/w NaCl solution as the osmotic agent. The experiments were conducted at four trials with different batches of reserve pit water where the operation in each trial was continuous until reclamation of 70% of the wastewater.

The pilot tests confirmed that the FO system successfully reclaimed 70% of the wastewater and allowed the reuse of the reserve pit wastewater as nano-pure base fluid for fracking actions after the removal of all suspended solids, solutes and heavy metals. Moreover, it was suggested using wastewater of TDS lower than 25,000 ppm, since the production rate was reduced by 50% due to deficiency in the osmotic driving force noticed when wastewater concentration increased more and approached the concentration of 26% NaCl solution.

2.5.2.2. Project E

HTI and Beer Creek Services (now named by Emerald Surf Services) have operated two different models of the portable FO system at commercial scale for O&G wastewater reuse as completion fluid in hydraulic fracture [23]. The pilot unit consists of 20 to 280 vertical long spiral wound FO membrane and was designed to accommodate a capacity of 8-170 gal/min of O&G wastewater. The system runs under recirculation mode, where the concentrated feed stream returns back to the primary feed tank, the 26% w/w NaCl DS recirculates inside the membrane envelope and goes to initial concentrated draw solution tank after it is diluted.

In addition, the testing results showed that the process is able to concentrate the O&G wastewater to more than 3.5 times the original concentration of 25,000 $mg.L^{-1}$ TDS and

achieve a recovery higher than 70% while osmotically dilutes the NaCl draw solution to less than 70,000 mg.L^{-1}.

2.5.2.3. Project F

An optimized pilot green machine FO based system was tested using customized CTA FO membrane cell. The main aim of the pilot experiments was to recover 50% of the wastewater generated during drilling. Following the conducted experiments, the results were analyzed and presented how the FO system was able to increase the concentration of the O&G wastewater up to three times. Above all, it was observed that FO system possesses high rejection of organics and inorganics along with irreversible fouling features [64].

2.6. FO applications for volume reduction of O&G wastewater

The main challenge encountered during oil and gas industries' rapid development is the management of generated process and produced water (PPW) streams while ensuring profitable and safe operation. Commonly, the global practice of disposing the wastewater in the onshore facilities is the re-injection to the deep drilled wells. However, the growth in E&P operations and expansion are bounded by the insufficient capacity of injection wells [169]. In addition, the attempted discharge of wastewater into municipal treatment plants showed deficient management option, and encouraged having practical solutions at reduced capital and operating costs. As a consequence, the single filtration step in FO technology was applied alone providing an osmotic concentration and volume reduction of PPW [199].

2.6.1. Bench-scale project in USA

Volume reduction of drilling wastewater from shale gas well was evaluated using FO system at bench scale in 2013 by Hickenbottom et al. [55]. The study was performed to assess the organic and inorganic contaminants rejection, water permeation flux and fouling. For the experimental investigation, the tested FO membrane was made of cellulose triacetate (CTA) polymer that was placed in custom-made FO test cells.

The treatment of drilling wastewater obtained from Northern Louisiana was done using draw solution of 260 g/L NaCl solution. Three sets of experiments were conducted with differently positioned membrane cell in horizontal direction with feed facing active layer, vertical direction with both solutions across the membrane flowing upward and horizontal direction with feed facing the support layer respectively. The first two sets of experiments were continued until reaching 80% feed recovery while 50% recovery was targeted for

third experiment. Resulted outcomes demonstrate the flux trend starting from around 14.00 LMH at the beginning of the two experimental sets and ending with 2.00 LMH flux. While for the third experiment, the initial acquired flux of 14.00 LMH had declined to 4.00 LMH when 50% of feed was recovered. The draw solution became diluted to 50 g/L NaCl for the two experimental sets and to 75 g/L NaCl for the 50% feed recovery experiment. The combined influence of fouling causing hydraulic resistance on membrane surface and reduced osmotic driving force contribute to the descended flux.

The effect of flow velocities was also studied in which high velocity stimulated membrane scouring and reduced the rate of flux decline. Besides, the increased conductivity of feed stream was a consequence to the reverse solute diffusion and reduced feed volume. Also, ions analysis results demonstrated that Al^{+3}, Ba^{+2}, Ca^{+2}, Fe^{+3}, K^{+}, Mg^{+2} and Si remained in FS, while Na^{+}, Cl^{-} and $SO4^{-2}$ were exposed to dilution. Lastly, the rejection of organics by membrane was measured by chemical oxygen demand (COD), dissolved organic carbon (DOC) and fluorescence spectroscopy. COD results showed around 5.8 mg/L decrease between original DS and diluted DS at the end. Moreover, 1.17 mg/L increase in DOC was a reason to the complex organics that appeared through combustion in DOC, as they were not digested by the COD analysis. Lastly, the cake layer accumulated on membrane surface was removed successfully by osmotic backwashing where DS was replaced with deionized water. As a conclusion of the achieved work, FO showed an efficient operation for three times concentration of drilling wastewater more than initial concentration and volume recovery of 80%.

2.6.2. Bench-scale project in Qatar

Produced and process water management through the volume reduction is of growing interest in Qatar to comply with Ministry of Environment rules and Qatari vision for saving lands and environment. Therefore, the operators in North Field are requested for 50% cut of their wastewater injection and excluding the conventional practice of discharging the clean treated water to the Arabian Gulf [66]. Through Qatargas (QG) company, Qatar is the largest producer of liquefied natural gas (LNG) globally and has the world's largest plant for gas to liquid (GTL) production [200,201]. Considerable amounts of PPW are generated from the production facilities in which are being treated currently with two constructed plants for wastewater recycle and reduction (WRR) as part of the long-term sustainability strategy [66]. Five different streams of process water are combined to a total flow of 176 m^3/h and treated in each WRR plant involving both conventional and advanced treatment technologies. The figure below (*Figure 2-16*) highlights the advanced technologies adapted in the plant in red, while the remaining units are considered as auxiliary treatment stages. The role of conventional auxiliary treatment stages is securing the removal of emulsified oil, hydrogen sulfide gas (H_2S), suspended solids and organic contaminants.

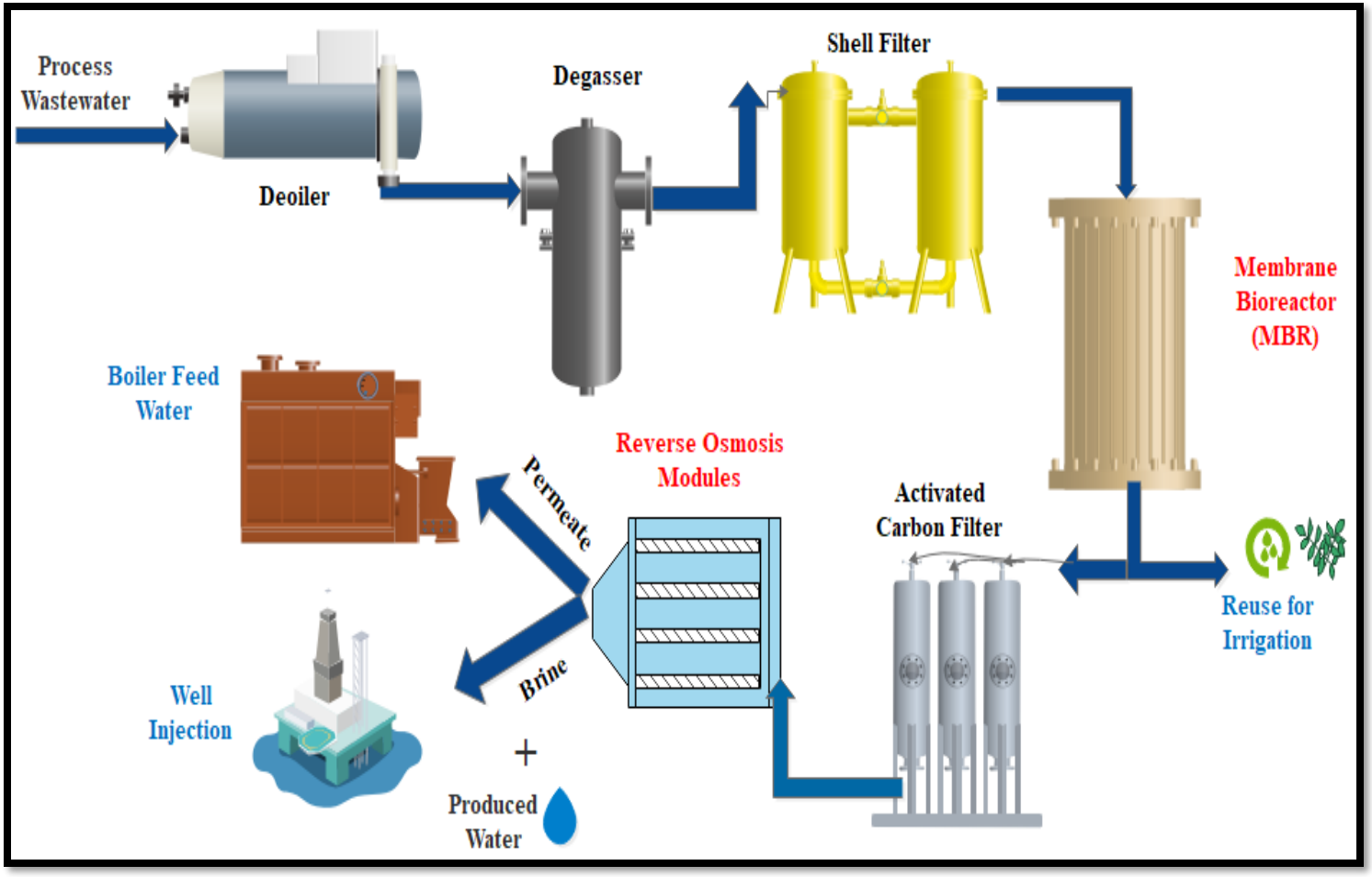

Figure 2-16: Process water treatment plant of Qatargas adapted from [57,66].

The fundamental advantages of the plant are represented by reusing the treated process water's permeate as boiler feed water and reducing its volume for deep well injection after being blended with PW. As the MBR precedes the RO treatment step, the design enables the water reached the MBR treatment to be reused for controlled irrigation utilization avoiding any operational challenges encountered by RO. The quality of supplied irrigation water drawn after the MBR should obey the following specifications:

Table 2-11: Qatar Gas WRR plant MBR effluent composition sent to irrigation [66].

Parameter	Value (mg/L)
TDS	2000
TSS	50
COD	150
Oil and Grease	10

The constructed WRR plants and the results obtained during the operation have opened the opportunities for laboratory treatability investigations of several membrane processes and whether or not their applicability will achieve the same intended objectives or even enhance it. Among the investigations, osmotic concentration with FO is proposed as a treatment solution replacing the RO and ensuring further volume reduction.

Indeed, FO is considered a low-energy intensive alternative for future facilities supporting in cutting off the significant cost of the advanced wastewater treatment plant for planned WRR project. Proposing FO for volume reduction of PPW also plays an essential role in resolving the problem of brine discharge from thermal desalination plants by being readily utilized as the DS for FO process. The exploitation of brine as DS contributes to substantial improvements in the process performance by driving high water flux, as well as alleviates the energy requirement by eliminating the energy-intensive DS re-concentration step of conventional FO process by directly discharging the diluted brine to the sea [199].

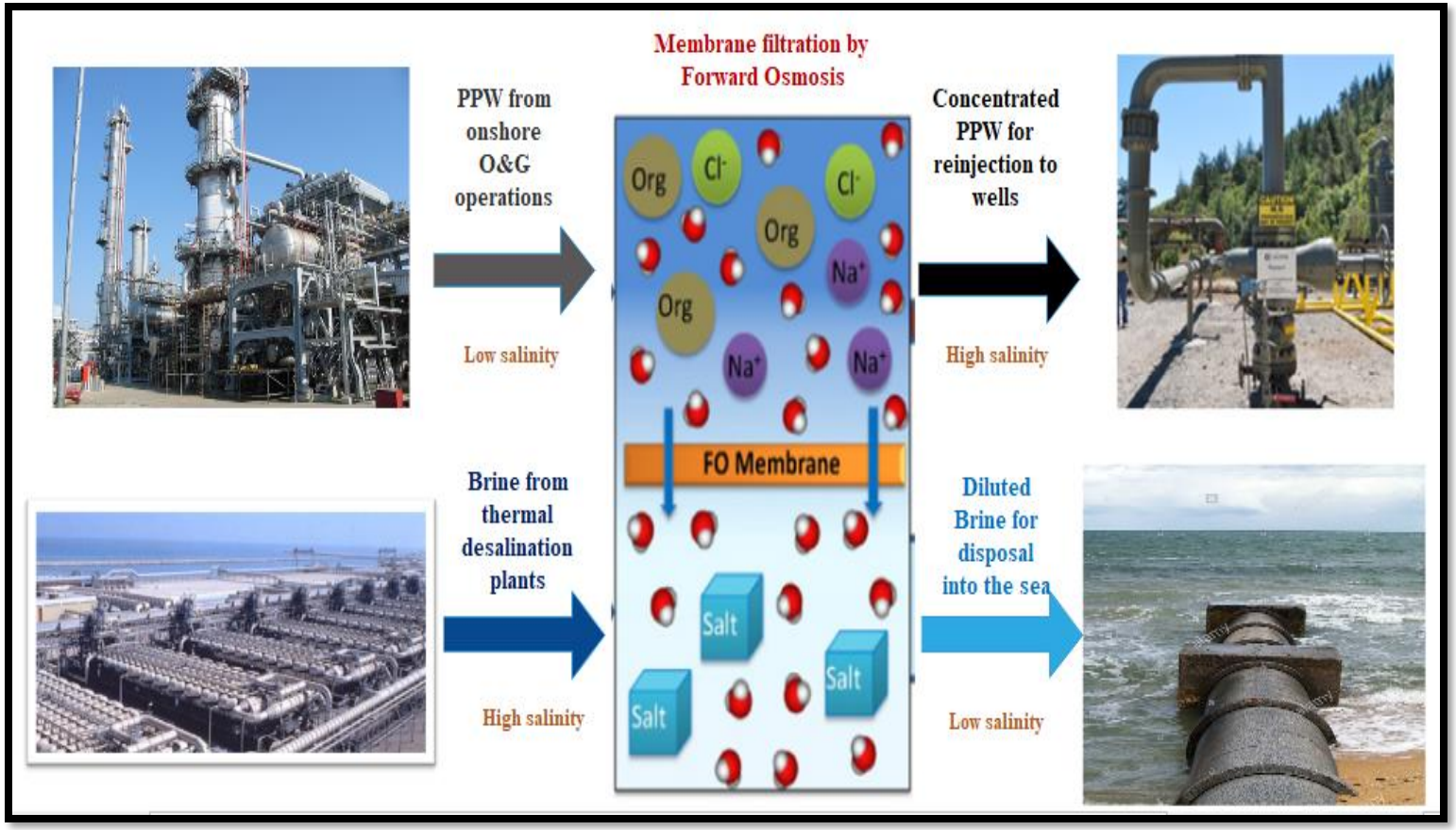

Figure 2-17: Osmotic concentration with FO for volume reduction of PPW [202].

As a proof of concept, Qatar National Research Fund (QNRF) has funded a bench scale study investigating the feasibility of FO for such application and examining the possibility for full scale implementation [65,80,199,202]. The objective of the study came to assure the 50% reduction of PPW volume by testing several membrane modules and understanding the impact of parameters on FO performance.

2.6.2.1. Bench-scale system

A bench-scale FO unit was customized for OD/OC process as per the following process scheme (Figure 2-18). In closed loops and counter current recirculation, the FS and DS were pumped to the membrane after controlling the temperature by water bath. To ensure constant DS concentration through the complete duration of the experiment, concentrated DS tank was used to balance the DS concentration getting diluting with time. Temperature, pressure and flow were all monitored from the on-line positioned transmitters.

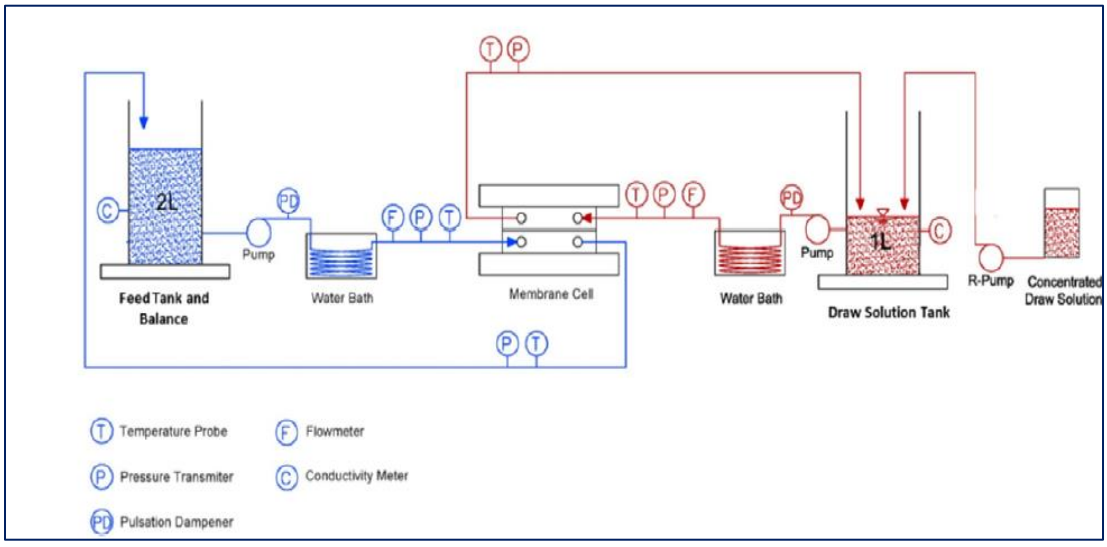

Figure 2-18: Bench-scale osmotic concentration unit for volume reduction of PPW feed.

2.6.2.2. Membranes

Thin film composite (TFC) FO membranes from both types of commercial flat sheet (FSH) [203] and hollow fiber (HF) obtained from Singapore Membrane Technology Center [204,205] were tested with an effective membrane area of 0.014 and 0.0106 m^2 respectively.

2.6.2.3. Feed and draw solutions

The used PPW blend consists of produced to process water with ratio of 1:5 after removal of oil, H_2S. The produced water was obtained from a gas field and went through filtration using cartridge filter (2 μm). The analysis results of PPW illustrated a TDS content of 1526 ppm with TOC of 132 ppm. In contrast, synthetically prepared draw solution of similar properties to seawater and brines was used.

2.6.2.4. Role of operating parameters

Experiments for evaluating the influence of DS concentration, temperature, crossflow velocity and active layer orientation on the water flux were first conducted using the commercial flat sheet membrane (FSH). The experiments for effect of operating parameters were carried out with deionized water as FS, 1 NaCl solution as DS, temperature of 25 °C and active layer facing the FS (AL-FS).

The tested DS concentration ranges from 35-175 g/L NaCl solution and it was indicated through the tests that flux and DS concentration have logarithmic relation ending with a plateau due to internal concentration polarization (ICP) initiated by dilution of DS in porous support layer. Additionally, 60% rise in water flux was observed when temperature

was increased from 20 to 40 °C. Crossflow velocity alteration from 9 to 22 cm/s on feed and draw solutions loops was done. The results proved that water flux is not linked to any change in crossflow velocity within the range tested. When FS faces the active layer, the dilution of DS in support layer increases the ICP. Therefore, enhanced water flux was achieved when DS was put on the active layer side. Minier-Mater et al. suggested the pretreatment for the challenging and high TOC content PPW with powdered activated carbon (PAC) exhibiting maximum TOC removal compared to examined organosilica adsorbent and ceramic membrane filtration.

2.6.2.5. System performance with HF and FSH membranes for volume reduction

With TFC-FSH FO membrane, the study succeeded in proving FO capability of attaining 50% PPW volume reduction at flux of 12 LMH when 70 g/L NaCl solution was utilized as DS with its concentration was maintained constant to perform similarly to a brine from thermal desalination plants [202]. Long-term stability experiments were achieved with TFC-HF membrane after proving its improved performance while obtaining a flux of 18 LMH compared to 13 LMH obtained by TFC-FSH at the same set of operating conditions [199]. The long-term experiments were performed for 80 hours of continuous operation with PPW blend feed and collected brine from thermal desalination plants at 40 °C as DS. The crossflow velocity of FS and DS were maintained at 40 and 80 cm/s respectively. The experiments were effective in accomplishing 50% reduction in the initial 42 L of PPW and 50% dilution of brine concentration from the initial 21 L. Besides, for higher than 50% reduction in osmotic pressure across the membrane sides, the flux decline throughout the whole duration was estimated by 30%. Overall, results clarified that TFC-HF possesses

high tendency for contaminants rejection with highest flow of sodium and chloride. Although nitrogen was observed to be existent in DS after transfer from FS, the detected concentration was below the Qatari discharge limits of diluted brine.

With reference to the presented OC projects in literature, the technology is still being under investigation where not many projects are implemented. Currently, the status of OC implementation is still at bench-scale testing and no pilot-scale project is demonstrated for the volume reduction application. In addition, the literature lacks studies showing the economic situation of the novel FO technology over the widespread RO process. Apparently, there is no presented technoeconomic analysis that has been performed for the whole-life costs of FO-based process for the wastewater reclamation.

Chapter 3 : Methodology

3.1. Technoeconomic analysis materials and methods

The economic feasibility of FO for wastewater treatment/reclamation is demonstrated through life cycle cost analysis (LCCA) where the net present value (NPV) indicating the cash inflow and outflow difference at the present value over the project lifespan is determined. NPV is estimated from the capital expenditure (CAPEX) and operating expenditure (OPEX) contributions. The OPEX arises primarily from the specific energy demand (SED) in $kWh.m^{-3}$ and critical component life.

The treatment options depicted in (*Figure 3-1*) are considered, namely:

1. Classical treatment by membrane bioreactor technology followed by reverse osmosis (MBR-RO) (*Figure 3-1*,a);
2. Novel treatment by an open-loop MBR-FO (*Figure 3-1*,b);

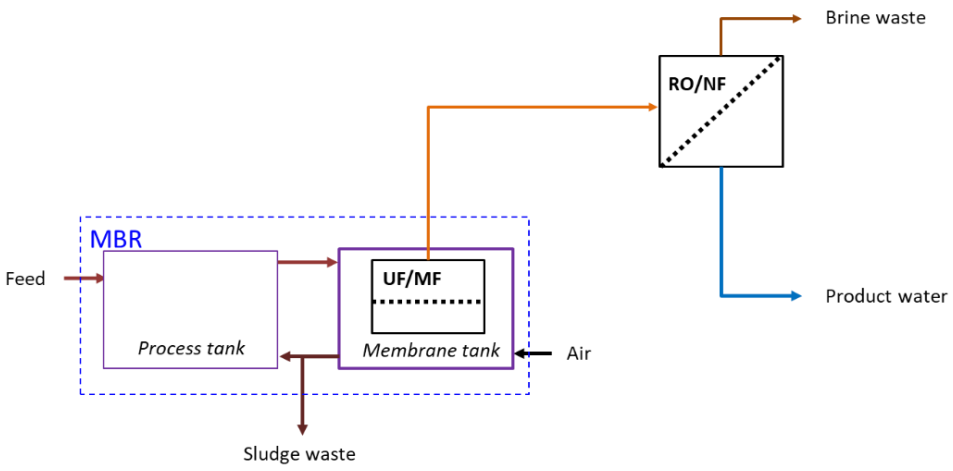

(a)

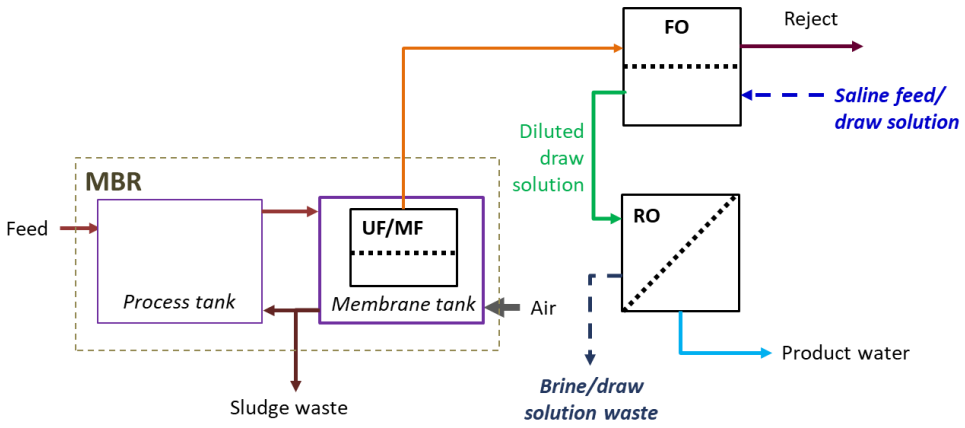

(b)

Figure 3-1: Process alternatives for wastewater reclamation: (a) classical MBR-RO and (b) open-loop MBR-FO.

The empirical analysis proceeded by using published cost and O&M data from existing full-scale MBR and RO installations, these then being used to infer the cost of a full-scale FO installations. An analysis was presented of the costs incurred by wastewater purification and seawater desalination combined treatment objective. Calculation of the normalised net present value (NPV/permeate flow) performed through developing a series of empirical equations based on available individual capital and operating cost data. Cost curves (cost vs. flow capacity) were generated for each option using literature MBR and RO data and making appropriate assumptions regarding the design and operation of the novel FO technology.

3.1.1. Information and data source

The analysis captured or made use of:

a) published CAPEX data and data trends (specifically cost as function of flow rate, or "cost curves") from existing installations,
b) classical analytical expressions for (i) aeration and pumping energy demand, and (ii) process biological aeration for the MBR, and
c) proprietary CAD software for the determination of energy demand and chemicals consumption for both the RO and FO technologies.

A feed water composition typical for medium-strength municipal wastewater [206] was selected, supplemented with elevated hardness, alkalinity and salinity levels (*Table 3-1*). The impact of salinity on RO energy demand was determined over a 20-7500 mg/L sodium concentration range, balancing with chloride. Process biology energy demand was calculated based on classical biochemical stoichiometry [146,206] for absolute COD and TKN removals of 500 and 40 mg/L respectively. Labor and waste disposal costs were both ignored: it was assumed that no significant differences in staffing levels existed between the two options, and that waste disposal costs were also similar.

Table 3-1: Feed water quality.

Parameter	Concentration, mg/L
Total dissolved solids	500-5000
Chemical oxygen demand removed (ΔCOD)	500-2500

Table 3-1: Feed water quality.

Parameter	Concentration, mg/L
Total Kjeldal nitrogen removed (ΔTKN)	40
Nitrate	0
Hardness (as $CaCO_3$)	180
Alkalinity (as $CaCO_3$)	150

3.1.2. Assumptions

Calculations proceeded through determining CAPEX as a function of flow capacity for all three technologies (MBR, RO and FO) using the data trends of Loutatidou et al. [207] for seawater (SW) and brackish water (BW) RO desalination plants. OPEX was calculated as a function of the membrane flux and the TDS and COD concentrations for the RO and MBR respectively. In the absence of available CAPEX data for the FO technology, a number of key assumptions were made in adapting the available RO and MBR data:

A. SWRO and BWRO installations were assumed to operate respectively above and below a threshold pressure of 15 bar. This threshold pressure was used to differentiate the BWRO and SWRO CAPEX curve data sets provided by Loutatidou et al. [207].
B. FO CAPEX was equated to that of a BWRO with FO membrane elements replacing the RO ones, the membrane area being adjusted according to the design flux. The FO plant CAPEX was then determined as:

$$L_{C,FO} = L_{C,BWRO} - L_{M,RO}A_{RO} + L_{M,FO}A_{FO} \quad (3\text{-}1)$$

Where A refers to installation membrane area, given by the ratio of the permeate flow (Qp) to the flux(J), and L_M is the membrane cost per unit area.

C. The SED of FO was equated to that of the equivalent BWRO array operating at zero osmotic pressure and a reduced flux appropriate to the FO. This corresponds to the energy associated with pumping through the membrane channels and pipework, as determined from the RO CAD software (Section 3.1.4.2).

D. The MBR step was assumed to provide sufficient pre-treatment for sustainable operation of the FO at the stipulated net flux for the MBR-FO option.

A CAPEX benefit of FO over RO associated with the lower-pressure operation thus exists at feed pressures above ~15 bar, since below this threshold the same low-pressure materials (e.g. fibre-reinforced plastic) and equipment can be used for both technologies. Above this threshold higher-grade materials (e.g. 316L stainless steel) must be used for RO, whereas the FO technology - always operating at low pressure - can always employ the less expensive materials. Below the threshold the CAPEX difference between RO and FO installations relates only to the difference in the total cost of the membrane modules.

The MBR-FO-RO scheme yields an energy benefit associated with dilution of the RO saline feed by the FO (*Figure 3-1*,b), translating to a proportional OPEX benefit (ΔOPEX = f(*C*)). However, this benefit is only obtained by increasing the capacity of the RO desalination step, which incurs a CAPEX penalty (ΔCAPEX = f(*Q*)). Both of these cost components can be normalised against the permeate volume generated over the plant life as part of the NPV determination.

The MBR technology have a process biological operational limit imposed by the feed water salinity; biological activity is adversely affected by high salinities. The analysis was based on a recovery of 95% for the MBR. An immersed MBR configuration was assumed throughout. A recent study [208] has indicated the immersed configuration (iMBR) to be economically favored at flow capacities above 7,000 $m^3.d^{-1}$.

Historical CAPEX data [207] suggests that the CAPEX of RO installations decreased between the years 2000 and 2012. This trend was extrapolated to 2019 to obtain the 2019 CAPEX figures for the RO and FO plants. The change in value of money over time was taken into account through introducing the discount factor. The subsequent NPV calculations nonetheless assumed a discount factor (**D)** of 2%, and were based on the approach of Verrecht et al. [209].

3.1.3. MBR costs

3.1.3.1. CAPEX

Published MBR CAPEX information includes cost curves interpreted from data provided by Itokawa et al. [210] and Iglesias et al. [211] for Japanese and Spanish full-scale installations respectively, and costs determined from the commercial software *CAPDETWorks* [212]. The Japanese and Spanish research studies evaluated MBR as a cost competitive alternative for medium to large plants of capacity reaching 15,000 $m^3.d^{-1}$. Additionally, CAPEX values at specific flow capacities have been provided by several authors [213–217]. All captured data was normalised against permeate flow rate (Q_p) to give the specific CAPEX (L_C) in k\$ $.m^3.d^{-1}$.

3.1.3.2. OPEX

MBR OPEX was determined through:

(a) capture of data relating to design and operation of a representative iMBRs treating municipal wastewater, including membrane module costs, chemical usage and costs, and membrane life (*Table 3-2*), and

(b) calculation of the SED in kWh per m^3 permeate from known analytical equations (*Table 3-3*). The biological process was assumed to follow the Modified Ludzack-Ettinger (MLE) process configuration for wastewater denitrification.

In MBR, part of the consumed energy is due to the shear application that is used for air scouring of immersed membrane [218]. In case of air scouring, the energy is described by a parameter called specific aeration demand (SAD) in $Nm^3.m^2.h^{-1}$.

Table 3-2: MBR operational process parameters base values.

Parameter	Symbol	Value(s): Base, range
Oxygen content of air, %	C'_A	21%
Mass consumption of oxygen, $g.m^{-3}$	D_{O2}	Calculated
SED, biological aeration, $kWh.m^{-3}$	$E_{A,bio}$	Calculated
SED, membrane aeration (air), $kWh.Nm^{-3}$	$E^{a}_{A,m}$	Calculated

Table 3-2: MBR operational process parameters base values.

Parameter	Symbol	Value(s): Base, range
SED, membrane aeration (permeate), kWh.m^{-3}	$E^{b}_{A,m}$	Calculated
SED, membrane permeation, kWh.m^{-3}	$E^{c}_{L,m}$	0.008
SED, sludge pumping, kWh.m^{-3}	$E^{d}_{L,sludge}$	0.016.R
Depth of aerator in tank, m	h	5
Specific capital cost, k$/(m^3.h^{-1})	L_C	Calculated
Permeate net flux, L.m^{-2}.h^{-1}	J_{MBR}	15[f]-22
Chemicals consumption costs, $.m^{-3} permeate	$L_{Chem,MBR}$	0.01[g]
Electricity supply cost, $.kWh^{-1}	L_E	0.1
Membrane cost, $.m^{-2} membrane area	$L_{M,MBR}$	30
Operating cost, $.m^{-3} permeate	L_O	Calculated
Oxygen transfer efficiency per unit depth, m^{-1}	OTE	0.045
Permeate flow rate, m^3.h^{-1}	Q_P	Variable
Membrane-biological process tank recycle ratio	R	5
SAD, membrane scouring, Nm^3.m^{-2}.h^{-1}	SAD^{e}_{m}	0.35

Table 3-2: MBR operational process parameters base values.

Parameter	Symbol	Value(s): Base, range
Change in COD, TKN, NO_3^- conc., $g.m^{-3}$	ΔS_{COD}, ΔS_{TKN} $\Delta S_{Nitrate}$	500, 40, 0
Membrane life, hrs	t_{MBR}	70080
MLSS conc., process, membrane tanks, $kg.m^{-3}$	X, X_m	8, 10
Observed sludge yield, $kgSS.kgCOD^{-1}$	Y_{obs}	0.35
Mass transfer correction factors	β, γ	0.95, 0.89
Biomass COD, TKN content, $kg.kgSS^{-1}$	λ_{COD}, λ_{TKN}	1.1, 0.095
Total pumping electrical energy efficiency	ε_{tot}	65%
Air density, $g.m^{-3}$	ρ_A	1.23
Conversion (permeate/feed flow)	Θ_{MBR}	95%

SAD Specific aeration demand; SED specific energy demand; [a] Blower power/air flow rate; [b] Blower power/permeate flow rate; [c] Pump power/permeate flow rate; [d] Pump power/sludge flow rate; [e] Air flow rate/membrane area for air scour; [f] Lower limit at high TDS, upper limit at low TDS; [g] Based on sodium hypochlorite and citric acid costs and usage [146] . Calculation of parameters is as indicated in Table 3-3.

The baseline net flux (J), air-scour specific aeration demand (SAD_m, $Nm^3.h^{-1}$ air flow per m^2 membrane area), and permeation energy ($E_{L,m}$, kWh per m^3) values were based on that typical of installed full-scale iMBRs [218]. The omission of labor costs means that OPEX is not a significant function of flow capacity [208].

Table 3-3: MBR OPEX- related equations (adapted from ([146,208,219])).

Parameter	Symbol	Equation
Membrane		
SED, $kWh.m^{-3}$	E_m	$1000\ E'_{A,m}\frac{SAD_m}{J} + E_{L,sludge}R + E_{L,m}$
Process biology (assuming MLE process denitrification)		
Oxygen demand, $kg.m^{-3}$	D_{O_2}	$\Delta S_{COD}\ (1 - \lambda_{COD}\ Y_{obs} - 1.71\lambda_{TKN}Y_{obs}\ )$ $+ 1.71\Delta S_{TKN} - 2.86\Delta S_{Nitrate}$
SAD, $Nm^3.m^{-2}.h^{-1}$	SAD^a_{bio}	$\frac{D_{O_2}}{\rho_A C'_A\ SOTE\ \alpha\beta\gamma} = \frac{Q_{A,bio}}{Q_F}$
α factor	α	$e^{-0.084\ X}$
SED, aeration, $kWh.Nm^{-3}$	E'_A	$\frac{k((0.0943h + 1)^{0.283} - 1)}{\varepsilon_{tot}}$
SED, permeate, $kWh.m^{-3}$	$E_{A,bio}$	$E'_{A,m}\ SAD_{bio}$
OPEX		
Cost m^{-3} permeate, $\$.m^{-3}$	$L_{O,MBR}$	$L_E(E_m + E_{A,bio}) + \frac{L_M}{J_t} + L_C + L_W$

3.1.4. RO and FO costs

3.1.4.1. CAPEX

RO CAPEX data was extracted from the comprehensive data set provided for installed, full-scale brackish and seawater RO desalination plants [207]. This data set refers to CAPEX trends based on Engineering, Procurement & Construction (EPC) contracts for RO installations in the GCC and Southern European geographical regions. In the research of Loutatidou et al. [207] and after the assessment of parameters influencing the CAPEX such as plant capacity, type, region and year; it was found that EPC costs are most affected by the plant capacity. It was assumed that the civil engineering (CE) cost component included in the MBR cost data applied to the complete installation, i.e. that no supplementary CE cost was required for either the RO or FO components.

3.1.4.2. OPEX

RO OPEX was calculated using the proprietary RO CAD design tool *ROPRO* (Koch Membrane Systems, Wilmington, MA) to estimate the SED and the pH-adjustment chemical (sulfuric acid) consumption rate for a commercial BW or SW membrane (*8822HR400* and *8822XR400*, Koch Membrane Systems, Wilmington, MA) based on a two-stage 2:1 RO array (i.e. yielding a conversion of 75%). The required acid dose was determined based on a Langelier Saturation Index (LSI) of 0-0.01 for the pretreated water. Required doses and costs of other specialist RO chemicals per each 1 m^3 of desalinated water through SWRO plants were estimated from suppliers' information and published literature data [128,135,220]. The cost comprises the consumed antiscalants and chemicals for the purpose of scale removal and membrane cleaning such as: sodium hypochlorite, sodium metabisulphite, caustic soda, citric and sulfuric acid [220]. FO OPEX was

estimated using the same *ROPRO* design tool, based on the lower design flux low-pressure operation (*Table 3-4*), the FO flux estimated from reported pilot-scale studies [5]. The overall specific OPEX ($L_{O,RO}$) is then analogous to that of an MBR but without the process biological energy component ($E_{A,bio}$).

Table 3-4: RO and FO operational process parameters base values.

Parameter	Symbol	Units	RO	FO
Permeate net flux, $L.m^{-2}.h^{-1}$	J_{RO}, J_{FO}	LMH	20	6
Process conversion	Θ_{RO}, Θ_{FO}	-	75%	75%
Membrane life, y	t_{RO}, t_{FO}	hrs	43800	70080
Membrane cost	$L_{M,RO}$, $L_{M,FO}$	$\$.m^{-2}$	13	50
Sulphuric acid cost (98% stock)	$LAcid_{Acid}$	$\$.t\ acid^{-2}$	270	
Antiscalants dose costs	$L_{Antiscalant}$	$\$.m^3$ permeate	0.011	
Target Langelier Scaling Index value	LSI	-	0-0.01	

3.2. Osmotic concentration process materials

3.2.1. Pilot-scale FO osmotic concentration unit

Pilot-scale FO based osmotic concentration system was constructed for the purpose of the oil/gas field produced and process water volume reduction. The schematic flow diagram is illustrated in *Figure 3-2* and the associated utilization of accessories is summarized in *Table 3-5*. The real constructed pilot system is shown in Figure *3-3* where four tanks with capacity of $5m^3$ were used for storing the feed solution, draw solution, concentrated feed and diluted draw solutions. The level of water inside the tanks was controlled by installing pressure transmitters (Omega, UK). Two diaphragm pumps (Model KNF Liquiport, Sterlitech, Switzerland) of variable speed were connected to the feed and draw solution tanks for supplying the solutions into the membrane and hence produces the crossflow velocity (Figure *3-3*). Thereafter, the pumped solutions were filtered in two cartridge filters (ATLAS FILTRI, Switzerland) before entering the membrane to prevent the membrane fouling in case of solid traces existence. The main objective of the unit is to investigate the performance of two hollow fiber (HF) FO membranes. Additionally, the plant was ensuring on-line monitoring of flow, pressure and temperature with positioned flowmeters and sensors (Omega, UK). Digital conductivity meters (Model Orion VersaStar Pro, by Thermo Fisher Scientific, US) were used to measure the salinity of the two inlet streams (FS and DS) and the two outlet streams (concentrated FS and diluted DS). The pilot plant encompasses a control panel for all wiring and electrical connections. The system operates automatically after complete programming work done using LabVIEW software (National Instrument, US). The LabVIEW interface screen for operating the system is shown in *Figure 3-4*. The interface allows the surveillance of pressure, temperature, flow and

conductivity along with controlling the inlet FS and DS flowrates. Besides, the system is programed to record the measured conductivity, temperature, pressure, tank levels, streams flowrates and flux every 30 seconds during the operation. The recorded data can be saved and exported into Excel file for analysis. Lastly, the program considers operational safety by setting alarms to detect potential hazards such as high pressure in pipes, high water level in tanks or any leak. Whenever one of the mentioned parameter deviates from the allowable limit, the pilot-system is automatically switched off.

Table 3-5: Osmotic concentration pilot -unit equipment.

Description	Specifications	Manufacturer
Feed pump	KNF Diaphragm pump - Liquiport - 0.5 to 3 l/min - Remote Control - PP/PTFE/FFPM - 90 PSI (3/8" NPT)	Sterlitech
Draw solution pump	KNF Diaphragm pump - Liquiport - 0.2 to 1.3 l/min - Remote Control - PP/PTFE/FFPM - 90 PSI (3/8" NPT)	Sterlitech
Pulsation dampener	KNF pulsation dampener -NF1.300 - Polypropelene, FFPM (069276/152350) - 3/8 FNPT	Sterlitech
Pump, transfer, feed offloading	Transfer pump, portable, nominal 40 L/m at 5 m head; corrosion resistant	Tyco
Temperature transmitter	RTD 1/4" MNPT, 1/2" NOSE, 72" leads, SST braided	Omega
Pressure transmitter	Pressure transmitter, 0-15 PSIG, 1/4"MNPT; output: 4-20MA, input: 9-30VDC, 1.5M CABLE, IP65	Omega
Level transmitter (pressure)	Pressure transmitter, 0-5 PSIG, 1/4"MNPT; output: 4-20MA, input: 9-30VDC, 5M CABLE, IP65	Omega

Table 3-5: Osmotic concentration pilot -unit equipment.

Description	Specifications	Manufacturer
Flow transmitter	PTFE Liquid Flow Sensor, 0.5-5.0 L/min	Omega
Flow transmitter	PTFE Liquid Flow Sensor, 0.2-2.0 L/min	Omega
Conductivity Meter	Orion Versa Star Pro (VSTAR20) benchtop meter with conductivity/TDS/salinity/resistivity module and stand	Thermo Scientific
Cable for conductivity meter	Thermo Scientific Orion Star Series RS232 Printer Computer Cable	Thermo Scientific
Conductivity Probe	Thermo Scientific™ Orion™ DuraProbe™ 4-Electrode Conductivity Cells - 013605MD - 10 m cable	Thermo Scientific
12 VDC power supply (for 4 flowmeters)	230VAC TO 12VDC EUROPEAN PLUG, 4A	Local Supply
Filter	Housing with replaceable filter, 5 micron, connections TBD based on availability on local market	Local Supply
Cartridges for filters	Based on availability on local market	Local Supply

Table 3-5: Osmotic concentration pilot -unit equipment.

Description	Specifications	Manufacturer
Isolation valve	316 Stainless Steel Quarter Turn Instrument Plug Valve, 3/8 in. Swagelok Tube Fitting, 6.4 Cv	Swagelok
Tank drain valve	1.5" or 2", corrosion resistant, design pending	Local Supply
Membrane module	Membrane module with 3/8" Tube connectors.	TOYOBO and NTU
Tubing	PFA tubing, 3/8" OD x 0.062 in. wall x 100'; Qty 1 refers to 100'of tubing in a box; priced per box	Swagelok
Adaptor	Adaptor, 3/8" OD tube to 3/8" MNPT, straight, PFA	Swagelok
Adapter, pump	Reducer, 3/8" OD tube to 3/8" MNPT, straight, PFA	Swagelok
Reducer, pump	PFA Swagelok Tube Fitting, Male Connector, 1/4 in. Tube Fitting x 1/8 in. Male NPT	Swagelok
Adapter, pump	Reducer, 3/8" OD tube to 3/8" OD Tube straight, PFA	Swagelok

Table 3-5: Osmotic concentration pilot -unit equipment.

Description	Specifications	Manufacturer
Control system connection cable	8 core 7/0.2 + drain screened cable with PVC insulation, 30 m reel	Omega
Controller	cRIO-9035 Compact RIO Controller, 1.33 GHz Dual-Core, 8-Slot, Kintex-7 70T FPGA, -20 °C to 55 °C	National Instruments
	DIN Rail Mounting Kit for 8-Slot NI cRIO-903x and NI cDAQ-9133/35	National Instruments
	NI PS-16 Power Supply, 24 VDC, 10 A, 100-120/200-240 VAC Input	National Instruments
	Panel Mounting Kit for NI PS-14/15/16/17	National Instruments
	Desktop Power Supply (12 VDC, 3.33 A, 90-240 VAC)	National Instruments

Table 3-5: Osmotic concentration pilot -unit equipment.

Description	Specifications	Manufacturer
Pressure and level transmitter	NI 9208, 24-bit current input module with D-Sub 16-ch	National Instruments
	NI 9923 Front-mount terminal block for 37-pin D-Sub Modules	National Instruments
Flow meter	NI 9201 Spring Term, +/-10 V, 12-Bit, 500 kS/s, 8-Ch AI Module	National Instruments
	NI 9981, Strain Relief and Operator Protection (qty 1)	National Instruments
Temperature input	NI 9216 Spring, 8-Ch RTD, PT100, 24-bit, 50S/s/ch AI module	National Instruments

Table 3-5: Osmotic concentration pilot -unit equipment.

Description	Specifications	Manufacturer
Pump flow control	NI 9269 4ch voltage output, ±10V, ch-ch ISO	National Instruments
	NI 9971 Backshell for 2-pos connector block (qty 4)	National Instruments
Pump startup/shutdown	NI 9481 4-Ch 30 V, 60 V, 250 VAC EM Form A SPST Relay	National Instruments
	NI 9927, Strain Relief and Operator Protection(Qty 1)	National Instruments
Conductivity meter input	NI 9870 4-Port RS232 Serial Module W/ 4 10P10C-DE9 Cables	National Instruments

Table 3-5: Osmotic concentration pilot -unit equipment.

Description	Specifications	Manufacturer
LabVIEW software	LabVIEW Full Development System, English. Includes Standard Service for Software., Include 1 Year SSP	National Instruments
	LabVIEW Real-Time Module., Include 1 Year SSP	National Instruments
	LabVIEW FPGA Module., Include 1 Year SSP	National Instruments

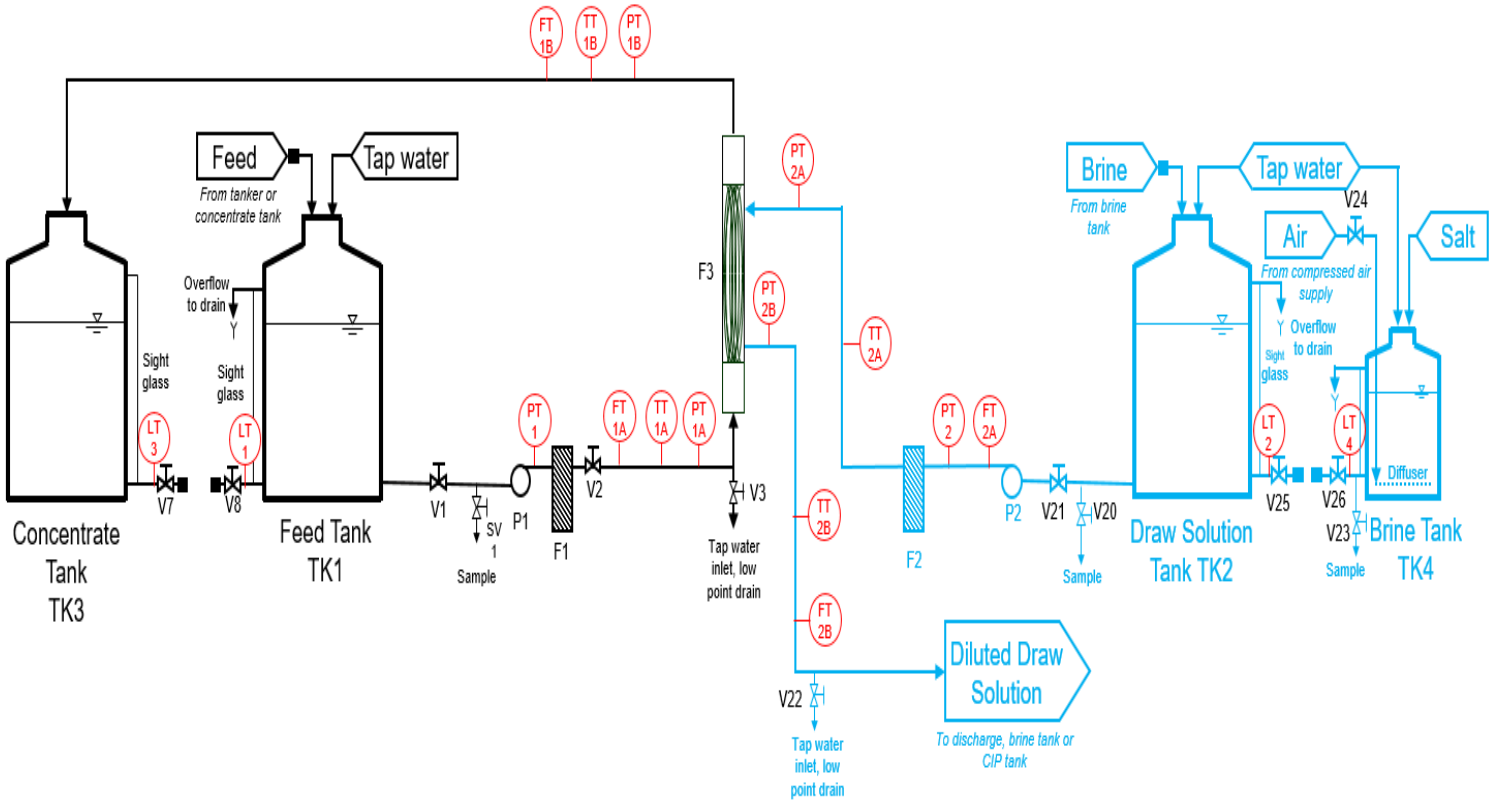

Figure 3-2: Schematic flow diagram of the pilot-scale osmotic concentration unit.

(a) (b)

Figure 3-3: Overall Osmotic concentration unit: (a) Overall view of the pilot unit (b) top view of the membrane and pipe connections.

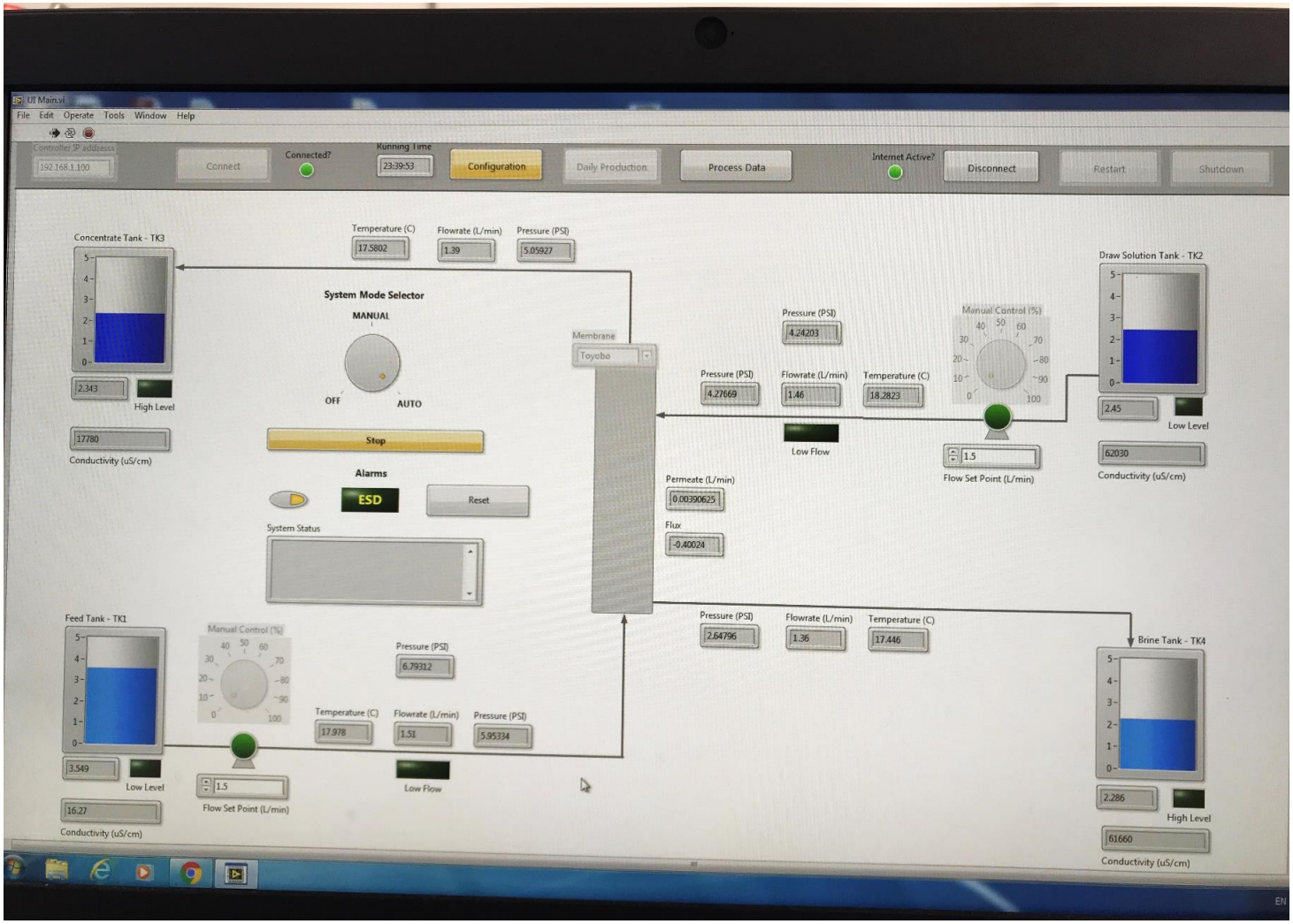

Figure 3-4: LabVIEW interface screenshot for pilot-plant monitoring.

3.2.2. Membranes

3.2.2.1. TOYOBO membrane

TOYOBO membrane is commercial scale hollow fiber (HF) FO membrane manufactured by TOYOBO, Japan. The membrane model is HPC3205 and is produced from the cellulose triacetate (CTA) to offer an enhanced tolerance to chlorine, high efficiency and lower osmotic pressure loss. The tremendous number of fibers placed in the pressure vessel increases the surface area of the membrane and leads to superior performance. The specifications of the membrane are illustrated in *Table 3-6*.

Table 3-6: TOYOBO membrane specifications.

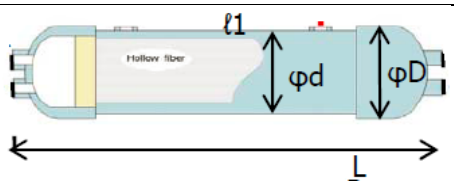

Membrane	Membrane Type	Hollow fiber
	OD of hollow fiber	175 µm
	ID of hollow fiber	85 µm
	Membrane Surface Area	31.5 m^2

Table 3-6: TOYOBO membrane specifications.

	Vessel material	polyvinyl chloride (PVC)
Module	Dimension Φ D, L	103 mm,830 mm
	Φ d, ℓ1	90 mm, 480 mm
Operating	Pressure	Shell side <0.49 MPa, Bore side < 0.2
Conditions		MPa
	Temperature	5-40 °C
	pH	3-8
	Residual Chlorine	≤ 1 mg.L^{-1}

3.2.2.2. NTU membrane

NTU membrane is also hollow fiber (HF) FO membrane manufactured by Singapore membrane technology center (SMTC) under the Nanyang Technological University (NTU). The membrane is made of polyethersulfone substrate with polyamide selective layer. The active layer is at the lumen of hollow fiber where it should face the feed water and the draw solution is pumped towards the shell side. The specifications of the membrane are demonstrated in *Table 3-7*.

Table 3-7: NTU membrane specifications.

	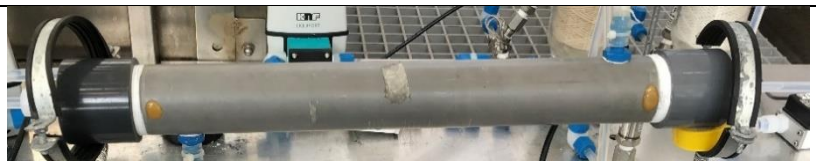	
Membrane	Membrane Surface Area	0.5 m^2
	Dimension OD	1.00 mm
	ID	0.67 mm
Operating	Recommended FS and DS flowrates	1.5 $L.min^{-1}$
Conditions	Pressure of FS (inside-out) (FS is facing inside of fiber)	3 Bar
	Pressure of DS (DS is facing outside of fiber, towards the shell side)	1 Bar
	Temperature	5-50 °C

3.2.3. Feed and draw solutions preparations

3.2.3.1. Sodium chloride salt

For the preparation of synthetic FS and DS, the industrial-grade sodium chloride (NaCl) salt was obtained from Essential Systems & Services (ESS-Middle East) after testing a variety of commercial salts available in the Qatari local market. The salt is manufactured by Concord Overseas in India and the brand is named by ECO pure salt tablets. The chosen salt is of 99.62% NaCl purity received in pellets shape with 20 mm diameter and 10 mm thickness (see *Table 3-8*, *Figure 3-5*), more information is summarized in *Table 3-8*.

Table 3-8: Industrial-grade sodium chloride salt specifications and composition.

Physical Analysis of Salt	
Appearance	White pellets
Whiteness Index (with $BaSO_4$)	94
Chemical Analysis of Salt	
Calcium as Ca	0.019 %
Magnesium as Mg	0.018 %
Sulphate as SO_4	0.015 %
Sodium chloride as NaCl	99.62 %
Moisture	0.189 %
Water Insoluble	0.020 %

Figure 3-5: NaCl salt pellets used for solutions preparation.

3.2.3.2. Feed solution (FS)

The feed solution was synthetically prepared from industrial-grade NaCl salt dissolution in tap water. The tap water was filtered using triple filtration stages filter with one activated carbon and two polypropylene cartridges of 5 microns size (ATLAS FILTRI, Switzerland) (*Figure 3-6*). The main aim of passing the tap water to the activated carbon cartridge is to assure the removal of chlorine, whereas the two remaining cartridges remove all traces of suspended solids from the tap water. The chlorine in filtered tap water was 0.04 $mg.L^{-1}$ measured using the chlorine kit (HACH, US) (*Figure 3-7*) and maintained to be lower than the tolerated level by membrane module. The prepared feed water salinity is 2000 $mg.L^{-1}$ to mimic real produced and process water (PPW) blended stream. The targeted produced and process water stream is a blend with ratio of 1:5 from the Qatari oil and gas industries after treatment with membrane bioreactor (MBR).

Figure 3-6: Triple filtration stage for tap water by ATLAS FILTRI.

Figure 3-7: Chlorine test kit by HACH.

3.2.3.3. Draw solution (DS)

The draw solution is prepared by dissolving the same industrial-grade NaCl salt in the tap water filtered similarly as in feed solution preparation by (ATLAS FILTRI). The DS concentration is made of 40000 $mg.L^{-1}$ salinity to be comparable with the gulf seawater salinity.

3.3. Experimental methods

All sets of experiments with each membrane were duplicated to check how successful the system is in giving reproducible data. Therefore, experimental outcomes were reproducible with less than 5% error (i.e. difference between the duplicated experiments).

3.3.1. FS and DS characterization experiments

3.3.1.1. Total suspended solids (TSS) and total dissolved solids (TDS).

Total suspended solids (TSS) and total dissolved solids (TDS) were measured by conventional filtration of FS and DS samples. TSS indicates the weight of the dry suspended solids that are not dissolved in water and can be trapped on filter paper surface after the filtration process. While, TDS is the dry weight of the small size solids that succeed in penetrating the filter paper pores. Despite the expected TDS in FS and DS as the solutions were prepared for specific concentration (mentioned in section 3.2.3), TDS test was done to assure that prepared solutions are of same required concentration.

The tests were initially performed by drying two small beakers and two filter papers for both solutions in the oven (Model: Dry Line, by VWR, US) at temperature of 105 °C for 2 hours (*Figure 3-8*). The utilized filter papers are glass fiber filters of grade GF 92 and 47 mm diameter (Whatman, GE Healthcare Life Sciences, US). The weight of dry filter papers and beakers were recorded using an analytical balance (ISOLAB Laborgeräte GmbH, Germany) (*Figure 3-9*).

Figure 3-8: VWR Dry-Line oven.

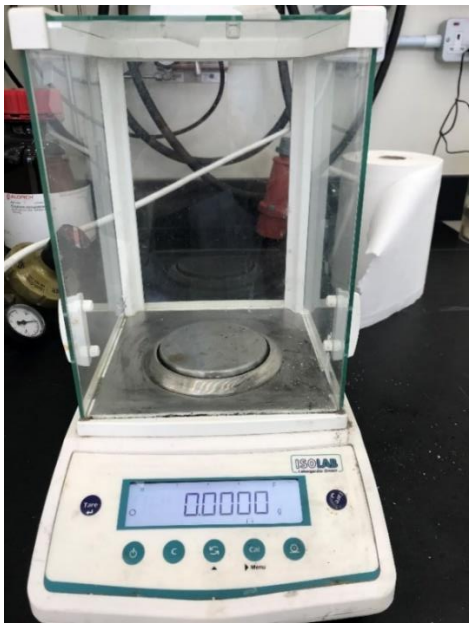

Figure 3-9: ISOLAB analytical balance.

Following that, 1 L of each solution was filtered as shown in the filtration apparatus setup (Fisherbrand, by Fisher Scientific, US) (*Figure 3-10*). The wet filter papers with trapped

solids were taken to the same oven again and kept inside it for two hours at 105 °C for drying them. Besides, around 40 ml of filtrate solutions were poured into the dried beakers and dried at 180 °C.

Figure 3-10: Fisherbrand filtration setup.

Finally, the weight difference between the initial dry filter paper and the dry filter paper after filtration provides the amount of total suspended solids collected on filter paper surface as per Eq. (3-2). In addition, the weight difference of dry beaker before and after filtration indicated the weight of total dissolved solids (Eq. (3-3)).

$$TSS = \frac{Weight\ difference\ of\ dry\ filter\ paper\ before\ and\ after\ filtration}{1\ L\ of\ solution} \quad (3\text{-}2)$$

$$TDS = \frac{Weight\ difference\ of\ dry\ beaker\ before\ and\ after\ filtration}{40\ mL\ of\ filtrate\ solution} \qquad (3\text{-}3)$$

3.3.1.2. Total organic carbon (TOC) and inorganic carbon (IC).

Total organic carbon (TOC) and inorganic carbon (IC) were measured in TOC-L analyzer shown (SHIMADZU, Japan) shown in *Figure 3-11*. The equipment involves catalytic oxidation and acidification of the sample to release CO_2 that can be detected and displayed in units of carbon mass per volume of the sample ($mg.L^{-1}$). The TOC is estimated by subtracting the total carbon detected by CO_2 released from the catalytic oxidation from the inorganic carbon detected by CO_2 released from the acidification reaction.

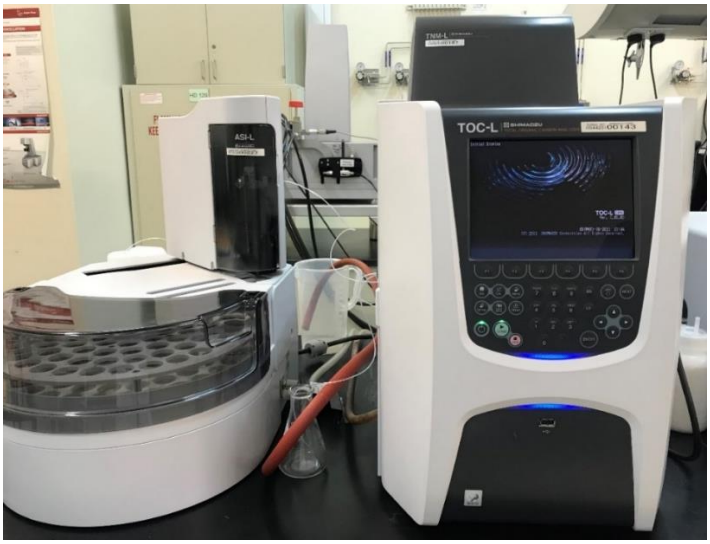

Figure 3-11: SHIMADZU TOC analyzer.

3.3.1.3. Turbidity, conductivity and pH.

The turbidity measurement helped in recognizing the clarity of the solutions and suspended traces contained in FS and DS. The turbidity measured in Nephelometric Turbidity Units

(NTU) was found using HACH 2100N Turbidimeter (*Figure 3-12*). Furthermore, the conductivity and pH were measured by immersing the probes of presented Orion VersaStar Pro conductivity meter (Thermo Fisher Scientific, US) and HQ11d pH meter (HACH, US) in (Figure *3-13*) inside both solutions.

Figure 3-12: Turbidimeter apparatus.

(a) (b)

Figure 3-13: (a) HACH pH meter, (b) Thermo Fisher Scientific Conductivity meter.

3.3.2. Experiments for achieving different feed recovery rates

The objective of these experiments is to investigate the pilot system capability to recover various rates of initial feed water. The pilot system was tested using the two different HF FO membranes (TOYOBO and NTU) described earlier in section 4.1.2. The experiments were conducted for 60%, 68%, 75% and 90% feed recovery and constant 75% dilution of DS at an operational temperature of 27 °C according to the laboratory surrounding conditions.

3.3.2.1. Experiments using TOYOBO membrane

The experiments started by exposing the membrane into countercurrent flow of feed and draw solutions. The membrane is positioned horizontally with applying the feed solution to the shell side outside the hollow fiber and the draw solution to the bore side inside the hollow fiber (outside-in configuration) as in *Figure 3-14*. Through TOYOBO operation, FS and DS are both in once-through mode where concentrated FS outlet and diluted DS outlet are sent into separate storage tanks.

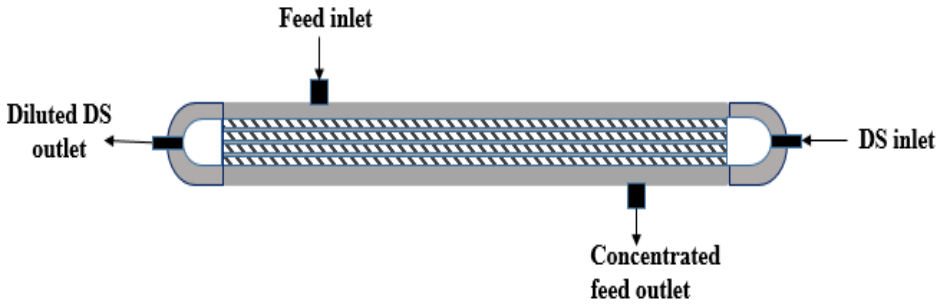

Figure 3-14: Outside-in configuration for TOYOBO membrane.

The key aim of the pilot testing is to investigate the capability of achieving several percentages of feed recovery. Various experiments were accomplished for achieving four feed recovery rates of 60%, 68%, 75% and 90%. Using TOYOBO membrane, each intended feed recovery was obtained by the manipulation in the flowrates of both feed and draw solutions from the 5 m^3 tanks and allowing the pilot system to run for several hours. The feed recovery rate percentage at each adjusted FS flowrate is calculated based on Eq. (3-4) and the DS dilution is calculated from DS flowrate according to Eq. (3-5). After several trials and manipulation in flowrates to achieve required recovery percentages, the outcomes of required flowrates at each recovery will be presented in chapter 5.

$$FR\ \% = \frac{Q_{F_{in}} - Q_{F_{out}}}{Q_{F_{in}}} \times 100 \quad (3\text{-}4)$$

$$DS\ Dilution\% = \frac{Q_{DS_{in}}}{Q_{DS_{out}}} \times 100 \quad (3\text{-}5)$$

where FR% is the feed recovery percentage, $Q_{F_{in}}$ and $Q_{F_{out}}$ are the volumetric flowrate of feed water inlet and outlet streams respectively. $Q_{DS_{in}}$ and $Q_{DS_{out}}$ are the flowrates of the inlet and outlet DS streams.

The water flux ($L.m^{-2}.h^{-1}$ or LMH) is calculated based on the flow difference between inlet feed water and outlet concentrated feed water over the membrane area. The change in FS and DS flowrates was translated into average flux value (Eq. (3-6) & (3-7)):

$$J_{W,FS} = \frac{Q_{F_{in}} - Q_{F_{out}}}{A_m} \quad (3\text{-}6)$$

$$J_{w,DS} = \frac{Q_{DS_{out}} - Q_{DS_{in}}}{A_m} \quad (3\text{-}7)$$

where $J_{W,FS}$ and $J_{w,DS}$ are the FS water flux and DS water flux respectively. $Q_{F_{in}} - Q_{F_{out}}$ is the change in inlet and outlet feed flowrates, $Q_{DS_{out}} - Q_{DS_{in}}$ is the change in inlet and outlet DS flowrates and A_m is the membrane area.

In addition, reverse solute flux (RSF) resulted from the diffusion of DS solutes to the feed side is another parameter of concern during TOYOBO membrane testing. The conductivity of solutions detected from the measurements of conductivity detectors was transferred into NaCl mass flowrate and overall mass balance assisted in the determination of RSF at the four feed water recovery values. The RSF was calculated from the following equation Eq. (3-8):

$$J_s = \frac{C_t Q_t - C_i Q_i}{A} \quad (3\text{-}8)$$

where C_t is the feed mass concentration (mg.L^{-1}) at time (t), C_i is the initial feed mass concentration (mg.L^{-1}), Q_t and Q_i are the volumetric flowrates at time t and initial time respectively and A is the membrane area.

3.3.2.2. Experiments using NTU membrane

The feed and draw solutions were flowing in countercurrent manner. Unlike TOYOBO testing protocol, the feed solution was applied to the bore side inside the hollow fiber (inside-out configuration) and the draw solution was subjected to flow over the shell side on the outer surface of the hollow fiber as in *Figure 3-15*.

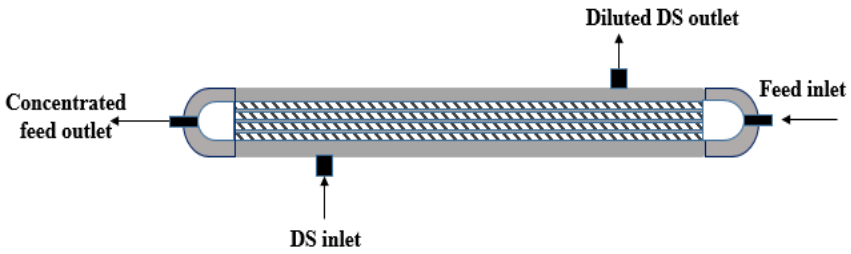

Figure 3-15: Inside-out configuration for NTU membrane.

The experiments were performed with small feed tank of 20 L that was placed on a digital balance (Mettler Toledo, USA) as in *Figure 3-16*. For the NTU membrane of small area, if feed water was taken directly from the tank of 5m^3 capacity; only few millimeters of water will be permeated by the membrane and accurate determination of water flux will not be feasible. However, the DS was taken normally from the original big tank of 5 m^3. For the same membrane's small area limitation, higher percentages of feed water recovery will not be achieved by the once-through flow of FS. Therefore, the FS was made in recirculation mode by placing the outlet concentrated FS stream in the same inlet FS tank and the DS flow was kept in once-through mode. Recirculation mode of FS helps in concentrating the initial feed water tank with experimental time and makes the membrane capable of achieving higher recovery rates. When the feed tank concentration gets higher with time, the inlet feed water concentration to the membrane also increases. Following that and after the membrane separation stage, the outlet FS stream will be poured to the initial small feed tank with higher concentration and lower volume. As a result, the increase in concentration and decrease in volume enhances the recovery of feed water. This indicates that in this case the recovery rates were achieved by changing the concentration of feed water rather than manipulating the FS and DS flowrates as in TOYOBO. The FS

and DS flowrates were both maintained constant at 1.5 L.min^{-1} through conducted experiments for different rates of feed recovery achievement. Experiments proceeded for recovering 60%, 68%, 75% and 90% of feed water. Higher rate of feed recovery obtained at higher concentration of feed tank. Whenever the required recovery was reached, more feed water was added to keep steady operation at the same recovery.

The weight difference of feed tank was recorded by the data acquisition system (LabVIEW, National Instrument, US) and was transferred into water flux values (LMH) as in Eq. (3-9). RSF was calculated from the conductivity measurements transferred into mass balance as explained earlier in Eq. (3-8).

$$J_w = \frac{W_{initial\ feed} - W_{final\ feed}}{t \times A_m} \tag{3-9}$$

where, J_w: is the water flux (LMH) and calculated from difference between weight of initial feed water ($W_{initial\ feed}$) and final weight of water in feed tank ($W_{final\ feed}$) over the membrane area (A_m) and time of experiment t (hours).

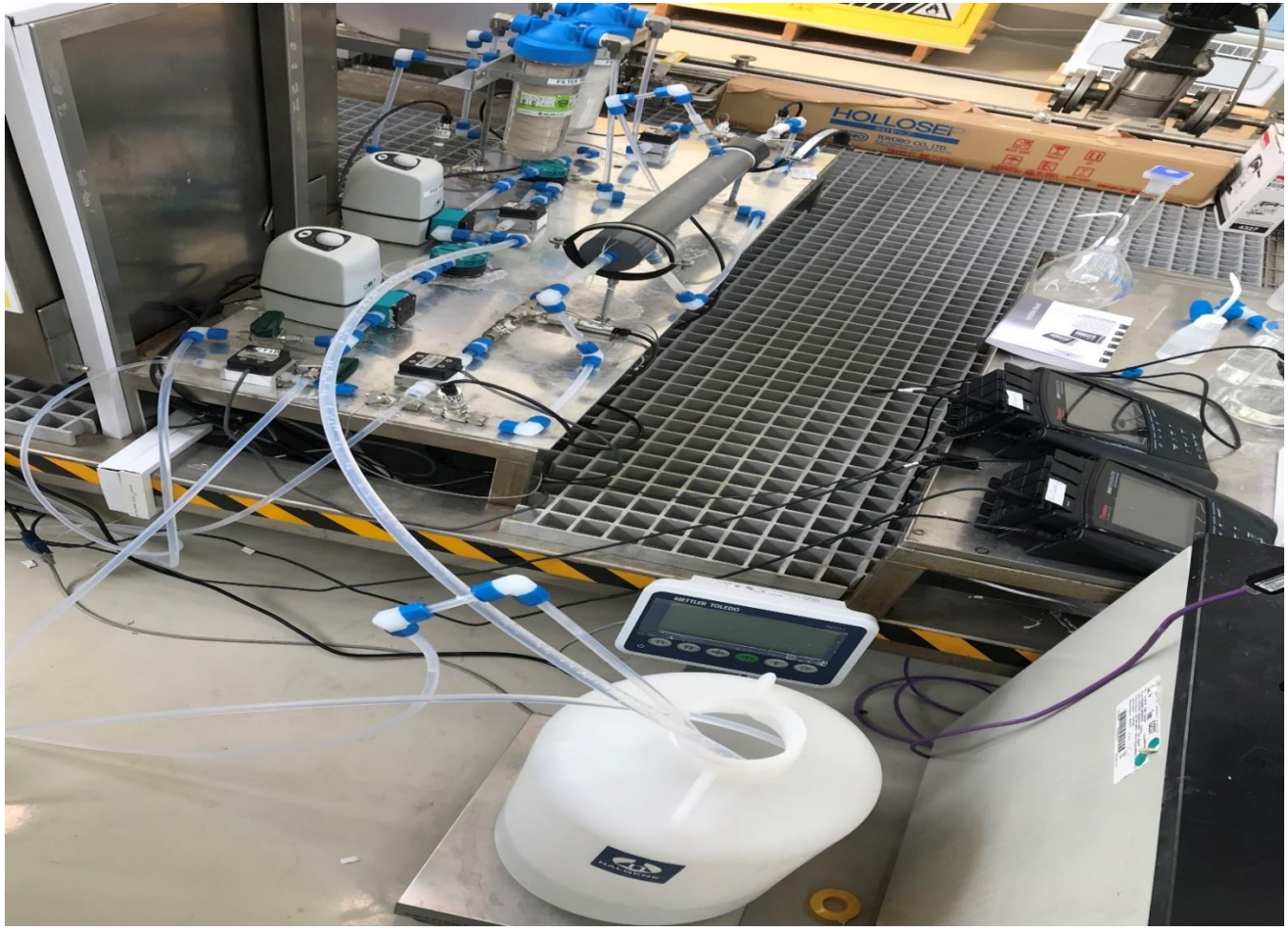

Figure 3-16: NTU membrane experimental setup.

3.3.3. Experiments for the effect of changing the draw solution flowrate

The effect of changing the DS flowrate was assessed on the performance of pilot-unit osmotic concentration when TOYOBO and NTU membrane modules are used in the system. The pilot-unit with each membrane was operated as explained earlier in section 4.2.2. For TOYOBO membrane, the FS and DS are in once-through mode, whereas NTU operation required the recirculation mode of FS and the once-through mode of the DS. Additionally, the setup of pilot-unit with TOYOBO and NTU were the same as in Figure *3-3* and *Figure 3-16*. Three experiments with DS flowrate of 0.28, 0.35 and 0.45 $L.min^{-1}$ were operated at constant FS flowrate of 1.10 $L.min^{-1}$ to investigate the performance on water flux, RSF, feed recovery and DS dilution. The experiments were conducted on both membranes at an operation temperature of 17.00 °C according to the surrounding conditions in the laboratory.

3.3.4. Experiments for the effect of changing the draw solution flowrate and operation temperature

The influence of temperature known to make changes on the water flux and reverse solute flux was assessed using the commercial TOYOBO HF-FO module. Three experiments conducted with TOYOBO membrane for different DS flowrates (0.28, 0.35 and 0.45 $L.min^{-1}$) and constant DS flowrate of 1.10 $L.min^{-1}$ at 17 °C (section 3.3.3) were repeated in summer time at an operation temperature of 27.00 °C according to the surrounding conditions in the laboratory.

3.3.5. Experiments for the long-term stability using TOYOBO and NTU membranes

The long-term stability experiments involved two runs for the pilot FO based osmotic concentration unit with TOYOBO and NTU membranes. The performance of each membrane was evaluated for 48 hours of continuous operation. According to the operating principles of each membrane (explained in 3.3.2), the conditions were set to achieve 75% feed recovery. The experiments were conducted where the surrounding temperature in the laboratory was around 17 °C, which was reflected onto the temperature of inlet FS and DS streams.

3.3.6. Experiments for evaluating the membrane intrinsic properties at different temperatures

The pure water permeability coefficient (A) and salt permeability coefficient (B) are two parameters determining the performance of the FO membrane. The value of coefficient A is a characteristic of the membrane active layer that indicates the water flux for specific osmotic pressure across the membrane sides. The greater the value of coefficient A, the better the membrane performance and the higher the water flux. For the two membranes used (TOYOBO and NUT), the experimental protocol followed to determine the value of coefficient A involved:

1- Using deionized (DI) water as FS.
2- Pressurizing the system to 2 and 4.9 bar in case of using NTU and TOYOBO membranes respectively and waiting for the stability of permeate flow.
3- After reaching the equilibrium, the permeate water was collected for 60 seconds.

4- Lastly, applying the following equation Eq. (3-10) facilitated the finding of value of coefficient A:

$$A = \frac{weight\ of\ permeate\ (kg)}{Membrane\ Area\ (m^2)\ x\ Pressure\ (bar)\ x\ time\ (hour)} \quad (3\text{-}10)$$

Value of coefficient B indicates the performance of the membrane from the reverse diffusion of DS solutes perspective at specific osmotic gradient (concentration difference) across the membrane sides. The value of coefficient B is also known as another property of the membrane active layer in which the higher value reflects higher reverse solute diffusion showing unsatisfactory performance of FO membrane. The value of coefficient B was calculated from the water flux (J_w) and salt rejection (R_{NaCl}) correlations according to Eq. (3-11) :

$$B = J_w \frac{1 - R_{NaCl}}{R_{NaCl}} \quad (3\text{-}11)$$

The water flux was obtained using the calculated value of coefficient A and the effective osmotic pressure gradient from Eq. (3-12):

$$J_w = A\Delta\pi_{eff} \quad (3\text{-}12)$$

In addition, the salt rejection (R_{NaCl}) was specified by:

1- Using NaCl rich solution of 500 mg.L^{-1} salinity as FS.

2- Pressurizing the system to 2 and 4.9 bar in case of using NTU and TOYOBO membranes respectively and waiting for the stability of permeate flow.

3- After reaching the equilibrium, around 5 ml of permeate water were collected for conductivity measurement. Additionally, the conductivity measurement was taken for the FS.

4- Finally, the value of coefficient B was found from the following expression (Eq. (3-13)):

$$R_{NaCl} = \left(1 - \frac{Conductivity\ of\ permeate}{Conductivity\ of\ feed}\right) x100\% \qquad (3\text{-}13)$$

The coefficients A and B determination experiments for TOYOBO membrane were conducted at operational temperatures of 20.00, 24.70 and 29.30 °C. However, for NTU membrane the coefficients A and B determination experiments were conducted at 19.70, 24.40 and 30.50 °C.

3.3.7. Membranes flushing method

Since the solutions across the membrane sides are salty with no complicated organic compounds, the cleaning was restricted to simple flushing of the membrane lumen after each experiment. The cleaning of the two membranes (TOYOBO and NTU) was done by replacing the inlet DS stream to the membrane with inlet FS stream. Therefore, FS was fed to both sides of membrane and remained flowing for 30 minutes until both sides approached the same salinity.

Chapter 4 : An Empirical Determination of the Whole Life-Cost Forward Osmosis Based Open-Loop Wastewater Reclamation Technologies

4.1. Introduction

Over the past 5-10 years it has become obvious that the considerable energy benefit given by forward osmosis (FO) for desalination emerges when the draw solution re-concentration step used to recover the DS and remove the permeate water transferred during the membrane separation is obviated. It is widely recognized that the DS recovery represents the greatest challenge to the technical and economic feasibility of the FO process [38,75]. It has, for example, been calculated that recovery of the permeate and draw solution incurs costs 65-140% higher than conventional RO for agricultural or diluted mining wastewater reclamation [9,10]. FO has nonetheless been mooted as an alternative to the conventional demineralization by RO for wastewater treatment and reclamation [25,32]. It is claimed that the technology can be energetically favored when a highly saline water source requires desalination in conjunction with the wastewater purification [25,47–51]. Under these circumstances, the process is configured as an open loop system where the FO stage dilutes the feed from an upstream RO stage. Therefore, the FO acts to dilute the osmotic pressure and reduces the energy consumption by the RO.

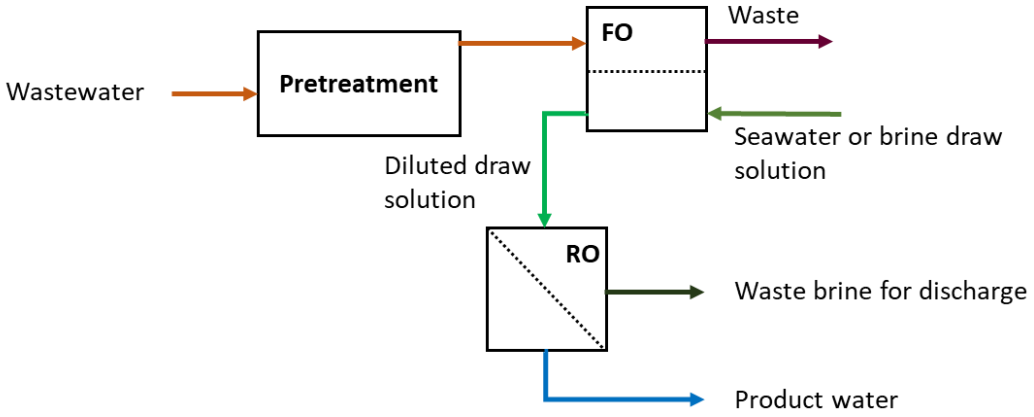

Figure 4-1: Open- loop combined wastewater reclamation and desalination.

It has been suggested that, for such an "open loop" system (*Figure 4-1*), the FO technology offers a lower-cost water reclamation option than the conventional process based on reverse osmosis (RO). Limited attention has been paid to the whole-life costs of the various FO-based process options for wastewater reclamation specifically, compared to the conventional MBR-RO option. Of the few studies which have considered open-loop FO systems [78,129], the outcomes suggest a small economic benefit.

In view of the above, the current chapter provides the results obtained by the life cycle cost analysis (LCCA) of FO for wastewater treatment/reclamation. The LCCA was conducted according to the methodology explained earlier in chapter 3 (section 3.1). The LCCA considers determining the net present value (NPV) indicating the cash inflow and outflow difference at the present value over the project lifespan.

4.2. Results and discussion

4.2.1. MBR costs

4.2.1.1. CAPEX

The specific CAPEX ($L_{C,MBR}$) in k$ per $m^3.d^{-1}$, was determined for each of the reported CAPEX: Q_P data sets over two decades of flow (500-50,000 $m^3.d^{-1}$) [210–212]. The data sets were fitted to a power law relationship (*Figure 4-2*):

$$L_{C,MBR} = mQ_P^n \quad (4\text{-}1)$$

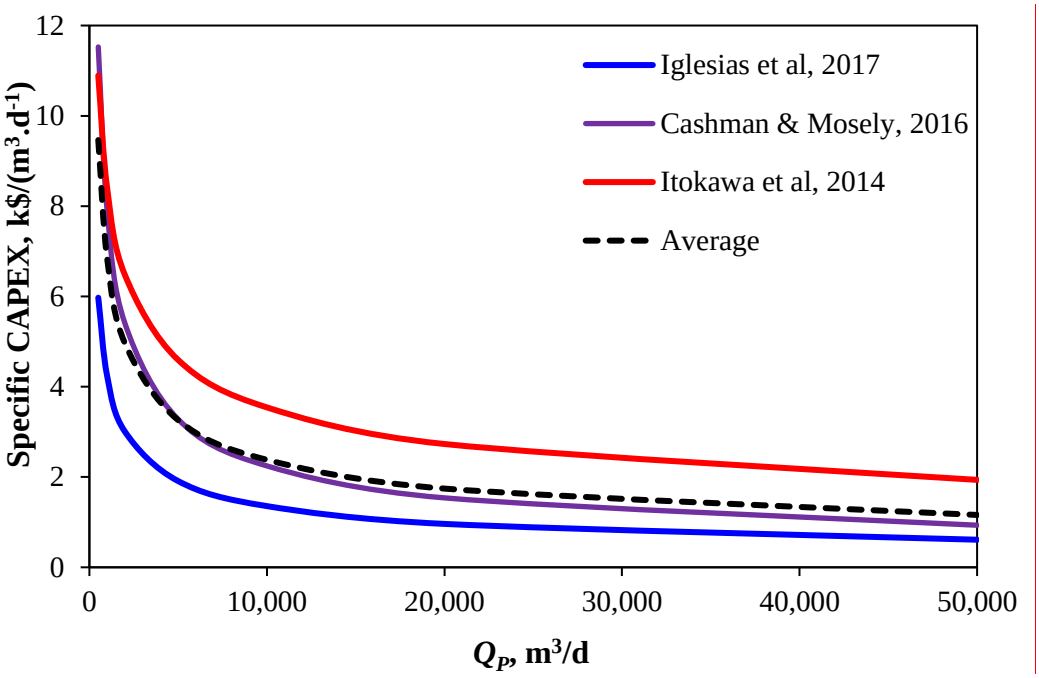

Figure 4-2: Specific iMBR CAPEX (correlated to 2019 USD) versus flow capacity based on outcomes of three studies.

Albeit with a high degree of data scatter in the case of the Itokawa et al., 2014 data (*Figure 4-2*). The disparity between the three data sets may either reflect regional differences or else result from the methodology used. The average of the three curves is very close to that interpolated from the study outputs of Cashman and Mosely [212] (*Figure 4-2* and *Table 4-1*).

Table 4-1: Specific CPEX correlations from published data, 2019 USD k$ per $m^3.d^{-1}$.

Source	Coefficient, m^1	Exponent, n^1	R^2
Iglesias et al. 2017	129	-0.495	0.94
Itokawa et al. 2014	112	-0.375	0.6
Cashman and Mosely, 2016	343	-0.546	
Average	167	-0.462	-

The MBR CAPEX equation based on average trend of data sets follows an exponential trend and is a function of permeate flow rate in $m^3.d^{-1}$:

$$L_{C,MBR} = 167\ Q_P^{-0.462} \quad (4\text{-}2)$$

According to this relationship, the specific CAPEX range between permeate flows of 3,800 and 19,000 $m^3.d^{-1}$ is \$1.76 to 3.71 k$ per $m^3.d^{-1}$, which is in reasonable agreement with the range of 2.03-3.09 k$ per $m^3.d^{-1}$ reported across four other studies [213,214,216,217].

It is further possible to recalculate the MBR CAPEX curve for a design flux of 15 LMH, appropriate for high TDS feed waters that form less filterable mixed liquors, by adjusting the membrane area accordingly:

$$L_{C,MBR,high\,TDS} = 139\,Q_P^{-0.424} \quad (4\text{-}3)$$

4.2.1.2. OPEX

The MBR specific OPEX $L_{O,MBR}$ in \$.m^{-3} permeate calculated from the base values listed in chapter 3 (*Table 3-2*) and the relationships given in chapter 3 (*Table 3-3*) can be expressed as a function of the flux J_{MBR} (in L.m^{-2}.h^{-1}) and the specific aeration demand SAD_m in (Nm^3.L^{-1}.m^{-2}) for membrane scouring:

$$L_{O,MBR} = 2.21\frac{SAD_m}{J} + 0.0164 + L_E\,E_{A,bio} \quad (4\text{-}4)$$

where L_E is the cost of electrical energy supply in kWh.m^{-3} (chapter 3, *Table 3-2*) and $E_{A,bio}$ is the SED for aeration of the process biological tank (determined from the process biology relationships in chapter 3, *Table 3-3*). Using the base values for the feed water quality given in *Table 3-2*:

$$E_{A,bio} = 5.08 \times 10^{-4} COD + 0.05 \quad (4\text{-}5)$$

4.2.2. RO and FO costs

4.2.2.1. CAPEX

The data of Loutatidou et al. [207] yields the following specific CAPEX correlations for saline and brackish water RO installations:

$$L_{C,SWRO} = 5.16\,Q_{P,RO}^{-0.0654} \quad (4\text{-}6)$$

$$L_{C,BWRO} = 2.42\ Q_{P,FO}^{-0.0502} \quad (4\text{-}7)$$

Based on the assumptions given in chapter 3, the FO plant CAPEX can be estimated from the BWRO CAPEX, assuming the RO elements to be replaced with sufficient FO elements to provide the same product flow capacity. This then yields the relationship:

$$L_{C,FO} = 2.41\ Q_{P,FO}^{-0.0502} \quad (4\text{-}8)$$

Published FO CAPEX data is scarce, but the $L_{C,FO}$ value of 1.35 k$ per $m^3.d^{-1}$ calculated for a flow $Q_{P,FO}$ of 100,000 $m^3.d^{-1}$ from Equation (7) is somewhat higher than the value of 0.79 determined by Valladares Linares et al. [25]. However, the respective CAPEX ratio values ($\frac{L_{C,FO}}{L_{C,SWRO}}$) of 0.65 [128] cf. 0.53 (this study) at this flow capacity are in reasonable agreement. Difference in absolute CAPEX values can be attributed to the low blanket EPC cost of $1.21 k$ per $m^3.d^{-1}$ assigned to SWRO by Valladares Linares et al. based on a 2007 study [221], about half the corresponding value determined in the current study.

4.2.2.2. OPEX

The commercial RO CAD package computed data for the total power consumption, the maximum operating pressure (i.e. the feed pressure), and the chemical consumption rate (*Table 4-2*). From these data the average chemical dosing cost ($L_{Chem,RO}$) and the instantaneous OPEX ($L'_{O,RO}$) were calculated for the range of ion compositions indicated in chapter 3 (*Table 3-4*) and otherwise based on the assumptions listed in chapter 3 (3.1.2). The overall RO specific OPEX ($L_{O,RO}$) was determined taking account of the membrane replacement cost factor $\frac{L_M}{J_t}$ analogous to MBR case.

Accordingly, the RO specific OPEX in $.m^{-3} follows a linear relation with the TDS in g/L:

$$L_{O,RO} = 0.0134\,TDS + 0.137 \quad (4\text{-}9)$$

Table 4-2: RO energy, chemicals and membrane replacement costs.

TDS, mg.L^{-1}	Power kW	Feed pressure bar	E_L kWh.m^{-3}	$L_{Chem,RO}$ $.m^{-3}	$\frac{L_M}{J_t}$ $.m^{-3}	$L'_{O,RO}$ $.m^{-3}	$L_{O,RO}$ $.m^{-3}
422	286	8.0	0.686	0.0244	0.0148	0.093	0.108
4182	453	12.7	1.087	0.0268	0.0148	0.136	0.151
19322	1157	32.5	2.777	0.0264	0.0148	0.304	0.312

Using the same software and extrapolating data trends to zero osmotic pressure while setting the flux to 6 LMH (chapter 3, *Table 3-4*) for the FO membrane, the computed FO process electricity cost (E_L) is constant at 0.215 kWh.m^{-3}. If pumping the draw solution is assumed to incur the same energy demand and the mean cost of chemical dosing ($L_{Chem,FO}$ = 0.0271 $.m^{-3}) and membrane replacement ($\frac{L_{M,FO}}{J_t}$ = 0.119 $.m^{-3}) are added:

$$L_{O,FO} = 0.189 \quad (4\text{-}10)$$

4.2.3. Overall treatment costs

A summary of the correlations for the CAPEX and OPEX components of the costs for the relevant technologies indicate widely differing trends in CAPEX for the two different generic types of process (*Table 4-3*, *Figure 4-3*). The MBR has a greater economy of scale, associated with the nature of the process that is based on the construction of large tanks for both the process biology and the membranes. The RO and FO technologies have a much reduced economy of scale, as indicated by the shallower cost curve slope (*Figure 4-3*). Although FO CAPEX data was assumed equal to BWRO CAPEX, FO curve in *Figure 4-3* showed a higher CAPEX than BWRO at all considered permeate flow capacities owing to higher FO membrane cost.

Table 4-3: Specific CAPEX (L_C, \$/(m^3.d)) and OPEX (L_O, \$/m^3) correlations for all technologies.

Technology	*CAPEX*, L_C , $\frac{\$}{m^3.d}$			*OPEX*, L_O , $\frac{\$}{m^3}$		
	m	variable	*n*	*m*	variable	*c*
MBR, low TDS	167	$Q_{P,MBR}$	-0.462	2.21	$\frac{SAD_m}{J}$	0.164 + $E_{A,bio}$
MBR, high TDS	139	$Q_{P,MBR}$	-0.424	2.21	$\frac{SAD_m}{J}$	0.164 + $E_{A,bio}$
SWRO (high TDS)	5.16	$Q_{P,RO}$	-0.0633	$1.34x10^{-5}$	TDS	0.137
BWRO (low TDS)	2.42	$Q_{P,RO}$	-0.0804	$1.34x10^{-5}$	TDS	0.137
FO	2.41	$Q_{P,FO}$	-0.0502	-	-	0.189
$E_{A,bio}$				0.408	COD	0.050

For the base conditions, the OPEX is a linear function of the membrane air scour rate, process biological aeration demand, and the inverse flux for the MBR, the process aeration being linearly related to the feed COD and TKN concentrations. For the fixed flux values of the RO and FO technologies, the OPEX is a function of the salinity (or TDS) for the RO but retains a constant value in the case of the FO. The FO OPEX is then most sensitive to the FO cost and replacement frequency.

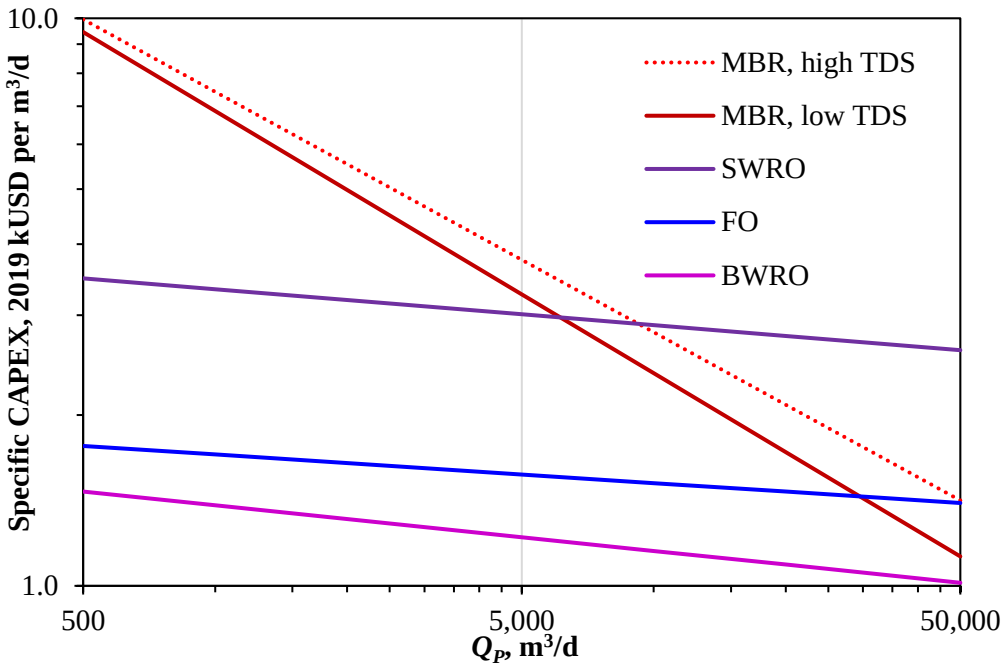

Figure 4-3: CAPEX trends with permeate flow.

The NPV is determined by combining the CAPEX and OPEX [209]:

$$NPV = \sum_{t=0}^{t=n} \frac{CAPEX_{t=0} + OPEX_t}{(1+D)^t} \tag{4-11}$$

D being the discount factor (assumed to be 2%) and n the total plant life (or amortization period), taken as 30 years. Annualizing all scheduled OPEX, including membrane replacement, simplifies this equation:

$$NPV = Q_P L_C + 365 Q_P L_O \sum_{t=0}^{t=n} \frac{1}{(1+\boldsymbol{D})^t} = Q_P (L_C + 8541 L_O) \tag{4-12}$$

The normalized NPV values (NPV/Q_P, Figure 4-4) demonstrate similar trends to those for the CAPEX (Figure 4-3), indicating the widely accepted sensitivity of total costs to CAPEX. However, the relatively high cost of the FO membranes is reflected in the higher overall costs of the FO technology compared with low-salinity RO (i.e. BWRO) and MBR technologies respectively.

As with the CAPEX trends, the flow-normalized (or specific) NPV can be fitted to a power law (NPV/Q_P =mQ_P^n), the R^2 values exceeding 0.995 in all cases (Table 4-4). These correlations can then be used to determine the specific NPV of the overall open loop treatment schemes based on a conversion of 95% for the MBR and 75% for the RO/FO technologies.

For the FO system, two other cost factors are taken into account:

i. The cost penalty of the increased capacity of the downstream RO step, and
ii. The cost benefit of the reduced SED of this step due to the dilution afforded by the FO.

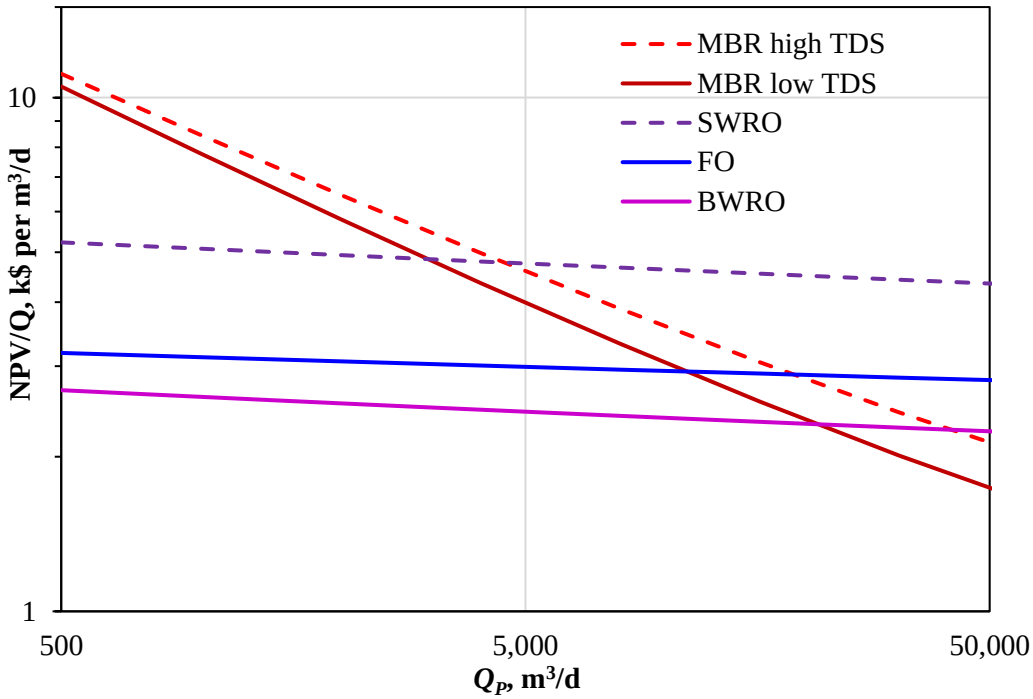

Figure 4-4: Normalized NPV versus permeate flow rate for individual unit operations.

Table 4-4: Specific NPV (NPV/Q_P, \$/ (m^3.d)) correlations for all technologies.

Technology	$\frac{NPV}{Q_P}, \frac{\$}{m^3.d}$			
	m	variable	*n*	R^2
MBR, low TDS	103	$Q_{P,MBR}$	-0.377	0.996
MBR, high TDS	91.6	$Q_{P,MBR}$	-0.348	0.997
SWRO (high TDS)	6.67	$Q_{P,RO}$	-0.0396	0.999
BWRO (low TDS)	3.43	$Q_{P,RO}$	-0.0393	1.000
FO	3.74	$Q_{P,FO}$	-0.0261	1.000

Subtracting (i) from (ii) above yields the net cost benefit ($\Delta\varepsilon$) of saline dilution. $\Delta\varepsilon$ was calculated assuming a saline feed water of 3.5 wt% salinity (i.e. normal seawater) and a 20% dilution of this stream by the FO permeate. Under these conditions, the contribution of $\Delta\varepsilon$ to the overall NPV is small, but increases proportionally from <1% to almost 10% as the permeate product flow increases from 500 to 50,000 $m^3.d^{-1}$ (*Figure 4-5*).

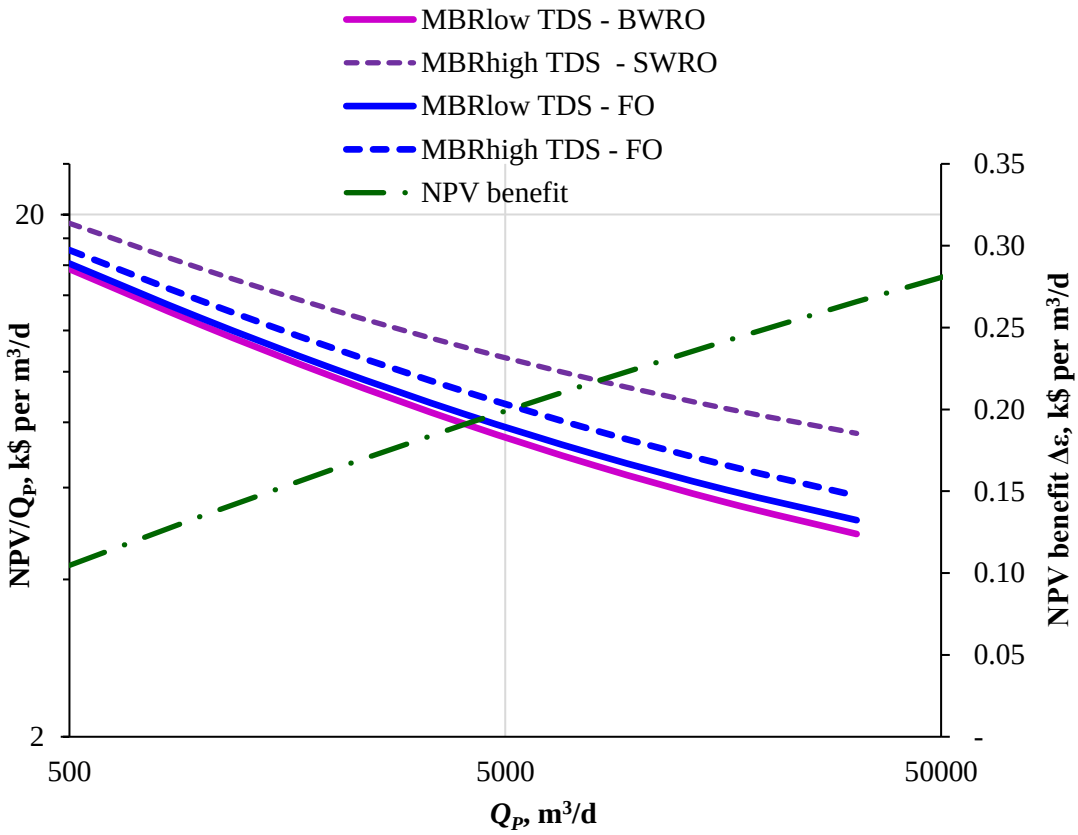

Figure 4-5: Normalized NPV versus permeate flow rate for the overall wastewater reclamation schemes shown in Figure 3-2.

Figure 4-5 otherwise reveals that over the range of permeate product flows considered (500-50,000 $m^3.d^{-1}$) and the base conditions indicated in chapter 3 (*Table 3-2*):

a. The MBR-FO option incurs an NPV 2-7% higher than that of the conventional MBR-BWRO option, the penalty increasing with increasing flow.
b. The same option provides an NPV benefit of 11-25% over the MBR-SWRO scheme used for a high feed TDS concentrations when higher RO pressures apply. This is in reasonable agreement with the outcomes of Teusner et al. [129], who reported an overall 12% cost saving from implementing an open loop system for combined wastewater reclamation and seawater desalination.

4.2.4. Sensitivity Analysis

Since there is evident significant variability in sustainable flux values reported from pilot and full-scale installations [5], this key parameter must subjected to a sensitivity analysis along with the membrane cost. Sensitivity can be demonstrated through correlating the % NPV/Q_P benefit compared with the classical MBR-RO scheme against the percentage change in these two base parameters. Accordingly, it is apparent that the NPV is more sensitive to membrane flux than to the cost of the material (*Figure 4-6*). Furthermore, the same figure (*Figure 4-6*) illustrates the high difference in flow normalized NPV benefit reaching 27% and 23% for FO process compared with SWRO when cost of membrane and flux are increased by their half values respectively. On the other hand, comparing FO with BWRO reveals that 50% increase in cost of membrane and flux in both processes provides a % NPV/Q_P benefit of 5% and 0% respectively lower than the case of FO compared with SWRO.

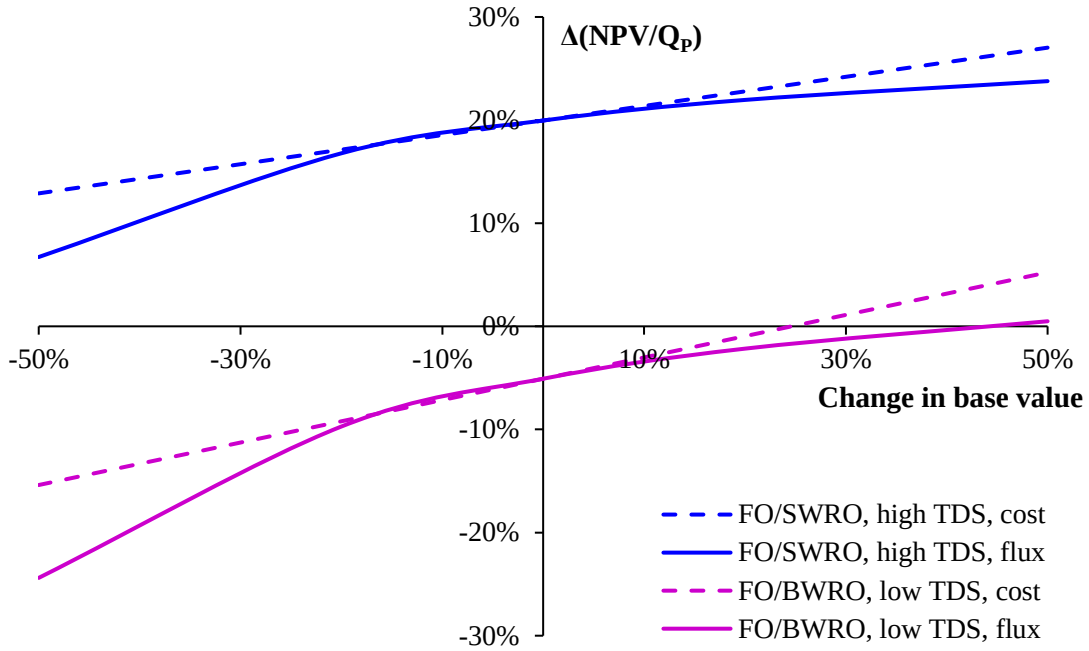

Figure 4-6: Sensitivity of the normalized NPV of the FO membrane-based wastewater reclamation schemes (Figure 3-1, b) to membrane cost and operational flux: % improvement in normalized NPV compared with classical MBR-RO scheme (Figure 3-1, a) versus % change in the membrane cost and operational flux base values, Qp=10,000 $m^3.d^{-1}$.

A number of caveats apply to the analysis as a whole:

1. It is assumed that there is no replication of CE and other cost elements between the MBR and RO cost components, which have been captured from different literature sources and for which no consistent cost breakdown was provided. On the other hand, the very low exponent value for the RO CAPEX curves (Table 4-3) suggest little economy of scale and, by implication, little impact of extensive site-related CE costs.

2. The primary cost impact of increasing the conversion of the RO or FO step of the two-stage processes is to reduce the required size of the upstream MBR, reducing the CAPEX and thus the overall cost. However, increasing the conversion beyond 75% is likely to be practically challenged by membrane organic fouling and scaling, substantially increasing the OPEX. Previous studies have identified an optimum conversion value of 63% for simultaneous seawater desalination and wastewater purification [47].
3. Of the two treatment options, only the conventional MBR-RO process recovers water directly. The recovery of the value of the water, diluting a saline feed stream for downstream desalination by RO, relies on the proximity of a saline stream requiring this desalination. Directing a saline feed water to a wastewater treatment works to recover the value of the FO permeate would incur significant infrastructure costs that would need to be accounted for.
4. The accuracy of the calculated absolute NPV values relies on the provenance of the CAPEX data and the validity of the OPEX assumptions. A recent published CAPEX data set [222] suggests greater economy of scale than the data set of Loutatidou et al. [207] indicates for SWRO installations (n = -0.185 vs. -0.0633), yielding lower $L_{C,SWRO}$ values at higher flows. The World Bank report [222] further suggests flow capacity dependency of OPEX, again leading to reduced specific costs at higher flows. This may reflect the importance of including labor costs, as noted elsewhere [208].
5. Notwithstanding the above limitations, the comparative normalised NPV values are likely to be valid since the assumptions made would have the same proportional impact across the two schemes. The two-stage MBR-FO process scheme appears to be more

cost effective than the two-stage MBR-SWRO process treating the same feed water with high TDS content.

4.3. Conclusions

An empirical cost analysis of two alternative treatment schemes for recovering the value of wastewater can be conducted with reference to available capital cost (CAPEX) data, along with classical correlations and/or commercial CAD packages to compute operating cost (OPEX). Available data for the established commercial membrane bioreactor (MBR) and reverse osmosis (RO) technologies can be used to estimate costs for the novel forward osmosis (FO) process. Assigning appropriate representative values for wastewater quality, process design and operation, and item costs reveals:

a. Flow capacity-normalised CAPEX and NPV follow an inverse power relationship (R^2>0.995) for all unit processes. The NPV-related exponent varies from low values (0.025-0.040) for RO/FO to high value (0.29) for MBR, reflecting the greater economy of scale of the latter.
b. The value of the water recovered by the extractive process (FO) is small if both the CAPEX penalty of increasing the downstream RO desalination plant size is taken into account in addition to the cost benefit of osmotic dilution of the feed. At flows below 30,000 m^3/d the CAPEX penalty is more than two-thirds of the OPEX benefit, and the net NPV benefit of this component ($\Delta\varepsilon$) equates to less than 10% of the total NPV benefit provided by the MBR-FO scheme compared to the MBR-BWRO.
c. At a permeate flow of 10,000 $m^3.d^{-1}$ and for a high salinity feed water, necessitating high-pressure SWRO desalination, the MBR-FO scheme has an NPV ~20% lower than that of the MBR-SWRO scheme. For a low-salinity feed water, the MBR-FO scheme offers no cost benefit over the classical MBR-BWRO scheme.

Whilst providing an apparent economic benefit, the full consequences of implementing the FO-based open loop system demands a consideration of the environmental impact through a life cycle analysis (LCA).

Chapter 5 : Pilot-Scale Testing of Two Hollow Fiber Forward Osmosis Membranes for Osmotic Concentration

5.1. Introduction

This chapter evaluates the performance of two different types of hollow fiber (HF) FO membrane modules for osmotic concentration. The two membranes are the commercial TOYOBO module and another pre-commercial NTU module fabricated by Nanyang Technological University. The HF made membranes were chosen as they provide a considerably high water production rate from their large surface/volume ratio. Besides, the HF module is a semi-permeable thin film membranes which alleviates the internal concentration polarization (ICP) problems from the eliminated porous support layer [205]. As mentioned earlier in chapter 3, the effective area of modules are different, where the NTU area represents around 1.6% of TOYOBO's membrane area. This difference in configuration translates into distinct operating procedures (discussed in chapter 4) and behavior for each module. Therefore, this chapter illustrates the differences between TOYOBO and NTU membranes operating at pilot scale level for osmotic concentration of large feed water volumes. The salinity of the prepared feed water is 2000 $mg.L^{-1}$ which is lower than the 40000 $mg.L^{-1}$ DS used to draw permeate from it. The characteristics of FS and DS are presented through this chapter. Both membranes are evaluated when operated for recovering various specified feed water percentages (60% up to 90%). This means that the experiments were conducted to examine the pilot-scale system capability to reduce the volume of feed water to a maximum of 90% using NTU and TOYOBO FO membranes. The performance of pilot-scale system in ensuring steady operation using each membrane was assessed from water productivity (represented by water flux) trend with time over the

testing period. Based on conditions of TOYOBO membrane, the experimental procedure for obtaining different feed recovery% has an effect on FS and DS flowrates which is illustrated in this chapter. On the other hand, the achievement of various feed recovery rates according to NTU experimental procedure linked to concentration change with time of operation at constant flowrates of FS and DS is to be illustrated. The feed recovery% is the main parameter studied and effects of its change were studied through trends of water flux and reverse solute flux for each membrane. Moreover, the effect of changing the DS flowrate on drawing the permeate water was tested through the experiments using TOYOBO and NTU membranes. The impact of DS flowrate was analyzed on trends of feed water recovery, water flux and reverse solute flux. Additionally, the effect of DS flowrate change with temperature is to be demonstrated from the experiments conducted using TOYOBO membrane. Further experiments were performed to evaluate the membranes' intrinsic properties with temperature and the results are to be described in this chapter. Above all, the stability of the pilot-unit for long-term osmotic concentration was demonstrated through investigated experiments for 2 days of continuous operation to recover 75% of feed. Lastly, it should be noted that the aim of the experimental works performed in this study is not intended to provide a decision about the best membrane module in response to results of pilot-scale testing and osmotic concentration of specified feed recovery rates; however, it represents how each module proceeds through each conducted experiment at pilot-scale.

5.2. Results and discussion

5.2.1. Feed and draw solutions characterization

The analysis results of the samples taken from the prepared feed and draw solutions are illustrated in *Table 5-1*. The total dissolved solids (TSS) produced by dissolving the industrial-scale NaCl salt was specified for each solution to mimic the process and produced water stream treated effluent of Qatargas as FS and the desalination brine as DS for the examined osmotic concentration process. As the solutions were prepared after passing the tape water through three filtration stages using activated carbon and traditional polypropylene cartridges, the suspended solids content was considered low. However, the large salt amount added to the DS contribute to increase its TSS content from the presence of contaminates traces in the salt. And owing to the nature of both feed and draw solutions being NaCl solutions with no organic pollutants, the IC was found to be much higher than TOC for both solutions. Moreover, the salinity difference contributes to a lower pH in case of DS with high salinity compared to higher pH of FS. At last, the lower salt content in FS makes its turbidity lower than that of DS. It should be noted that the FS prepared from using filtered tap water and 2 g NaCl. L^{-1} has a 58.5 % lower turbidity than normal tap water without filtration.

Table 5-1: Feed and draw solutions water characterization.

Parameter ($mg.L^{-1}$)	Feed Solution	Draw Solution
TDS	2000	40000
TSS	1.3	15.2
Inorganic carbon (IC)	18.75	15.4
Total Organic Carbon (TOC)	0.324	0.705
pH	8.19	7.74
Conductivity (mS/cm)	4.0	64.0
Turbidity	0.148	0.719

5.2.2. Experimental results of changing feed recovery rate.

5.2.2.1. Effect of changing the feed recovery rate on the flowrates of FS and DS during TOYOBO membrane evaluation in the osmotic concentration process.

During the TOYOBO FO membrane testing, obtaining different rates of feed recovery was possible by manipulating the flowrate of the FS inlet stream. The experiments were conducted for the aim of recovering 60%, 68%, 75% and 90% from 2000 ppm salinity feed water by the effect of 40000 ppm DS at temperature of 27 °C. Throughout all the experiments, the dilution rate of DS was maintained at 75%. Therefore, the DS flowrate was altered for achieving the same DS dilution rate at each feed recovery.

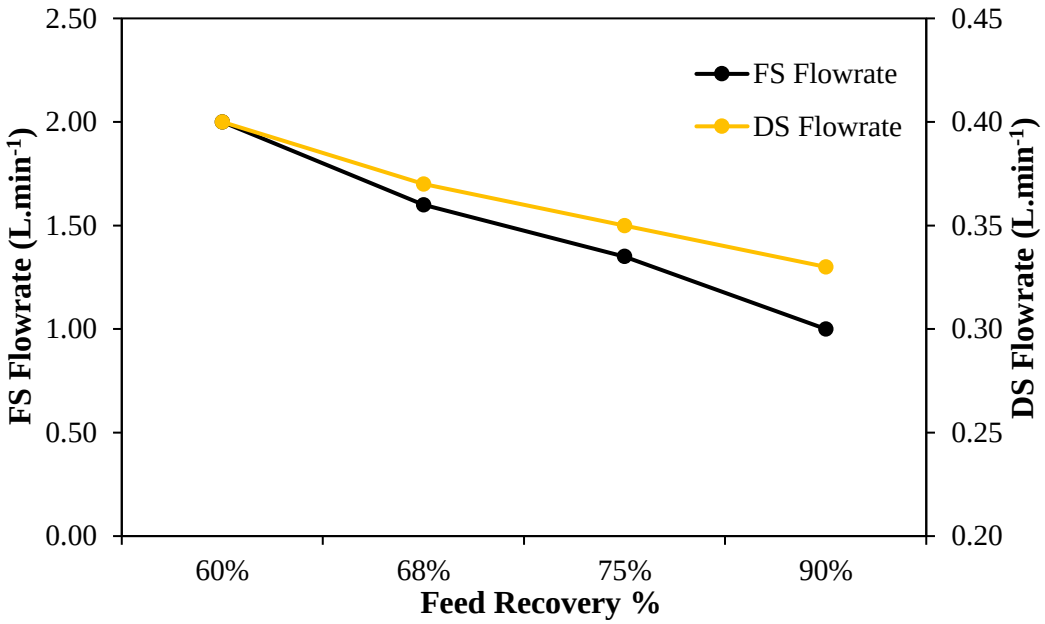

Figure 5-1: The relationship between FS and DS flowrates altered to obtain various feed recovery % and maintain constant DS dilution rate of 75%.

It was observed that the decrease in FS volumetric flowrate is responsible for producing high feed recovery rate (*Figure 5-1*) according to equation (5-1) described earlier in chapter 3. The low feed recovery was a consequence of the feed flowrate being higher than the permeate flow rate ($Q_{F_{in}} - Q_{F_{out}}$).

$$FR\ \% = \frac{Q_{F_{in}} - Q_{F_{out}}}{Q_{F_{in}}} \times 100 \qquad (5\text{-}1)$$

The same finding of the FS flowrate effect on the recovery rate was reported in a previous research study using spiral wound FO membrane [223]. In addition to the effect of increasing the feed flowrate on decreasing the recovery rate, the same study concluded the increase of recovery when DS flowrate increased at constant feed flowrate.

The results also showed that the highest recovery of 90% was achieved at FS flowrate of 1.00 $L.min^{-1}$ and DS flowrate of 0.33 $L.min^{-1}$ compared to 60% recovery obtained by 50% increase in the flowrates of FS to 2.00 $L.min^{-1}$ and 21.20% increase in DS flowrate to 0.40 $L.min^{-1}$. *Table 5-2* shows that the regulated flowrates of both FS and DS at each feed recovery%, a total of 50% increase in the recovery range tested (from 60% to 90%) requires a 50% and 17% decline in FS and DS flowrate respectively. Besides, the experiments also showed the need for 20% decrease in FS flowrate to achieve about 13% higher feed recovery rather than 60% feed recovery. The FS flowrate resulted from the operation at 68% feed recovery (increased by 13%) required 7.5% decrease in DS flowrate to maintain its dilution at 75%. Increasing from 68% to 75% feed recovery, the FS and DS flowrates were decreased to 1.35 $L.min^{-1}$ and 0.35 L $L.min^{-1}$ respectively, meaning a 15.60% decline in FS flow and a 5.40% decline in DS flow.

Table 5-2: The adjusted FS and DS flowrates at each targeted feed recovery rate for TOYOBO membrane module.

Feed Recovery (%)	FS Flowrate ($L.min^{-1}$)	DS Flowrate ($L.min^{-1}$)
60	2.00	0.40
68	1.60	0.37
75	1.35	0.35
90	1.00	0.33

As there are four conditions for feed recovery and as TOYOBO experiments was allowed to run for around 4 hours, a total of 1.43 m^3 of feed water was consumed. According to the adjusted feed flowrates and experiments time, the amount of water consumed and recovered at each recovery is shown in *Table 5-3*.

Table 5-3: Amount of feed water consumed and recovered at each experiment using TOYOBO membrane.

Feed Recovery%	Feed water consumed (L)	Feed water recovered (L)
60	480	288
68	384	261
75	324	243
90	240	216
Total	1428	1008

Based on the displayed amounts of water fed to the FO membrane system and recovered quantities, the pilot osmotic concentration process using the TOYOBO membrane module succeeded in recovering around 1.00 m^3 from 1.43 m^3 consumed. The water recovered was during four performed experiments for different feed recovery rates and at different flowrates of FS and DS. Lastly, the overall concentration and volume reduction of the 2000

mg.L^{-1} feed water by the effect of 40000 mg.L^{-1} DS reached to 70.5% from performing four experiments with different flowrates.

5.2.2.2. Effect of changing the feed recovery rate on the feed concentration during NTU membrane evaluation in the osmotic concentration.

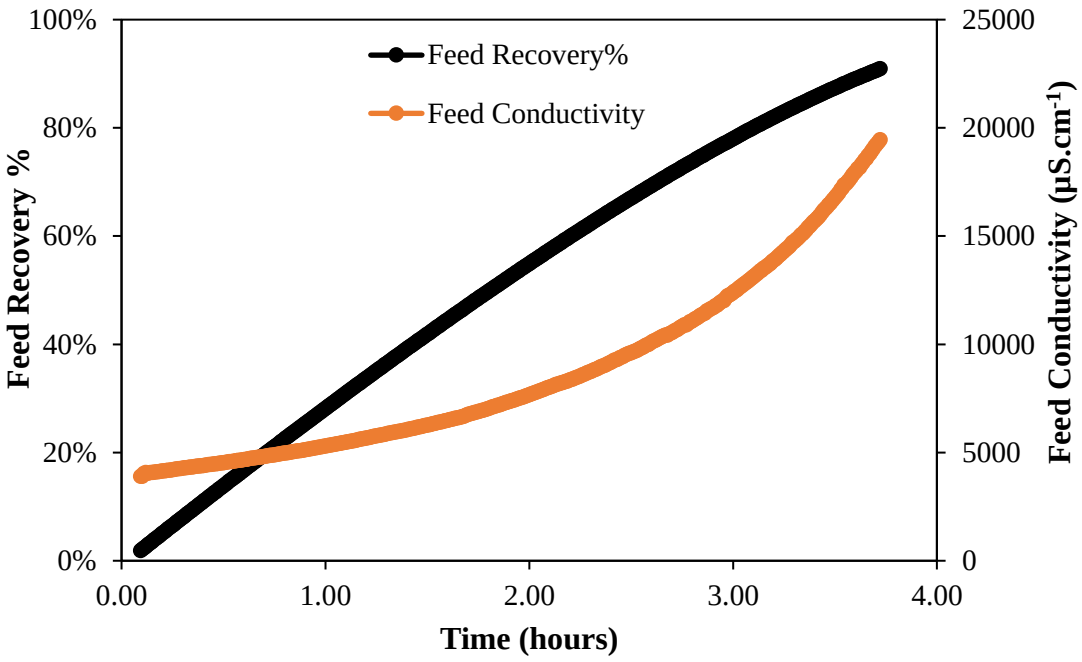

Figure 5-2: The relation between the feed concentration (expressed as conductivity values) and feed recovery rate with the time.

For the testing of NTU membrane module, the performed experiments to achieve various feed recovery rate percentages of the 20 L feed water tank were conducted at constant flowrate for both FS and DS at 1.50 L/min. In this case, various feed recovery percentages was achieved by changing the feed concentration level with time. It was observed that when the feed was operated in recirculation mode, the feed concentration in the intake tank

increased with the running time (*Figure 5-2*). This was caused from pouring the concentrated feed outlet stream after the membrane separation stage again into the intake feed tank. Therefore, the recirculation mode succeeded in concentrating the feed water that was reflected into obtaining high feed recovery rates. Moreover, longer runs of FO pilot-system allow recovering higher percentage of feed water rather than runs for shorter periods at the same flowrate conditions as the trend of recovery illustrates in *Figure 5-2*.

The 2000 $mg.L^{-1}$ feed solution has an initial measured conductivity approximated by 4000 $\mu S.cm^{-1}$ (*Table 5-1*) and increased to around 19460 $\mu S.cm^{-1}$ after a time duration of 3.70 hours where the feed recovery reached the maximum-targeted rate of 90%. However, the 60% feed recovery was achieved at 57% lower conductivity of feed water (lower concentration) measured as 8377 $\mu S.cm^{-1}$ and took around 2.20 hours to be reached at 1.50 $L.min^{-1}$ flow of FS and DS. The 68% and 75% feed recovery rate were attained when the conductivity of intake feed water was increased to 9805 $\mu S.cm^{-1}$ after 2.50 hours and 11450 $\mu S.cm^{-1}$ after 2.80 hours respectively.

The amount of feed water recovered from the initial 20.00 L for each experiment conducted to achieve different feed recovery rate is displayed in *Table 5-4*. For total of four set of experiments with the four presented feed recovery% required, total of 80.00 L feed water were consumed and a total 58.6 L were recovered resulting in overall recovery of 73.30%.

Table 5-4: Amount of feed water recovered at constant flowrate using NTU membrane.

Feed Recovery%	Feed water consumed (L)	Feed water recovered (L)
60		12
68	20	13.6
75		15
90		18
Total	80	58.6

5.2.2.3. Effect of changing feed recovery rate on the performance of hollow fiber membranes in osmotic concentration process.

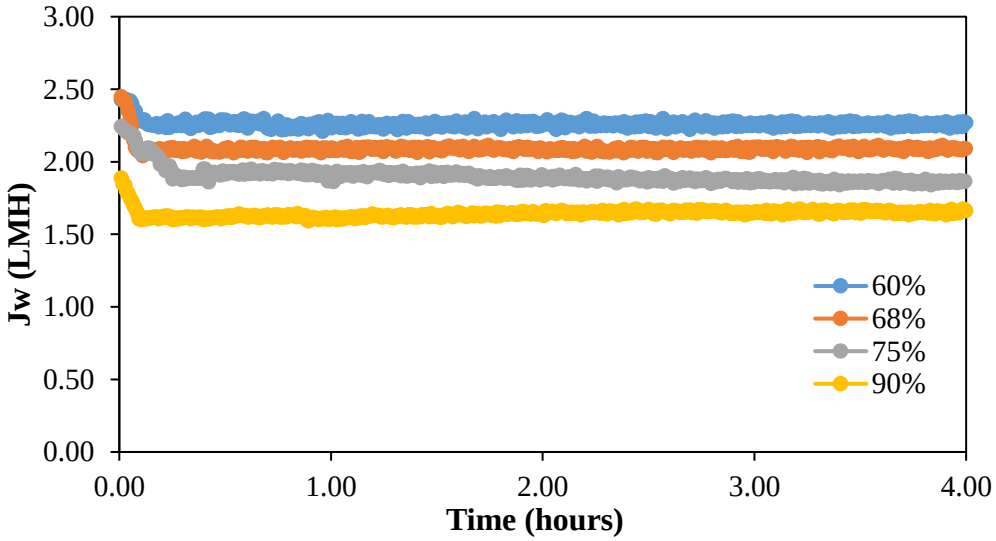

(a)

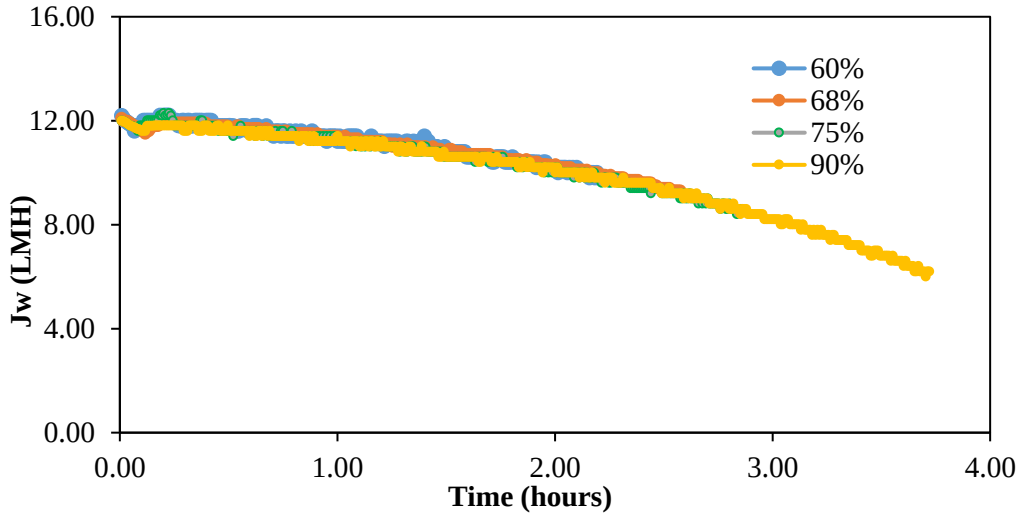

(b)

Figure 5-3: Performance of (a) TOYOBO and (b) NTU membrane modules through the experiments to produce a steady flux.

The performance of osmotic concentration process represented by the water flux (J_w) generated from using 2000 mg.L^{-1} FS and 40000 mg.L^{-1} DS using TOYOBO and NTU membranes is demonstrated in *Figure 5-3*. In the case of TOYOBO membrane (*Figure 5-3*(a)), the water flux was stable at each tested recovery during the entire operation time of the pilot-scale system. Once the FS and DS flowrates are specified and the system starts the operation, there will be few minutes spent until the water flow across the both sides of membrane attempts stability. Besides, the profiles in *Figure 5-3*(a) clearly illustrate that there was no flux decline throughout the 4 hours of operation. This indicates that the DS was not diminished and the osmotic driving force was maintained. Furthermore, the steady performance of the pilot system through the testing period proved its integrity for continuous operation. The obtained results confirm the capability of the programmed data acquisition system to measure efficiently the flowrates of inlet and outlet FS and DS streams that assisted in determining the water flux.

The trends of flux as a function of time during the NTU membrane experiments are shown in *Figure 5-3* (b). The figure shows the identical flux trend at the four different rcovery rates, however, the time needed to reach higher recovery rate was longer. This is due to the operational procedure of NTU membrane explained earlier in Chapter 3 which is based on increasing the feed concnetration level for obtaining different recovery rates. It was observed that operating the feed in recirculation mode facilitated in increasing the concentration of feed flowing to the membrane. The decline of flux at high recvoery rate was due to the reduced osmtoic driving force which was a consequence of the increase in the feed concentration. Lastly, the programmed system can be described by its successful

and robust operation during the entire testing time and the measured flux matches the expected trend.

5.2.2.4. Effect of changing the feed recovery rate on the water flux obtained by the hollow fiber membranes in osmotic concentration.

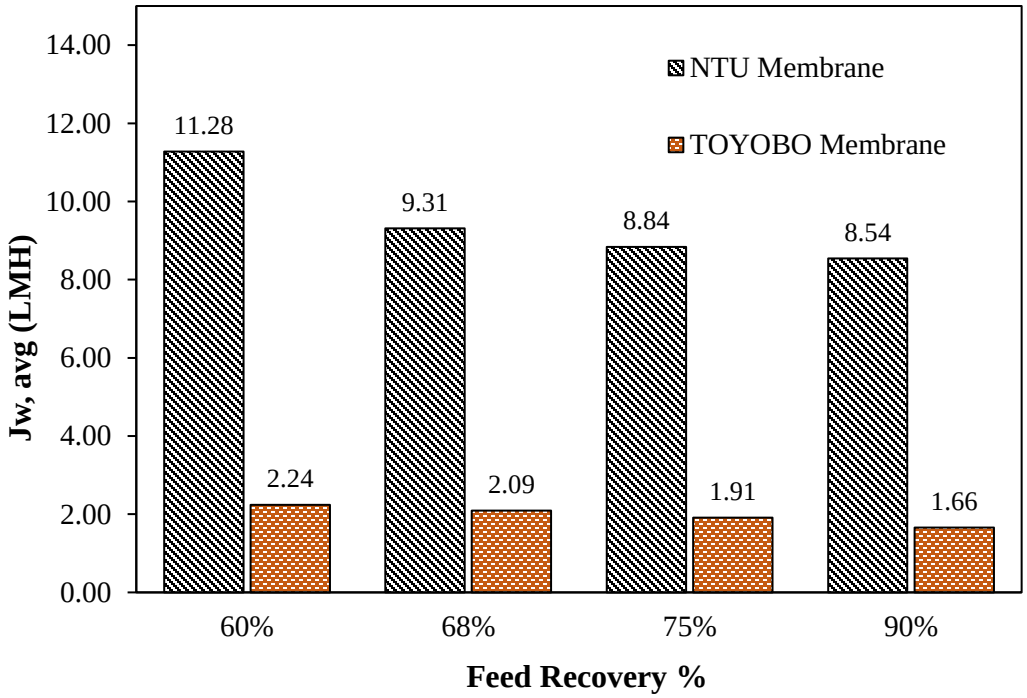

Figure 5-4: Effect of changing feed recovery rate on water flux during TOYOBO and NTU membranes testing.

The impact of pilot-scale unit operation for different feed recovery rate percentages on the water flux (J_w) measured in $L.m^{-2}.h^{-1}$ (LMH) was studied for TOYOBO and NTU FO membrane modules (*Figure 5-4*). The water flux generated by the two membrane modules was evaluated for the same four recovery rates that are 60%, 68%, 75% and 90% at laboratory temperature of 27 °C. *Figure 5-4* illustrates the average water flux of two experiments conducted for each feed recovery rate, and the declining trend with the increase in the feed recovery rate. The effect of increasing the feed recovery rate by the simultaneous decrease in the FS and DS flowrates fed to TOYOBO membrane modules was investigated. It was found that the flux decreased from 2.20 LMH at 60% recovery to 1.70 LMH at 90% feed recovery. The 22.70% flux decline was resulted from 50.00% and 17.50% decrease in flowrate of FS and DS respectively over 30% increase in recovery rate from 60% to 90%. The obtained trend was similar to the trend confirmed in the research of Hawari et al. [224], where the effect of changing both FS and DS flowrates was studied and high water flux of flat sheet thin film composite (TFC) FO membrane was produced at increased volumetric flowrates. Several studies on different FO membranes have confirmed the fruitful influence of the elevated flowrates on water flux [223,225,226].

In comparison of the two FO membrane modules with an identical HF configuration, the results of conducted experiments showed improved water productivity (amount of water permeated by the membrane) for NTU module. The low flux of TOYOBO could be caused by the large membrane area in which it increases the feed recovery and DS dilution rate at the module outlet. Eventually, the membrane of larger area reduces the water flux owing to osmotic driving force reduction [12]. The water flux obtained by the NTU membrane was much higher reaching its maximum of 11.30 LMH at 60% feed recovery. Throughout

the experiments, it was observed that operation at 60% recovery increases the flux by around 79% if compared to the performance of membrane recovering 90% of feed.

Comparing the maximum flux of the commercial TOYOBO membrane with NTU membrane at the same condition of feed recovery (60% recovery rate), the TOYOBO flux was around 80% lower than that of NTU. Increasing the feed recovery rate from 60% to 90% maintained 77.40%, 77.10% and 73.80% lower flux for TOYOBO than NTU at 68%, 75% and 90% feed recovery respectively. The obtained results emphasize the impact of the large effective membrane area on improving the water permeability.

The experimental results of both membrane modules have confirmed the inverse proportion of flux with the recovery rate, in which increasing the recovery percentage yields lower flux. The decline in flux at reduced FS and DS flowrates during TOYOBO membrane testing was attributed to the concentration polarization (CP) phenomenon. The high flowrates of FS and DS were capable to increase the module turbulence and minimize the effect of CP [227]. For instance, the high water flux obtained was a results of solute accumulation impediment after subjecting the membrane to high FS and DS flowrates [111]. The advantageous role of the high flowrate on both sides of the membrane on enhancing the mass transfer coefficient and increasing the flux was reported and demonstrated by many studies [12,109,228].

As it was mentioned earlier in the NTU membrane testing approach, higher recovery rates were achieved by running the system for higher feed concentration level. This explains that the decline in water flux was a consequence to the diminished separation driving force. To further clarify this, the FS got concentrated after diluting the DS through long membrane

operation and water permeation. Thus, this led to the reduction in the osmotic pressure difference across the membrane and caused the flux decline [50,107,227]. Furthermore, operation of the system at higher FS concentration level for high recovery rate decreases the salinity difference between FS and DS across the membrane and descends the water flux. Consequently, operation of FO at higher osmotic pressure is required for yielding greater water permeability.

5.2.2.5. Effect of changing the feed recovery rate on the reverse solute flux obtained by the hollow fiber membranes in osmotic concentration.

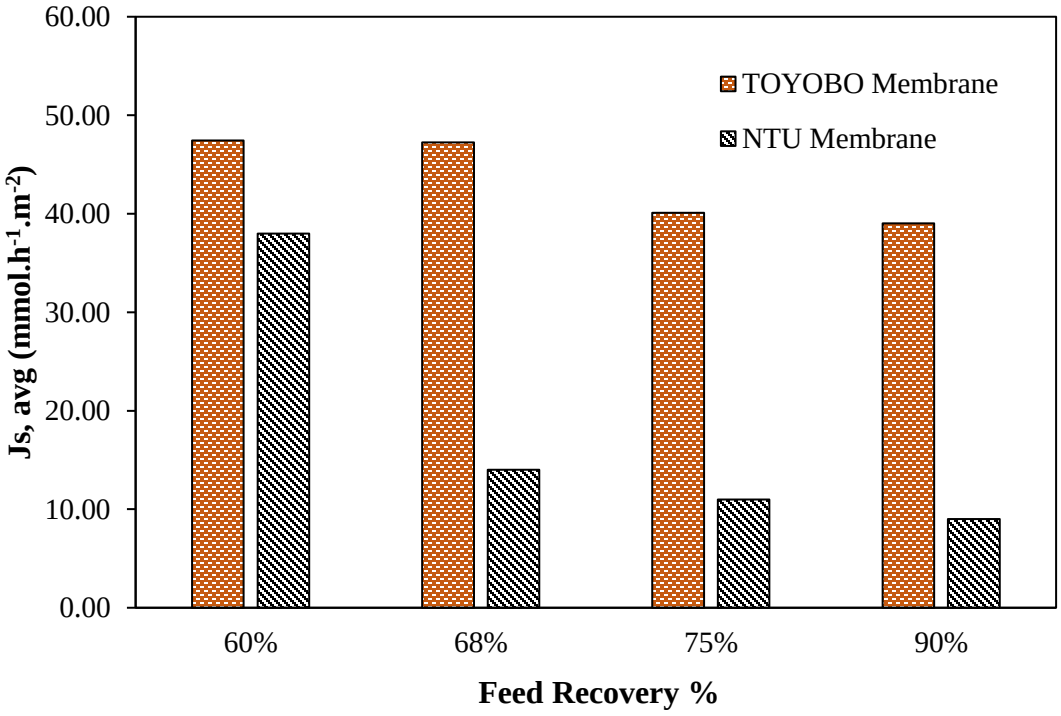

Figure 5-5: Effect of changing the feed recovery rate on reverse solute flux during TOYOBO and NTU membranes testing.

The impact of pilot-scale unit operation for different feed recovery rate percentages on the reverse solute flux (RSF, (J_s)) measured in $mmol.m^{-2}.h^{-1}$ was studied for TOYOBO and NTU FO membrane modules (*Figure 5-5*). The RSF was measured based on mass balance calculations determined by the water streams conductivity difference (Eq. (3-8) chapter 3). The RSF was obtained for the same four experiments performed for each membrane (i.e. 60%, 68%, 75% and 90% recovery rates) at 27 °C. Actually, the RSF is an indication for

salts- NaCl in this case- which reverse flowing from DS to FS and opposes the conventional water flow direction. Higher RSF is not desirable as it accelerates the decline of osmotic driving force and water flux [61]. Aside from the reduced driving force, high RSF rates elevates the periodical needs for replenishing the DS and recovering its high osmotic pressure [113]. The RSF trend illustrated in *Figure 5-5* shows the decrease in amount of solutes transferred from DS into FS with the increase in the feed recovery rate for both membrane modules.

During TOYOBO testing, the operation with highest flowrates of FS and DS for the lowest feed recovery rate of 60% was characterized by maximum reverse diffusion rate of DS solutes into the feed water. The maximum RSF for TOYOBO at 60% was estimated by 47.40 $mmol.h^{-1}.m^{-2}$ that is equivalent to 2770 $mg.h^{-1}.m^{-2}$ of NaCl available in DS reversing their diffusion into FS. This indicates that the DS flow at high rate induced the solutes to diffuse through membrane into the feed. On the other hand, the lowest RSF was during the recovery of 90% and low flowrate of inlet DS stream. The operation at 60% recovery produces 21.54% higher RSF than the produced at 90%. Therefore, adjusting low flowrates of FS and DS is preferable to minimize the RSF phenomenon across the TOYOBO membrane.

RSF values calculated using NTU module are lower than the obtained by TOYOBO membrane. The higher membrane area in TOYOBO modules facilitated higher diffusion of draw solutes into the feed side. In a similar trend to TOYOBO RSF, NTU RSF was at its maximum of 38.00 $mmol.h^{-1}.m^{-2}$ (2220 $mg/h.m^2$) for the recovery of 60% from the 20

L initial feed solution. However, there is around 76% change in RSF when operation for recovering 60% is compared with 90% feed recovery rate.

It is obvious that for both tested membrane modules, the water flux and RSF are directly proportional to each other. It was found that RSF was high at low feed recovery rates described by elevated average water flux rather than at higher feed recovery percentage. The relationship of flux and RSF was demonstrated in the research of Heo et al. [229] who studied the RSF trend with flux for several DS of different concentrations and reported the linear increase in RSF with the water flux increase.

Reverse solute flux normalization can be applied to clarify the differences between the TOYOBO and NTU membranes as illustrated in *Figure 5-6*. The normalization is interpreted by plotting the specific solute flux ($\frac{J_s}{J_w}$) which is a metric parameter usually used to determine the draw solutes loss per water pass with the four desired feed recovery rates. Low specific solute flux is translated into high FO membrane selectivity and separation capacity [230]. Despite the high selectivity, lower $\frac{J_s}{J_w}$ is favorable as it indicates minimal solutes loss from DS when operation in in FO mode where feed solution faces the active layer (FS-AL) in NTU case. Moreover, low $\frac{J_s}{J_w}$ helps in reducing the ICP in PRO mode operation where DS faces the active layer (DS-AL).

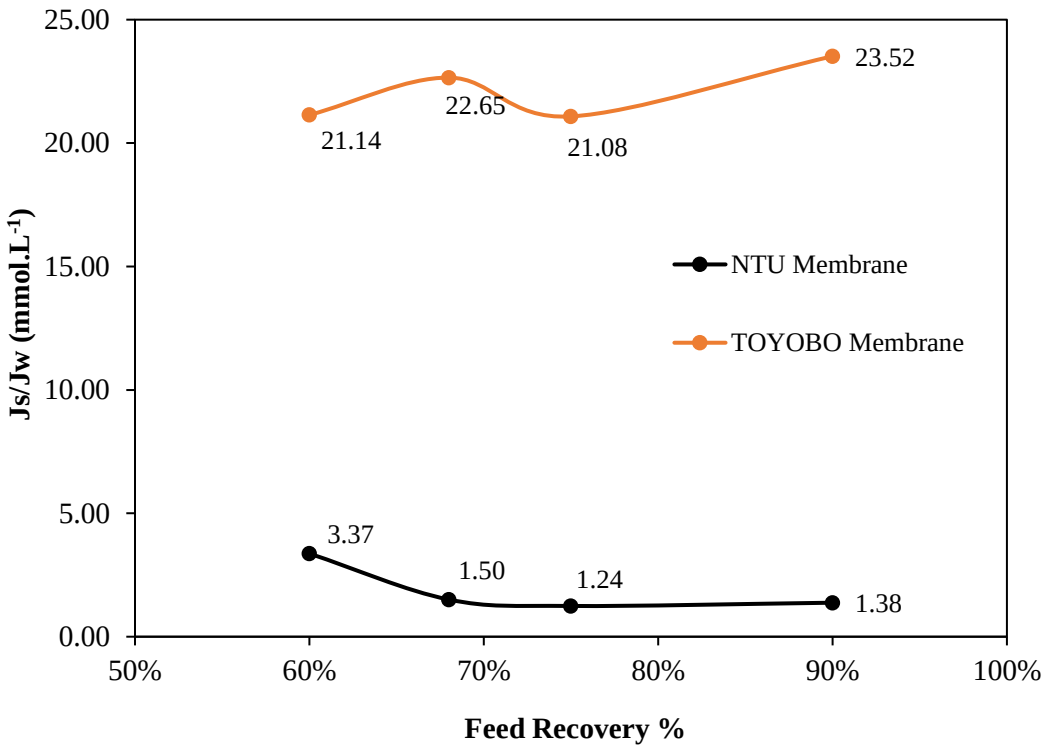

Figure 5-6: Specific solute flux versus feed recovery % for TOYOBO and NTU membranes.

Figure 5-6 demonstrates how the NTU membrane trend of $\frac{J_s}{J_w}$ is lower than that of TOYOBO membrane. To further explain this, the high specific solute flux produced by the commercial TOYOBO is a reason to its higher effective membrane area that was responsible in obtaining high J_s and low J_w compared to NTU (*Figure 5-4* and *Figure 5-5*). The $\frac{Js}{Jw}$ ratio of NTU has almost an apparent descending direction with the increase in feed recovery rate compared to the possessed increasing trend by TOYOBO. During TOYOBO testing, the increase of feed recovery rate by 30% from 60% to 90% results in a total of 11.3% increase in ratio of $\frac{Js}{Jw}$. Whereas, the NTU has experienced an overall decline in

$\frac{Js}{Jw}$ estimated by 59% with the increase in feed recovery. Consequently, the obtained results assert that NTU module outperforms the TOYOBO from the reduced loss of DS solutes perspective.

The increasing trend of $\frac{Js}{Jw}$ with the increase in the feed recovery rate when TOYOBO module was used can also be expressed with respect to the change in feed flowrate, since the various feed recovery rates were achieved by manipulating the feed flowrate (Figure 5-1 and *Table 5-2*). Therefore, Figure 5-6 results illustrate that $\frac{Js}{Jw}$ increases with the decrease in the adjusted feed flowrate and conflict the produced trend in a previous study where HF-FO membrane manufactured by Aquaporin was employed [231]. The difference in trends obtained here and in the research of Sanahuja-Embuena et al. [231] can be attributed to the smaller effective membrane area of Aquaporin module and to the difference in the osmotic pressure across the membrane. In the research of Sanahuja-Embuena et al. [231] DI as FS and 1 M NaCl as DS were fed to Aquaporin module compared to 0.2% wt NaCl FS and 4% wt NaCl fed to TOYOBO module in the current experimental testing.

Although the TOYOBO and NTU trends of $\frac{Js}{Jw}$ are of increasing and decreasing attitude respectively, there is one point in each data series which contrasts the recognized trend. As *Figure 5-6* shows, in the data series of TOYOBO the value of $\frac{Js}{Jw}$ at 75% recovery decreased by 6.9% from previous point and obviated the increasing trend. Besides, the decreasing trend of Js/Jw for NTU encountered around 11.3% increase in value of specific solute flux from 75% to 90% feed recovery.

5.2.3. Experimental results of changing draw solution flowrate.

The outcomes resulted from conducted experiments investigating the effect of changing the draw solution (DS) flowrate on the water and solute permeation are to be illustrated in this section. Additionally, some results related to the achieved level of feed recovery and DS dilution will be revealed as per the computations. The DS flowrate impact was evaluated on the two HF membrane modules (TOYOBO and NTU). Three experiments were performed for three different chosen DS flowrates where the DS temperature was around 17 °C similar to the surrounding temperature in the laboratory.

5.2.3.1. Effect of changing the DS flowrate on the osmotic concentration using TOYOBO membrane.

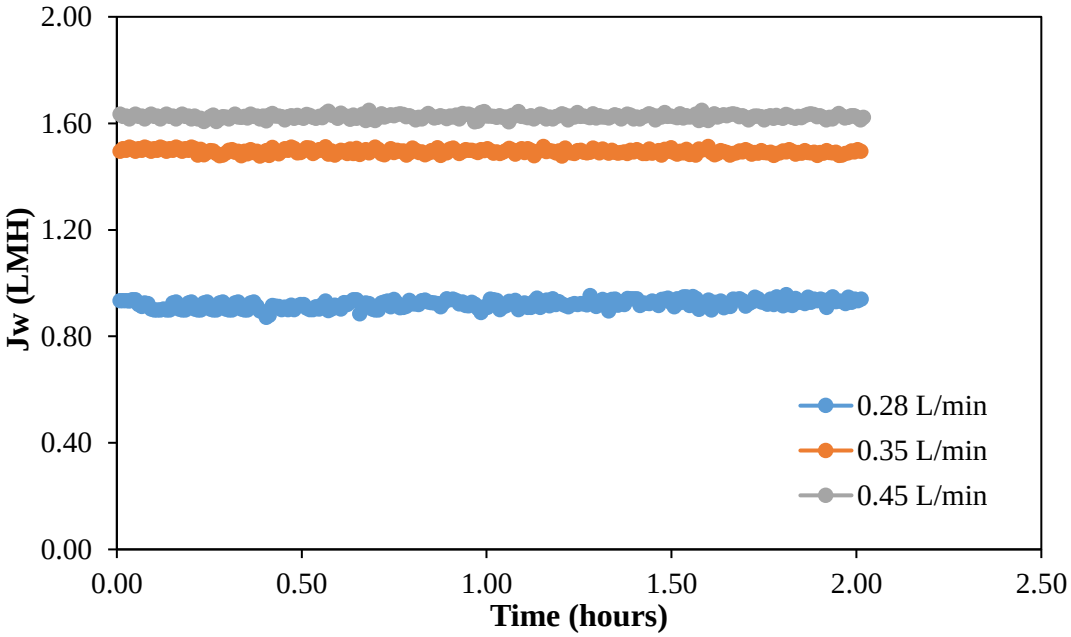

Figure 5-7: Water flux profile versus time for TOYOBO membrane under different DS flowrates at constant FS flowrate.

The effect of changing the DS flowrate at constant FS flowrate was investigated for TOYOBO membrane module. Three experiments were conducted by setting the DS flowrate to 0.28, 0.35 and 0.45 $L.min^{-1}$ at constant FS flowrate of 1.10 $L.min^{-1}$ and the performance of the pilot system was studied for 2.00 hours of continuous operation at a temperature of 17 °C. The profiles of water flux with time are shown in *Figure 5-7* for the three experiments where the influence of DS flowrate used to draw feed water on the permeate water productivity can be observed.

The higher the DS flowrate, the higher the permeation rate throughout the entire duration of the experiment. This was inferred by the observed remarkable increase in the water flux when DS flowrate was increased by 60.71% from 0.28 to 0.45 $L.min^{-1}$. Moreover, the trends illustrate the stable operation of the experiments at the obtained flux during the 2.00 hours. A negligible flux decline was experienced showing insignificant reduction in the osmotic gradient.

For the adjusted flowrates at each performed experiments, the feed recovery rate along with the DS dilution degree were approximated as in *Figure 5-8*. The trends presented are based on average values taken for the entire duration of each experiment. It is evident that elevated DS flowrate has an advantageous influence on increasing the feed recovery rate. Higher DS flowrate enables drawing higher amount of feed water .This suggests that small positive hydraulic pressure could be evolved in the direction of DS rendering higher permeation rate [227].

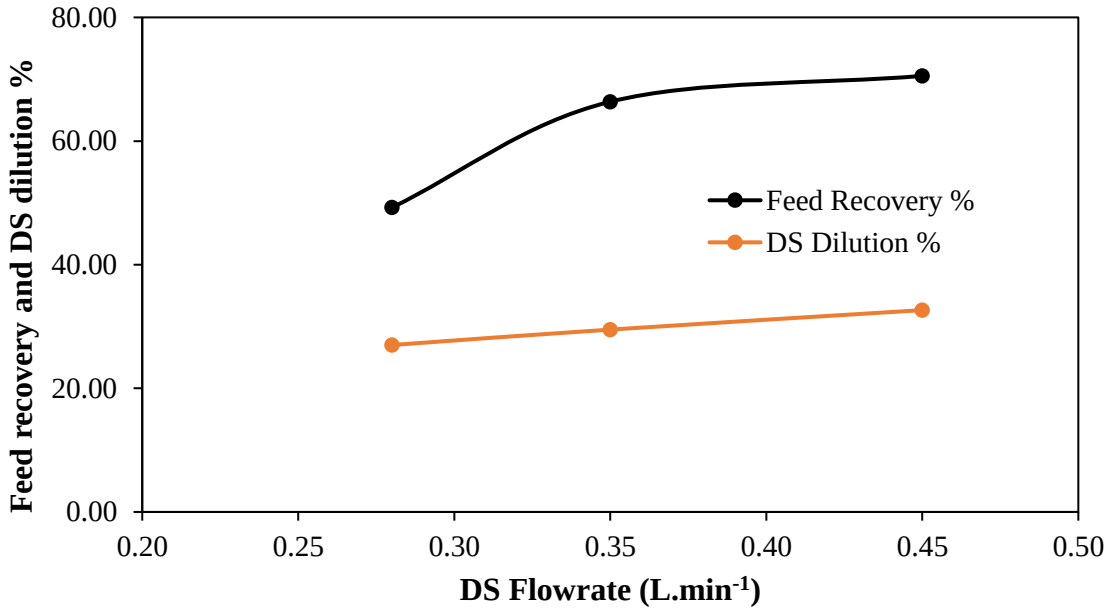

Figure 5-8: Effect of changing the DS flowrate at constant FS flowrate on the feed recovery and DS dilution rates using TOYOBO membrane.

The experimental results indicate that an overall increasing of DS flowrate by 60.71% contribute to 43.26% increase in feed recovery rate. When FS and DS flowrates were adjusted to 1.10 and 0.28 L.min^{-1} respectively, the osmotic concentration process successfully recovered around 49.24% of feed water. An additional of 34.77% increase in the recovery rate was distinguished when DS flowrate was turned higher into 0.35 L.min^{-1} at the same FS flowrate, rising the recovery rate of feed to around 66.36%. Further increasing the DS flowrate to 0.45 L.min^{-1}, the recovery rate was high reaching around 70.54%. Based on the obtained recovery rates, the amount of feed water recovered and change in volume can be determined. For all the three experiments, a FS flowrate of 1.10 L.min^{-1} during 2.00 hours operation means consuming 132.00 L per experiment.

Proceeding with the calculations for determining the volume of water recovered from the consumed amount leads to the results shown in *Table 5-5*. The outcomes of displayed water amounts disclose around 62.00% reduction in volume of feed water after three experiments running with different DS flowrate for unified operation time of 2.00 hours and FS flowrate of 1.10 $L.min^{-1}$.

Table 5-5: Amount of feed water recovered during operation at each DS flowrate where FS flowrate and operation time were maintained constant using TOYOBO membrane.

DS Flowrate (L/min)	Feed Water Consumed (L)	Feed water recovered (L)
0.28	132.00	64.99
0.35	132.00	87.59
0.45	132.00	93.11
Total	396.00	245.69

Table 5-5 shows that osmotic concentration process is effective in reducing the volume of feed water with increased feed recovery rate based on conditions of conducted experiments at the different DS flowrates. The initial 132.00 L of feed water needed to operate the experiments with the identified conditions are at feed recovery of zero. The charts in *Figure 5-9* reveals a descending trend of the unrecovered water with the increase in feed recovery

produced from alteration to high DS flowrate. This descending trend is a response to the increased amount of water being recovered at higher DS flowrate.

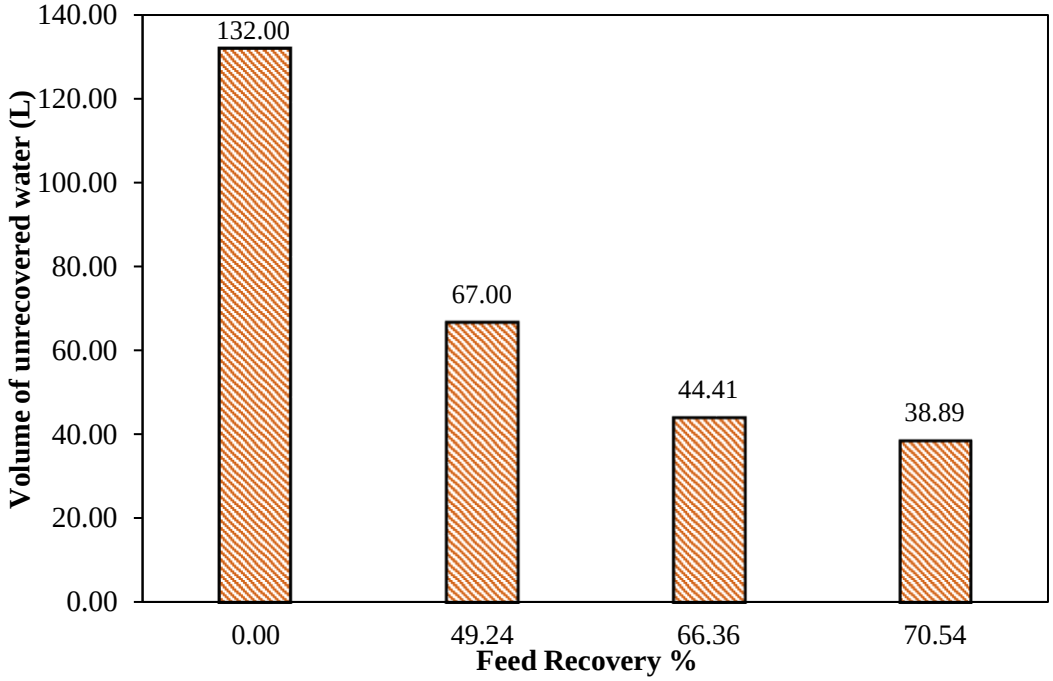

Figure 5-9: Change in the volume of feed water remaining unrecovered versus feed recovery rates resulted from testing different DS flowrates (0.28, 0.35, and 0.45 $L.min^{-1}$) at constant 1.1 $L.min^{-1}$ FS flowrate for 2 hours using TOYOBO membrane.

In addition to the positive relationship demonstrated between the feed recovery and the DS flowrate, *Figure 5-8* shows the effect of high DS flowrate causing more permeation rate on its dilution level. Throughout all the conducted experiments, the dilution rate of the DS found from equation (3-5) in chapter 3 slightly increased by 20.95% where DS flowrate increase was around 60.71%.

Adjusting the FS and DS flowrates to 1.10 and 0.28 L.min^{-1} respectively resulted in diluting the inlet DS stream by 27.00% which was determined from the increase in DS outlet stream flowrate. Increasing the DS flowrate to 0.35 L.min^{-1} dilutes the DS by around 29.50%. This indicates that shifting from 0.28 to 0.35 L.min^{-1} increased the DS dilution rate only by 2.50%. At the highest studied DS flowrate, the dilution of DS was estimated by 32.65%. The DS dilution trend emphasized the impact of high DS flowrate on drawing more permeate, thus the increased volume of water transferred to DS creates high reduction in its concentration.

Aside from the impact of DS flowrate on the rate of feed recovery, the water flux (J_w) and reverse solute flux (RSF) (J_s) trends were analyzed (*Figure 5-10*). Both J_w and J_s have increasing trends with the increase in the DS flowrate.

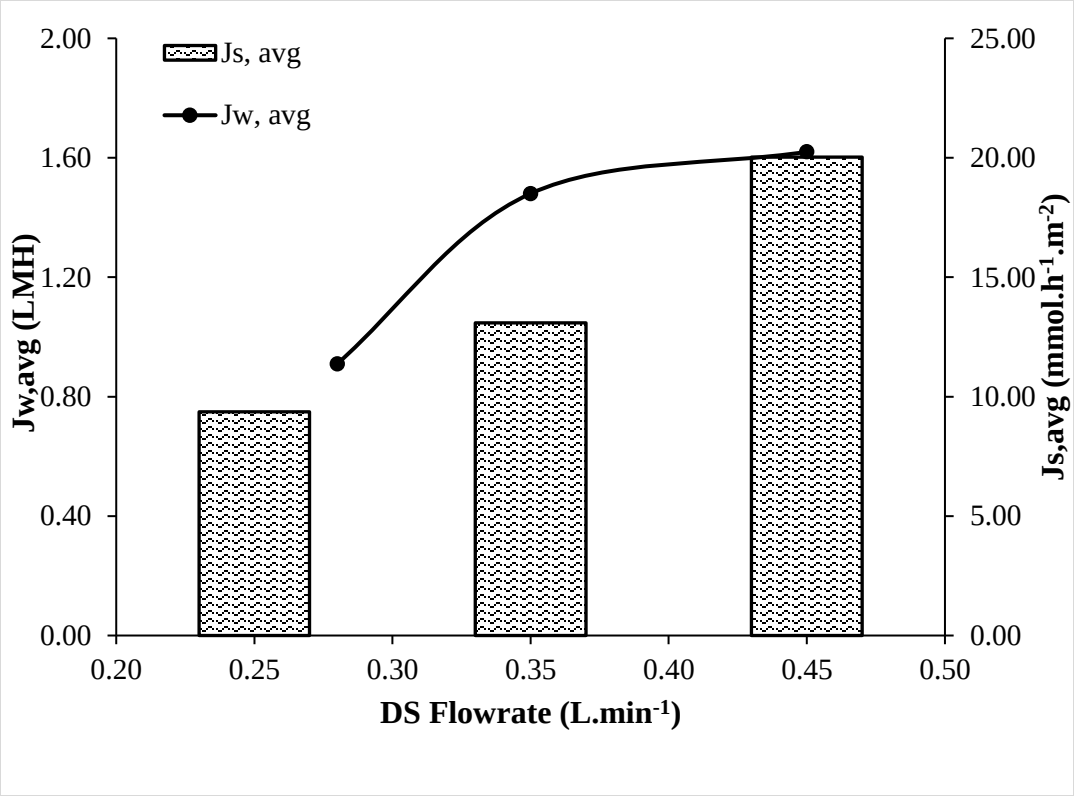

Figure 5-10: Effect of changing the DS flowrate at constant FS flowrate on the water flux (Jw) and reverse solute flux (Js) using TOYOBO membrane.

The average flux obtained at DS and FS flowrate of 0.28, 1.10 L.min^{-1} respectively is 0.91 LMH and increased by 62.64% to 1.48 LMH when the DS flowrate was increased by 25.00% to 0.35 L.min^{-1} at the same FS flowrate. Particular increase in the DS flowrate to 0.45 L.min^{-1} resulted in raising the average flux to 1.62 LMH. Therefore, the results show an approximate flux enhancement of 78.02% from 0.91 to 1.62 LMH when DS flowrate was increased by 60.71% from 0.28 to 0.45 L.min^{-1}.

The increase in the flux is a result to the high permeation rate induced by the high DS flowrate. This suggests that high DS flowrate generates high cross flow velocity shear force

which minimizes the cake enhanced concentration polarization (CECP) and dilution effect [12,223]. Therefore, the flux increases due to the increased driving force after replenishing the concentration of diluted DS at the membrane surface and this findings are in good agreement with the research of Hawari et al. who studied effect of high DS flowrate on water flux [224].

In a similar behavior to the possessed by the water flux (J_w), reverse solute diffusion to feed side increases at higher DS flowrates as indicated by the solute flux (J_s). Changing the DS flowrate from 0.28 to 0.45 prompted high occurrence of reverse solutes diffusion that was increased from 9.37 to 20.03 mmol.h^{-1}.m^{-2}. For a 25% increase in DS flowrate from 0.28 to 0.35 L.min^{-1}, the RSF increased by 39.70% from 9.37 to 13.09 mmol.h^{-1}.m^{-2}. The maximum reverse diffusion of solutes was determined at 0.45 L.min^{-1} for DS with flux reaching 20.03 mmol.h^{-1}.m^{2}. The RSF can be described by having a direct relation with water flux as described earlier in section 5.2.2.5.

5.2.3.2. Effect of changing the DS flowrate on the osmotic concentration process using NTU membrane.

The effect of changing the DS flowrate at constant FS flowrate was also investigated for NTU membrane module. Three experiments were conducted for the same flowrates conditions tested using TOYOBO membrane (DS flowrate of 0.28, 0.35 and 0.45 L.min^{-1} at constant FS flowrate of 1.1 L.min^{-1}). The performance of the pilot-scale system was evaluated during 2 hours of continuous operation where the temperature in the laboratory was around 17 °C. The profiles of water flux with time are shown in *Figure 5-11* for the

three experiments where the influence of DS flowrate used to draw feed water can be observed on the permeate water productivity.

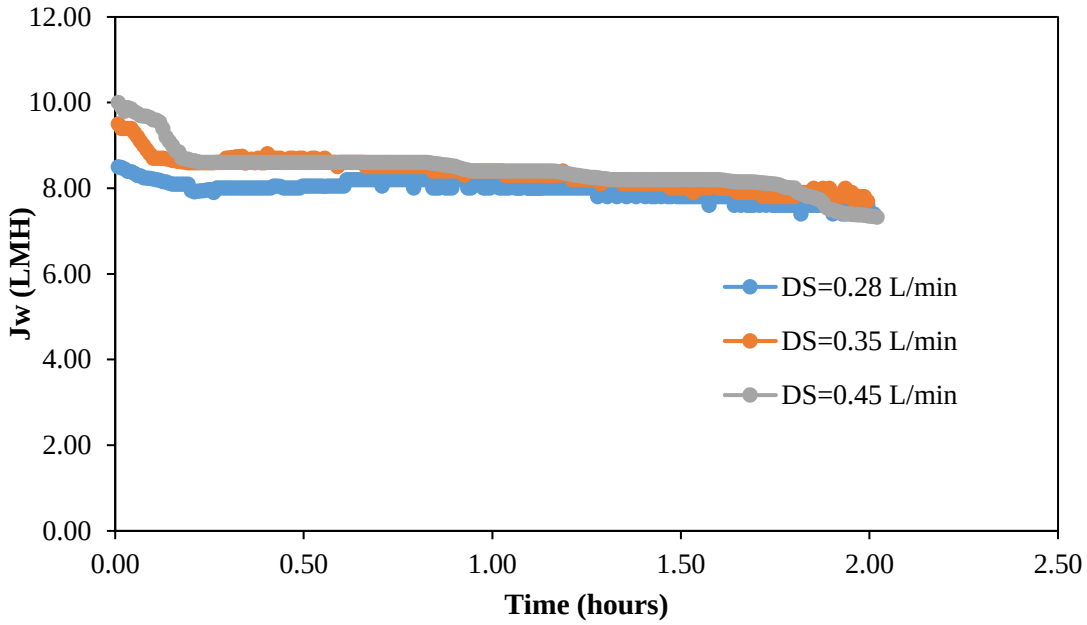

Figure 5-11: Water flux profile versus time of NTU membrane under different DS flowrates at constant FS flowrate.

The flux profiles show an increasing water permeability over the entire time of the experiment operated at high DS flowrate. At the high DS flowrate of 0.45 $L.min^{-1}$, the water flux reached 10.00 LMH compared to an obtained flux of 8.50 LMH as an effect of the lowest DS flowrate tested. In here, the nearly stable profiles also elucidates minimum decline in the osmotic driving force across the membrane sides and the ability of pilot system to work efficiently and produce reasonable data.

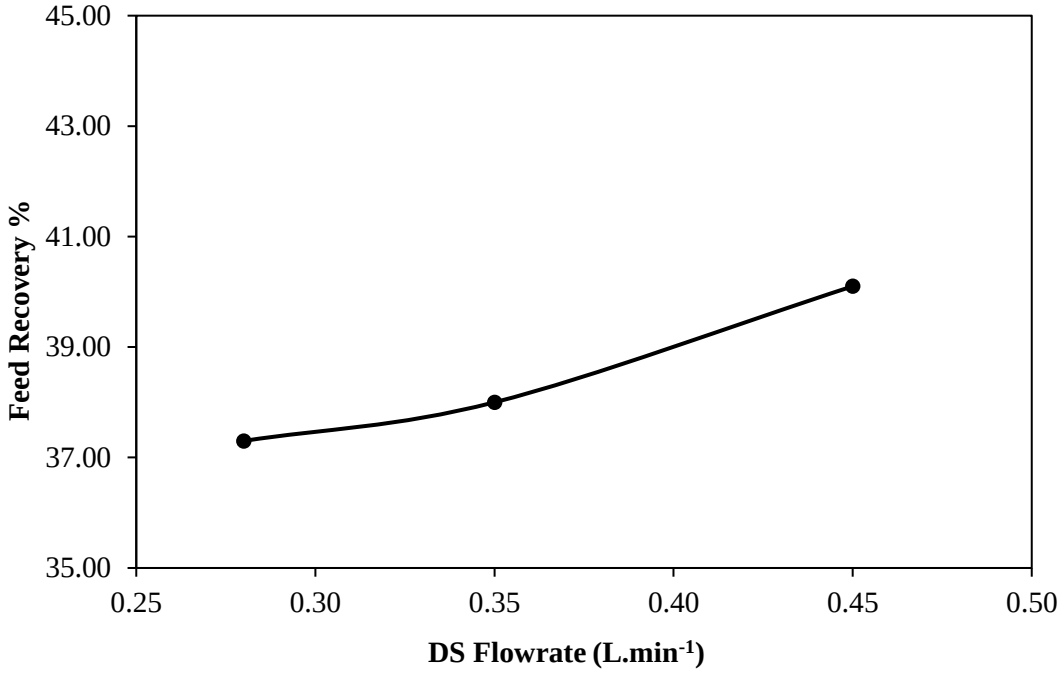

Figure 5-12: Effect of changing the DS flowrate at constant FS flowrate on the feed recovery rates using NTU membrane.

The examined effect of DS flowrate on the feed recovery rate was demonstrated in the trend of *Figure 5-12*. At the end of the experiment with DS flowrate of 0.28 $L.min^{-1}$, the NTU membrane was able to recover around 37.70% of feed water. Adjusting the DS flowrate to a 25% higher value (0.35 $L.min^{-1}$) enables recovering around 0.80% higher amount of feed water (38.00%). An overall increase in the DS flowrate by 60.70% up to 0.45 $L.min^{-1}$ results in 6.37% increase in the recovery rate, allowing the recovery of feed to reach 40.10%.

Based on the obtained recovery rates, the amount of feed water recovered and change in volume can be determined. For all the three experiments using NTU membrane, the FS

flowrate of 1.10 $L.min^{-1}$ was taken from initial 20.00 L feed water operated in recirculation mode where concentrated FS outlet stream pours inside it. Proceeding with the calculations for determining the volume of water recovered from the consumed feed water in recirculation mode leads to the results shown in *Table 5-6*.

Table 5-6: Amount of feed water recovered during operation at each DS flowrate where FS flowrate and operation time were maintained constant using NTU membrane.

DS Flowrate (L/min)	Initial feed water volume (L)	Feed water recovered (L)
0.28	20	7.46
0.35	20	7.60
0.45	20	8.02
Total	60	23.08

Figure 5-13 shows how the osmotic concentration process is effective in reducing the volume of feed water with increased feed recovery rate based on conditions of conducted experiments at the different DS flowrates. The initial 20.00 L of feed water needed to operate the experiments with the identified conditions are at zero feed. The plot in *Figure 5-13* reveals a descending trend of the unrecovered water with the increase in feed recovery

produced from alteration to high DS flowrate. This descending trend is a response to the increased amount of water being recovered at higher DS flowrate.

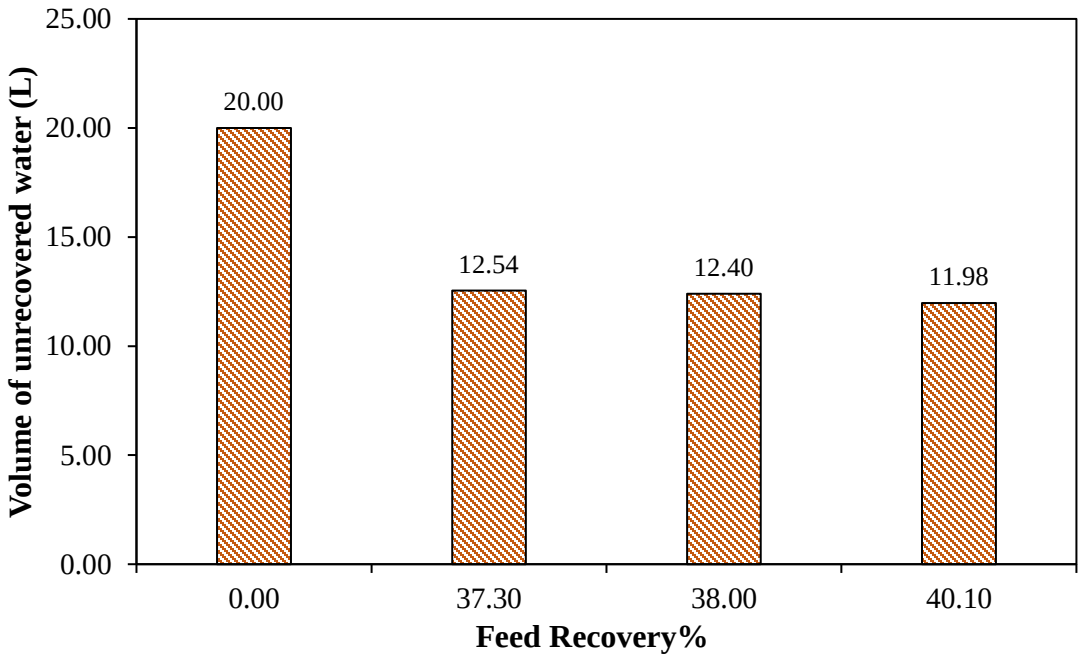

Figure 5-13: Change in the volume of feed water remaining unrecovered with the feed recovery rates resulted from testing different DS flowrates (0.28, 0.35, and 0.45 L.min^{-1}) at constant 1.1 L.min^{-1} FS flowrate for 2 hours using NTU membrane.

Figure 5-14 illustrates the influence of DS flowrate on producing increasing trends for the water flux (J_w) and reverse solute flux(J_s) as shown earlier for TOYOBO membrane. The positive role of high DS flowrate on increasing the feed recovery rate can certainly be translated into high J_w and J_s values due to the increased driving force. High DS flowrate stimulates high permeation of FS across the membrane, thus elevates the water flux as

described previously in 5.2.2.4. For the tested DS flowrate range (0.28-0.45 $L.min^{-1}$), the average flux obtained was in the range of 7.94 to 8.24 LMH. It is important to mention that the 60.70% increase in the DS flowrate was liable for a trivial improvement in water flux estimated by 3.77%.

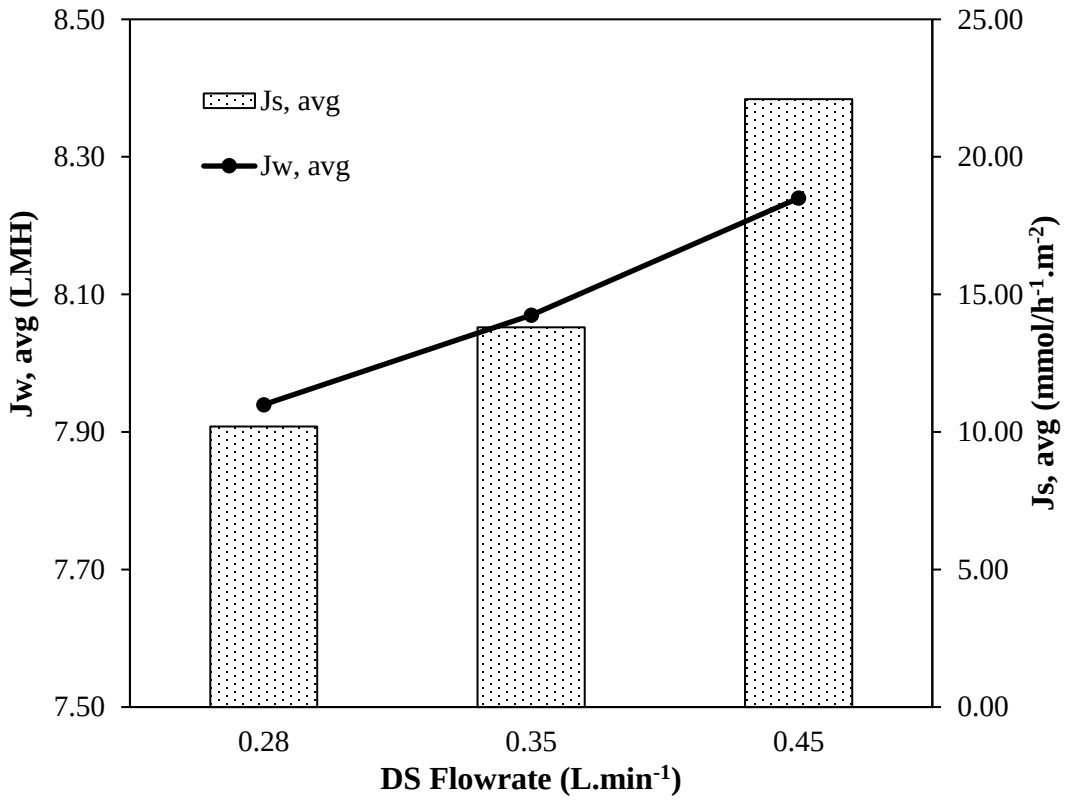

Figure 5-14: Effect of changing the DS flowrate on the water flux (Jw) and reverse solute flux (Js) using NTU membrane.

Likewise, the high DS flowrate induces higher transfer of DS solutes to the feed side as inferred by the NaCl salt mass balance calculations leading into high amount of reverse solute flux as shown in *Figure 5-14*. The straightforward relation of RSF with the water

flux is also confirmed in these experiments. RSF is desirable at the lowest DS flowrate of 0.28 $L.min^{-1}$ since it produces minimal reduction in the driving force and excludes the need for re-concentrating the DS. RSF was increased by 35.29% from 10.20 to 13.80 $mmol.h^{-1}.m^{-2}$ when DS flowrate changed by 25% from 0.28 to 0.35 $L.min^{-1}$. Further escalation in the DS flowrate to 0.45 $L.min^{-1}$ drives 60.14% increase in reverse diffusion of the solutes from 13.80 to 22.10 $mmol.h^{-1}.m^{-2}$. The increase in DS flowrate by 60.70% had a higher impact on RSF that was increased by 116.67% rather than the improving the water flux.

5.2.3.3. Two membrane modules comparison

In comparing with the results obtained at the same studied DS flowrates using the two HF membranes (TOYOBO and NTU), the different membrane area of each membrane has effect on RSF and water flux. The smaller area of NTU resulted in water flux in the range of 7.94 to 8.24 LMH when DS flowrate changed from 0.28 to 0.45 $L.min^{-1}$. Whereas, the flux attained using the larger TOYOBO module at the same three tested DS flowrates was in the range of 0.91 to 1.62 $L.min^{-1}$ smaller than NTU. The high water flux produced from smaller membrane module confirms the trends obtained earlier in section 5.2.2.4 which was proved by other studies [223,225,226].

5.2.4. Effect of changing the operation temperature on the osmotic concentration using TOYOBO membrane.

The experiments conducted with TOYOBO membrane for different DS flowrates (0.28, 0.35 and 0.45 L.min^{-1}) at 17 °C (section 5.2.3.1) were repeated when the surrounding temperature of the laboratory was increased to 27 °C during summer time. This section provides a comparison between the obtained trends for water flux and reverse solute flux at the two temperatures using the same membrane. Moreover, the determined effect of temperature on changing the feed recovery and DS dilution is to be demonstrated. This assists in drawing some conclusions about the role of temperature along with predicting the reasons for the changed behavior.

The impact of DS flowrate on the water flux (J_w) was compared at the two temperatures of 17 and 27 °C in *Figure 5-15*. It is demonstrated that adjusting high DS flowrate has an impact on increasing the amount of water permeates (J_w, LMH) at both temperatures. However, proceeding with the experiments during a warmer weather where the laboratory temperature was high supports in obtaining high flux values. The average flux of 0.91 LMH resulted from DS flowrate of 0.28 L.min^{-1} at temperature of 17 °C is increased by 37.36% when temperature raised by 10 °C. Besides, 25% increase in DS flowrate to 0.35 L.min^{-1} produced around 18.92% higher water flux estimated by 1.76 LMH at 27 °C rather than the 1.48 LMH generated at 17 °C. Lastly, the high temperature helped in improving the flux by 20.37% from 1.62 to 1.95 LMH at the highest tested DS flowrate of 0.45 L.min^{-1}. At the temperature of 27 °C, the flux increased by 56.00% when DS increased by 60.71% from 0.28 to 0.45 L.min^{-1}. It is worth mentioning that the J_w enhanced by 3.70% for each 1.00 °C increase moving from the operation at 17 °C to 27 °C when DS flowrate was 0.28

L.min^{-1}. Meanwhile, the improvement of flux was estimated by 2.00% for each 1.00 °C increase at DS flowrate of 0.35 and 0.45 L.min^{-1}. The influence of increasing both the DS flowrate from 0.28 to 0.45 L.min^{-1} and the temperature from 17 to 27 °C is determined by achieving 114.29% enhancement in the overall water flux. The useful role of increasing these two parameters simultaneously on improving the water flux was also confirmed previously [224]. Hawari et al. [224] elucidated around 93.30% flux improvement when DS flowrate is increased from 1.20 to 3.20 L.min^{-1} with temperature rise by 30% from 20 to 26 °C.

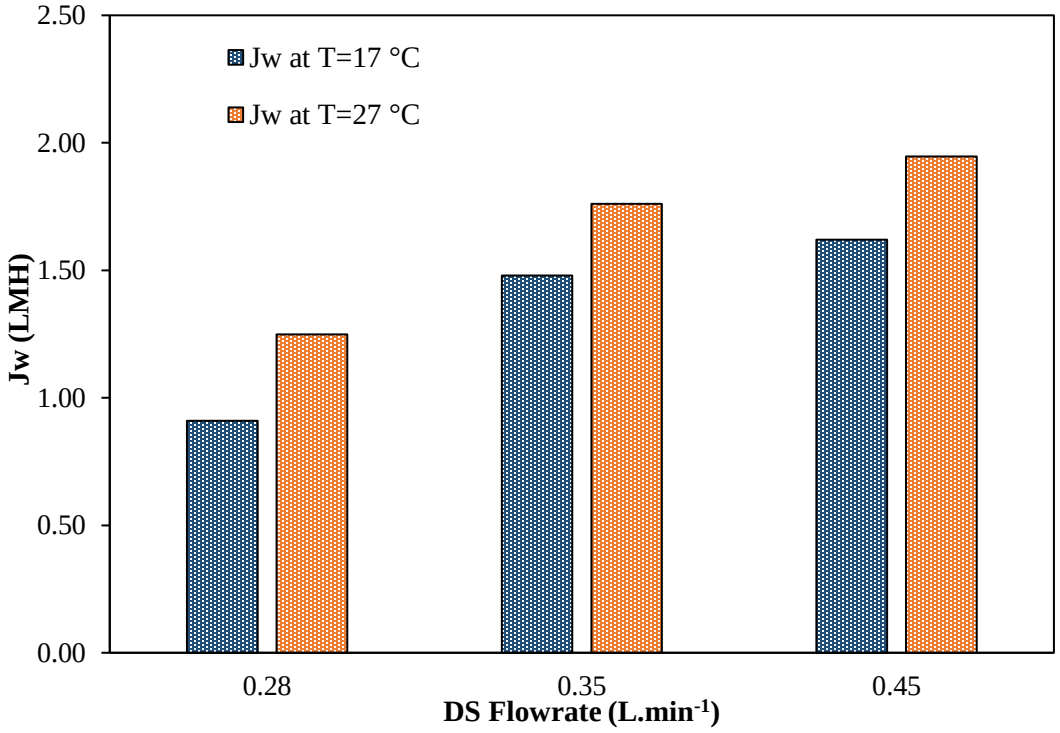

Figure 5-15: Comparison between the water fluxes (Jw) obtained at different DS flowrates with respect to temperature.

The acquired results indicated the favorable role of the high temperature in producing higher water flux values. The attained trends of flux at a higher temperature was confirmed by previous research studies on the FO process which investigated the temperature influence on the water and solute fluxes [111,232–237]. The high temperature of the surrounding leads to increase the temperature of the FS and DS inlet streams to the FO membrane modules. Thus, the increased temperature of the solutions works to alter the thermodynamic properties of the solutions represented by osmotic pressure, diffusivity and viscosity as reported earlier [238,239]. For instance, the direct impact of the temperature change on the osmotic pressure is presented by Van't Hoff's equation, in which any increase in temperature leads to higher osmotic pressure. Subsequently, the flux could be improved due to the enhanced osmotic pressure and driving force across the membrane. Furthermore, the high water flux is thought to be an output to the decreased viscosity that allows more diffusivity of water molecules through membrane's active and support layers, which in turn, increases the mass transfer. McCutcheon and Elimelech [85] designated the improved flux at high temperatures to the greatly reduced concentration polarization from the high diffusivity of the NaCl solutes. Higher diffusion coefficients of NaCl solutes in FS and DS reduces the impact of external concentration polarization (ECP) and lessens the solute resistivity in the porous layer of the membrane leading to reduced internal concentration polarization (ICP).

The reverse solute flux is known to be linearly related to the water flux as described in section 5.2.2.5, thus the improved J_w at higher temperature is accompanied with increased J_s at the same high temperature. The impact of DS flowrate on the RSF (J_s) was compared

for the two temperatures of 17 and 27 °C in *Figure 5-16*. The figure illustrates the higher reverse solute flux obtained for each DS flowrate at the higher temperature. To further explain the increasing trend of RSF with respect to temperature, the ICP got reduced at high temperature due to the less resistivity of NaCl solutes which boosted the back diffusivity of solutes to the feed side [229].

The comparison of the two RSF values obtained at each DS flowrate with respect to temperature yields 40.13%, 35.52% and 23.81% higher RSF for DS flowrate of 0.28, 0.35 and 0.45 $L.min^{-1}$ respectively at temperature of 27 °C. The obtained results indicate a decreasing trend for the flux enhancement at T= 27 °C with the increase in DS flowrate. For instance, the RSF improvement for each 1.00 °C when temperature raised from 17 °C to 27 °C is approximately equal to 4.00%, 3.55% and 2.38% for DS flowrate of 0.28, 0.35 and 0.45 $L.min^{-1}$.

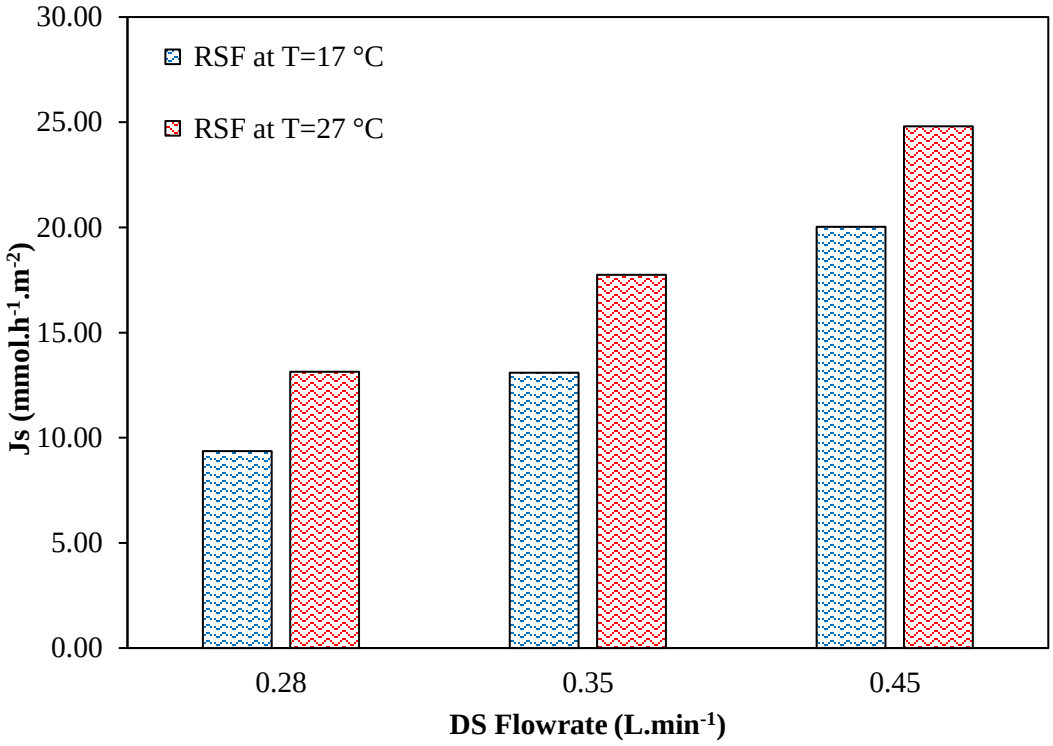

Figure 5-16: Comparison between the reverse solute fluxes (Js) obtained at different DS flowrates with respect to temperature.

Moreover, as the above-mentioned results proved the improvement of water flux with the temperature, it is of extreme significance to demonstrate the rate percentages of achieved feed recovery and DS dilution. *Figure 5-17* shows the effect of both temperature and DS flowrate change on the amount of feed recovered along with the attained DS dilution level. Despite the nearly constant DS dilution with DS flowrate change illustrated in the trends, it is obvious that DS dilution increases at higher temperature of DS. Besides, the feed recovery increases with changing both the DS flowrate and the solutions temperature. This indicates that the elevated feed recovery at the higher temperature is a result to the high water flux and amount of water permeated through the membrane. Therefore, high

permeation from FS to DS at high temperature will assure increased dilution rate from the initial concentration of the DS.

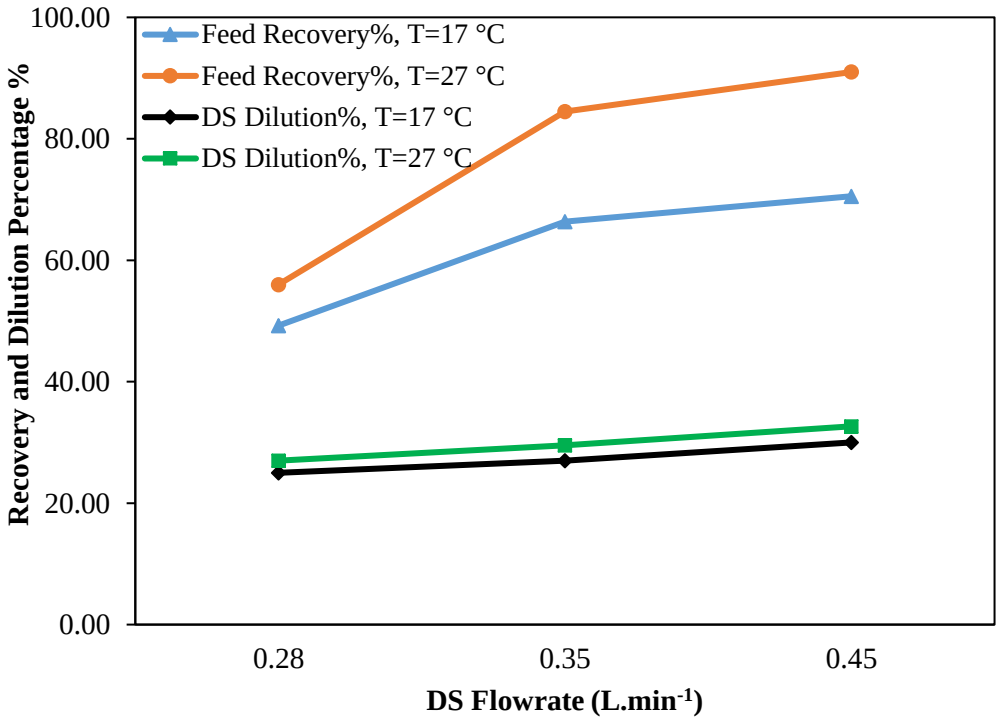

Figure 5-17: Comparison between the feed recovery and DS dilution obtained at different DS flowrate with respect to temperature.

For 58.8% and 60.71% increase in the temperature and DS flowrate respectively, the overall achieved feed recovery enhancement is estimated by 84.41%. At the lowest DS flowrate of 0.28 L.min^{-1} and temperature of 17 °C around 49.24% of feed water inlet stream was recovered compared to 91.00% of inlet feed water recovered at the highest DS flowrate of 0.45 L.min^{-1} and temperature of 27 °C. Around 49.24% of feed was recovered at the

initial DS flowrate of 0.28 L.min^{-1}, then 66.36% of feed water was recovered when DS flowrate was increased by 25% at the temperature of 17°C. Following that, feed water recovery was increased by 6.29% where 70.54% of feed water inlet stream was reclaimed at the same temperature. *Figure 5-17* interprets those results as trends showing that feed recovery approaches a plateau with further increase in DS flowrate after 0.35 L.min^{-1}. At temperature of 17 °C, the attained rates of feed recovery were 49.24%, 66.36% and 70.54% for DS flowrate of 0.28, 0.35 and 0.45 L.min^{-1} respectively. Moreover, the acquired rates of feed recovery at 27 °C were 56.00%, 84.50% and 91.00% for DS flowrate of 0.28, 0.35 and 0.45 L.min^{-1} respectively being higher at each tested flowrate.

In contrast, raising the temperature and DS flowrate by same percentages has insignificant impact on changing the DS dilution. The DS was diluted by around 30.60% when temperature increased from 17 to 27 °C and DS flowrate was adjusted into higher values from 0.28 to 0.45 L.min^{-1}. The obtained results show that dilution increased slightly from 25% to 30.00% and from 27% to 32.65% at temperature of 17 °C and 27 °C respectively.

5.2.5. Experimental results of evaluating the integrity and stability of osmotic concentration pilot-unit long-term run.

The integrity and operational stability of the constructed pilot FO unit were evaluated through long-term run. Additionally, the performance of the stability experiments conducted at 17 °C was evaluated for 48 hours of continuous operation to achieve 75% feed recovery. Lastly, for the sake of assessing the performance, the water flux (J_w) is the main parameter of interest that was monitored to check its stability throughout the entire run.

As stated earlier, the aim of the long-term stability experiment is recovering 75% of feed water and according to the explained previously in section 5.2.2.1; the manipulation in FS and DS flowrates is required for achieving the desired recovery rate using TOYBO membrane. Therefore, the FS and DS flowrates were adjusted to 1.00, 0.35 L.min^{-1} giving the 75% feed recovery at the temperature of 17 °C. The water flux trend obtained during the entire experiment is illustrated in *Figure 5-18*. The closely stable flux trend during the 48.00 hours indicates the successful operation of the pilot unit. For the objective of 75% feed recovery, the initial average flux achieved was around 1.60 LMH and reduced to 1.47 LMH with time because of the diminished driving force.

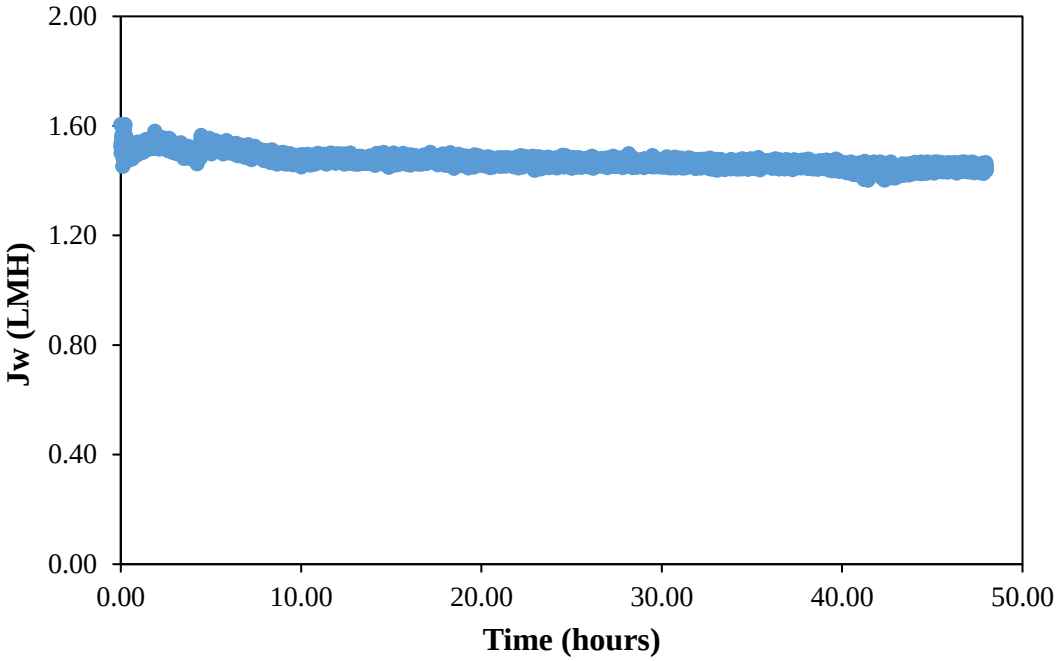

Figure 5-18: Water flux trend with time for long-term stability experiment using TOYOBO membrane.

In comparison with the experiment conducted at 27 °C for the same 75% feed recovery (section 5.2.2.1 and 5.2.2.4), difference in adjusted flowrates and obtained flux can be recognized. The 75% recovery was achieved at higher FS flowrate of 1.35 $L.min^{-1}$ at temperature of 27 °C compared to achieving it at lower FS flowrate of 1.00 $L.min^{-1}$ when temperature was 17 °C. The pumped flowrate at 27 °C has to be higher to account for the greater water flux at the elevated temperature. The DS flowrate in both cases was kept constant at 0.35 $L.min^{-1}$ for diluting the DS by 75%. Moreover, the average flux obtained during the experiment at 27 °C was around 1.90 LMH and reduced by 22.63% to 1.47 LMH at 17 °C.

In contrast to the manipulation with flowrates to achieve the target recovery rate using TOYOBO membrane, the operational methodology for NTU membrane requires changing the level of feed concentration at each desired recovery. The long-term testing for NTU membrane was performed at FS and DS flowrates of 1.50 $L.min^{-1}$ and at a surrounding temperature of 17 °C. By operating the FS at recirculation mode to increase the conductivity in inlet feed tank, the conductivity was maintained constant when 75% of initial feed water was recovered by diluting it with FS water whenever it gets increased.

Figure 5-19 demonstrates the water flux trend with time for the 48.00 hours of continuous operation. At the beginning of the experiment when recovery was very low around 0.45%, the obtained flux was 10.00 LMH. Following that with the increase in the feed recovery rate, approximately after 3.60 hours the flux declined to 6.20 LMH when 75% of feed water was recovered. Subsequently, the flux maintained steady trend at an average flux of 6.00 LMH throughout the remaining 44.40 hours of experimental time. Comparing the obtained flux of this test with the previous test at 27 °C, the flux at the higher temperature (27 °C) was 8.80 LMH and 46.6% higher than that at 17 °C. The main reason behind the flux decline at lower temperature is the increased solutions' viscosity and decreased diffusivity of water molecules passing through the membrane active layer as explained previously in section 5.2.4.

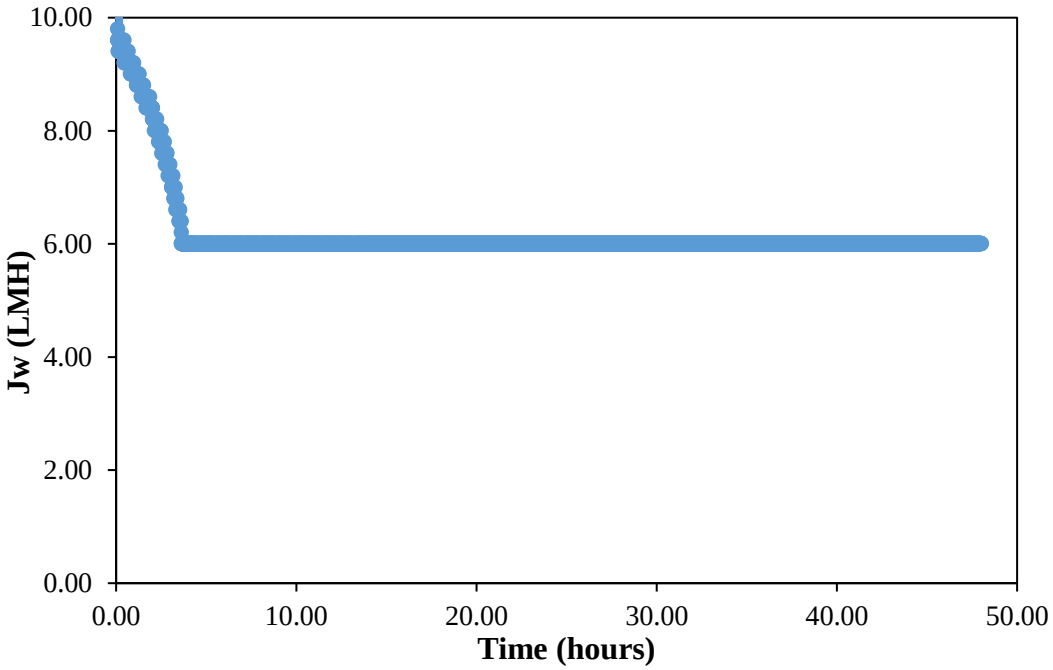

Figure 5-19: Water flux trend versus time for long-term stability experiment using NTU membrane.

5.2.6. Evaluation of membranes' intrinsic properties at different operating temperatures.

5.2.6.1. Water and salt permeability coefficient

The water and salt permeability coefficients (A and B) were determined according to the FO membrane testing protocol explained earlier in chapter 3. The transport parameters of FO membrane (A and B) are considered intrinsic properties since they are independent on the change in some of the operational conditions including flowrates and concentration of DS [235]. In addition, the permeability experiments were performed at different operation temperatures approximated by (20, 24, and 30 °C) to disclose the temperature effect on the permeability evolution. In *Figure 5-20* and *Figure 5-21* the water and salt permeability coefficients (A and B) values respectively are presented for both membranes. The depicted results demonstrate the high temperature effect on increasing both permeability coefficients. The temeprature effect on the intrinsic properties of several tested FO membranes represented by A and B values also proved the higher permeability coefficients at higher temepratures [235,236,239]. The higher permeability reffered to higher A and B values at elevated temperature is attributed to the enhanced solutions diffusivity and decreased viscosity. Thus, allowing the water and salt to transport through the memrbane's active layer at a higher rate [239].

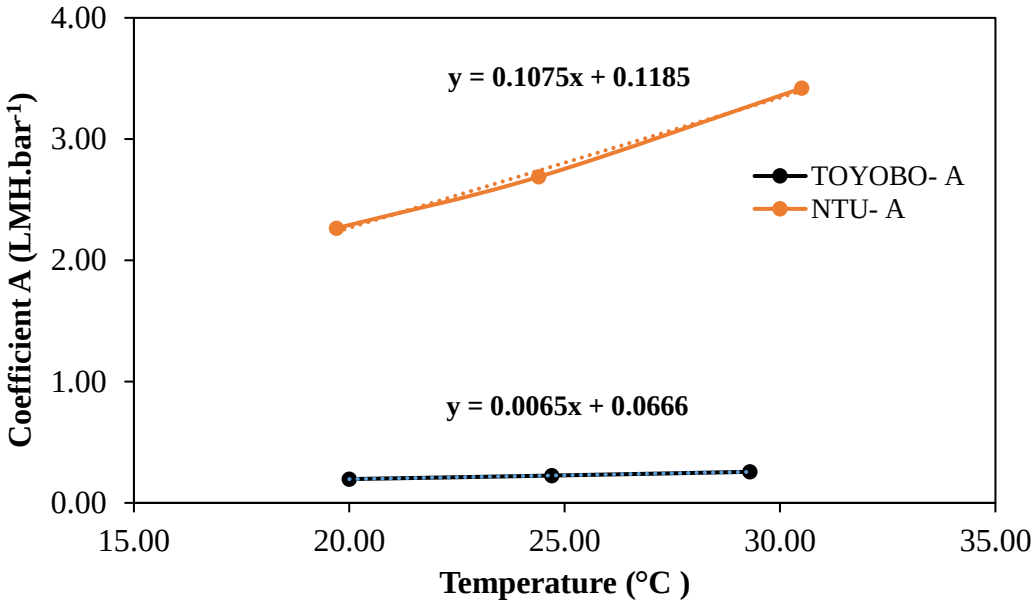

Figure 5-20: Water permeability coefficient (A) for TOYOBO and NTU membranes at different temperatures.

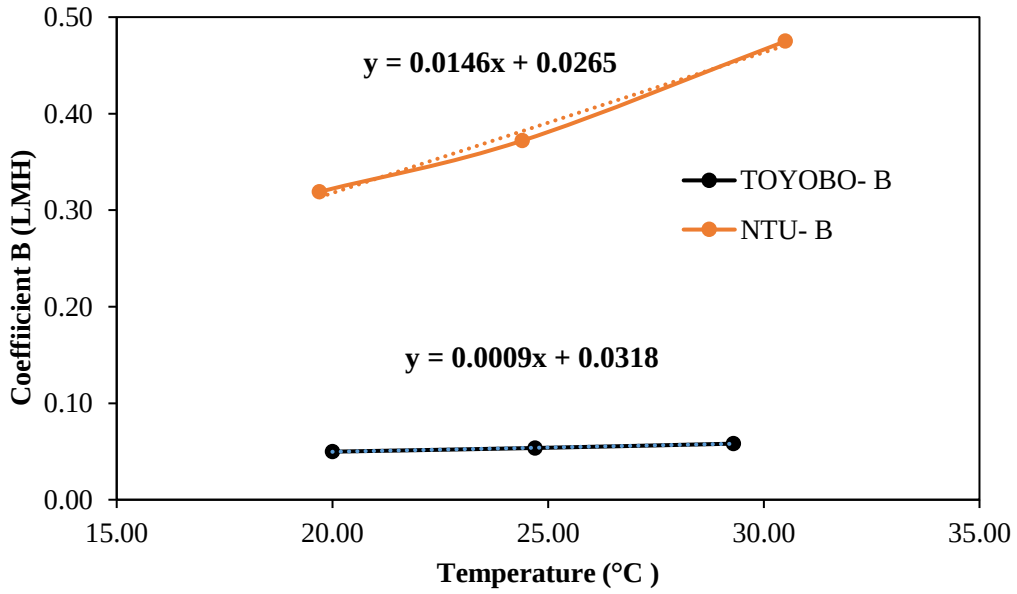

Figure 5-21: Salt permeability coefficient (B) for TOYOBO and NTU membranes at different temperatures.

The experiments illustrated higher water and salt permeability coefficients for NTU compared to TOYOBO memrbane. The large memrbane area of the commercial TOYOBO module is a factor resulting in lower A (LMH.bar^{-1}) and B (LMH) values. For TOYOBO memrbane, when temperature is increased by around 46.50% from 20.00 to 29.30 °C the A increased by 30.50% from 0.19 to 0.27 LMH.bar^{-1}. The water permeability coefficient A for TOYOBO relation with temperature fitted a linear model where the coefficient of determination is 0.9994.

$$A = 0.0065\,T + 0.0666 \qquad (5\text{-}2)$$

The salt permeability coefficient B for TOYOBO experienced slight change with the temperature increase. For instance, the 46.50% temperature elevation had rasied the B by 16.67% and had 13.93% lower impact on B compared to A. Higher coefficient B value indicates the membrane is capable to achieve high salt rejection rates. The attained B values are 0.049, 0.053 and 0.058 LMH at temperature of 20.00, 24.70 and 29.30 °C respectively.

$$B = 0.0009\,T + 0.0318 \qquad (5\text{-}3)$$

On the other hand, the A value for NTU increased by around 50.90% when 54.82% raise in temperature occurred. At a temperature of 19.70 °C A is 2.27 LMH.bar^{-1}, and increased to 2.69 and 3.42 LMH.bar^{-1} when operation temperature was shifted into 24.40 and 30.50 °C respectively. The data obtained can fit a linear model yielding 0.9941 determination coefficient.

$$A = 0.1073\,T + 0.1185 \qquad (5\text{-}4)$$

Moreover, B values of NTU membrane follow the same increasing trend with temperature. However, the 54.82% increase in temperature had increased the salt permeability coefficient by 48.90% making 2.00% less effect compared to *A* values. For the three experiments conducted at 19.70, 24.40 and 30.50 °C, the corresponding *B* values are 0.32, 0.37 and 0.48 LMH respectively and fitted to the following linear model with determination coefficient of 0.9883.

$$B = 0.0146\,T + 0.0265 \qquad (5\text{-}5)$$

Lastly, the empirical correlations obtained for temperature and permeability coefficients serve in the determination of the A and B values for these two membranes at any operation temperature other than in the tested range.

5.2.6.2. Water and salt permeability coefficients normalized with the membrane area.

The determination of water and salt permeability for the total area of each membrane can be achieved by normalizing the A and B values with respect to the area of each membrane. The normalization is done for the same discussed A and B values in section 5.2.6.1. *Figure 5-22* and *Figure 5-23* depict the trends of A and B for the total area of each membrane ($(A \times a_m)$ and $(B \times a_m)$) with temperature.

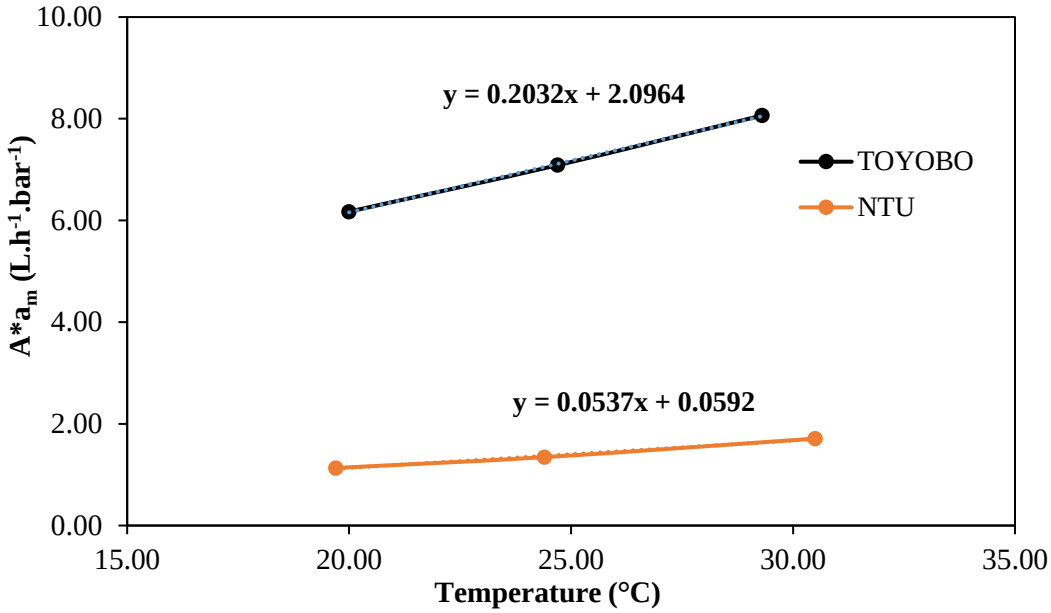

Figure 5-22: Water permeability of TOYOBO and NTU for the total area of each membrane.

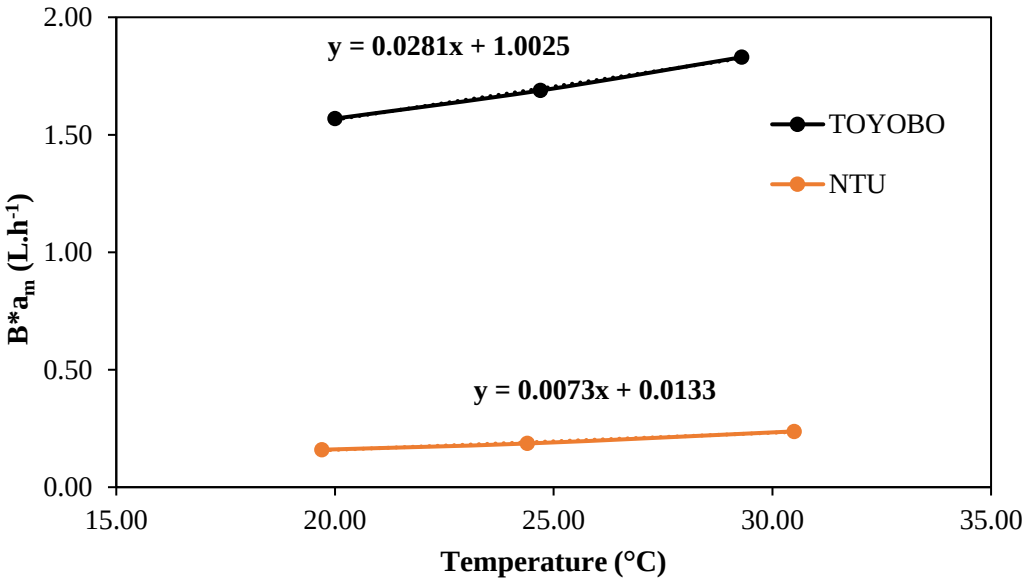

Figure 5-23: Salt permeability of TOYOBO and NTU for the total area of each membrane.

Looking at the graphs, the larger membrane area of TOYOBO has an advantageous influence on allowing higher water and salt permeability measured in $L.h^{-1}.bar^{-1}$ and $L.h^{-1}$ compared to NTU membrane. This indicates that the HF membrane with larger area ensures higher permeability of solvent and solute through all its fibers. The water permeated in TOYOBO ($L.h^{-1}.bar^{-1}$) through the operation temperature of 20.00, 24.70 and 29.30 °C is estimated by 6.17, 7.09 and 8.06 $L.h^{-1}.bar^{-1}$ respectively. The 46.50% temperature increase resulted in 30.60% enhancement to the water permeated through the membrane area. These data can also be fitted to a linear model with determination coefficient of 0.9994.

$$A \times a_m = 0.2032\,T + 2.0964 \qquad (5\text{-}6)$$

Perceiving the trend of water permeation through NTU membrane module, the amount of water in $L.h^{-1}.bar^{-1}$ is 81.60% less than that of TOYOBO at an approximated temperature of 20.00 °C. The water permeation evolution in NTU was estimated by 50.80% for 54.80% elevated temperature from initial of 19.70 °C. At the initial temperature of 19.70 °C, 1.13 $L.h^{-1}.bar^{-1}$ was permeated compared to 1.35 and 1.71 $L.h^{-1}.bar^{-1}$ permeated at 24.40 and 30.50 °C. In addition, these data can help in predicting the linear relationship between temperature and water permeation as per the following model with 0.9941 estimated determination coefficient.

$$A \times a_m = 0.0537\,T + 0.0592 \qquad (5\text{-}7)$$

In comparison, salt permeation was lower than the water permeation for both membrane modules as illustrated in Figure 5-23. However, the TOYOBO succeeds in maintaining higher salt permeation ($L.h^{-1}$) in addition to the water permeation ($L.h^{-1}.bar^{-1}$). For the first

tested operation temperature of 20.00 °C approximately, the salt permeation across NTU was 89.87% lower than in TOYOBO.

For TOYOBO and for the same 46.50% temperature increase from 20.00 to 29.30 °C, salt permeability increased from 1.57 to 1.83 $L.h^{-1}$ by around 16.63%. The linear model fitting these data is as following with a determination coefficient of 0.997:

$$B \times a_m = 0.0281\,T + 1.0025 \quad (5\text{-}8)$$

In the case of using NTU membrane, salt permeation was improved by 49.69% when temperature was raised by 54.80%. Moving from the operation at a temperature of 19.70 °C to the operation at a temperature of 29.30 °C, the salt permeability increased from 0.16 to 0.24 $L.h^{-1}$. The linear model of the obtained salt permeation with temperature trend is presented with determination coefficient of 0.9883.

$$B \times a_m = 0.0073\,T + 0.0133 \quad (5\text{-}9)$$

5.3. Conclusions

The pilot-scale evaluation of two FO hollow fiber membranes for the osmotic concentration of and volume reduction of feed water was accomplished through this study. The obtained results and trends revealed the following conclusions:

i- The two tested membranes (TOYOBO and NTU) succeeded in recovering up to 90% of feed water by manipulation in flowrates of FS and DS inlet streams, and feed concentration respectively according to their operating principles.

ii- The higher the rate of feed recovery achieved, the lower the produced water flux and reverse solute flux. The commercial TOYOBO membrane of larger area than NTU membrane in the pre-commercial stage produced lower water flux and higher reverse solute flux compared to NTU at the same investigated feed recovery rates.

iii- The pilot-scale osmotic concentration unit was capable for continuous operation of 48 hours and successfully recovered 75% of feed water. The water flux trends produced by two membranes were stable indicating minimal decline in the driving force.

iv- The higher the DS flowrate, the higher the permeation rate and the higher the achieved water flux through the two membranes. Besides, the greater permeation of feed water by high DS flowrate increased the rate of feed water recovered. However, high DS flowrate increased the undesired phenomenon of DS solutes reverse diffusion to FS.

v- The high temperature induces the production of high water flux by the altered thermodynamics properties and increased diffusivity of water molecules across the

membrane active layer. Nevertheless, operation at high temperature has favorable role in increasing the rate of feed water recovery and reducing feed volume.

vi- The evaluation of water and salt permeability coefficients of membranes at high temperature resulted in greater permeability coefficients values. Testing the permeability of TOYOBO membrane demonstrated lower water and salt permeability coefficients in $LMH.bar^{-1}$ and LMH respectively than NTU membrane. Despite the low permeability coefficients of TOYOBO when compared with NTU, normalizing the permeability coefficients by considering the area of each membrane discloses the higher amount of water permeation ($L.h^{-1}.bar^{-1}$) and salt permeation ($L.h^{-1}$) through TOYOBO membrane.

Chapter 6 : Conclusions and Future Prospects

6.1. Conclusions

The ultimate objective of this study is to demonstrate the cost-effectiveness of FO technology for wastewater reclamation and assess its technical viability when implemented for osmotic concentration (OC) at pilot-scale level. To accomplish this main objective, technoeconomic analysis of the whole-life cost of FO process needs to be established to estimate the net present value (NPV) of the process and declare its effectiveness over the other classical approaches (i.e. reverse osmosis (RO)). Additionally, a comprehensive knowledge of FO system's components and process parameters is required to construct the OC pilot-plant and evaluate its performance. Therefore, the following conclusions are drawn from this research study:

1- Economic study of two treatment options namely conventional membrane bioreactor-reverse osmosis (MBR-RO) and novel membrane bioreactor- forward osmosis (MBR-FO) processes is investigated for determining the net present value (NPV) for each process. This was complemented by capturing CAPEX data from published results of some existing installations and making use of analytical expressions and CAD software for energy demand estimation that is transferred into OPEX value. The resulted trend revealed that at a defined permeate flow of 10,000 $m^3.d^{-1}$, the cost benefit of MBR-FO is estimated by its 20% less NPV compared to MBR-RO. However, when low TDS wastewater treatment is compared using both options operating for 10,000 $m^3.d^{-1}$ permeate flow, the MBR-FO and MBR-RO processes have approximately the same NPV with no cost benefit of one over the other alternative.

2- OC pilot plant was constructed with a capacity of 5 m^3 from the synthetically prepared feed water mimicking the salinity of the Qatari's oil/gas produced and process water and for the purpose of concentrating it osmotically. The feed water salinity is 2000 $mg.L^{-1}$ and it got concentrated as part of it was transferred by the action of the 40000 $mg.L^{-1}$ draw solution (DS) mimicking the gulf seawater salinity. The examination of OC pilot plant performance was performed using two hollow fiber (HF) FO membranes, owing to the high water recovery of this configuration. Using the large TOYOBO membrane that is capable of approaching high water recovery rate in the pilot plant, the feed solution (FS) and the DS streams are in once-through mode. In comparison, the utilization of smaller NTU membrane restricted the achievement of high water recovery rates and induced the need for recirculating the outlet concentrated FS into the intake FS tank, while maintaining the one pass mode of DS.

3- Both HF FO membranes were tested for achieving 60%, 68%, 75% and 90% feed water recovery percentages. It was recognized that regulating low FS volumetric flowrate produced high feed recovery rate as a result of the high permeate water flow generated compared to the low permeate flow produced at high FS flowrate and translated into low recovery% during TOYOBO testing. The highest feed recovery of 90% was successfully achieved at a flowrate of 1.00 $L.min^{-1}$. On the other hand and during NTU membrane testing, the flowrates were maintained constant and 90% recovery of feed water was achieved when the conductivity of intake FS tank was increased from 4000 $\mu S.cm^{-1}$ to 19460 $\mu S.cm^{-1}$.

4- The effect of changing the feed recovery rate on the water productivity (water flux 'Jw') and reverse solute flux (RSF 'Js') trends were also studied. It was observed that

the increase in the rate of feed water recovery had a slightly negative impact on OC performance by lowering the produced water flux. The OC pilot plant using NTU membrane succeeded in recovering 60% of feed water at a maximum produced water flux of 11.28 LMH while producing a water flux of 6.54 LMH when 90% of feed was recovered at 27 °C. However, the reduced driving force through the large TOYOBO membrane attributed to the production of 2.24 LMH and 1.66 LMH water fluxes at 27 °C. In contrast, increasing the rate of feed recovery was advantageous in reducing the unfavorable reverse solute diffusion from DS side to FS side. Moreover, the stability of the OC pilot plant was investigated at the long-term by maintaining the continuous operation for 48 hours and at the conditions to recover 75% of feed water at an operational temperature of 17 °C. Consequently, the OC pilot plant had effectively recovered 75% of feed with an average produced flux of 1.47 LMH and 6.00 LMH using TOYOBO and NTU membranes respectively.

5- Effects of changing the operating conditions such as DS flowrate and operational temperature were also examined. It was proved that higher DS flowrate increases the water permeation, the maximum water flux values of 1.62 LMH and 8.24 LMH at DS flowrate of 0.45 $L.min^{-1}$ were obtained using TOYOBO and NTU membrane modules respectively. At the highest tested DS flowrate (0.45 $L.min^{-1}$), TOYOBO membrane was distinguished by recovering up to 70.54% of feed water, however maximum of 40.10% recovery rate was obtained during testing the NTU membrane. Moreover, the temperature effect on the performance of OC process was investigated by repeating the varied DS flowrate experiments at operation temperature of 27 °C. The acquired trends have indicated the desirable role of high temperature in improving the feed recovery

and water flux from the reduced viscosity and enhanced diffusivity of water; however, it has adverse role in increasing the RSF. At the highest tested DS flowrate (0.45 $L.min^{-1}$), the water flux was increased from 1.62 LMH (T= 17 °C) to 1.95 LMH (T=27 °C) and the higher temperature empowered the process to recover around 91% of feed water rather than 70.54% recovery rate achieved at lower temperature. Unfortunately, the lowered resistivity of solutes at the higher temperature (T=27 °C) boosted the back diffusivity of NaCl solutes to FS side by 23.80%.

6- The transport parameters of both tested HF FO membranes including water and salt permeability coefficients (A and B) were determined. This was accomplished by using deionized water and NaCl rich solution as FS for coefficient A and B experiments respectively, pressurizing the membrane and analyzing the collected permeate. Besides, the temperature effect on changing these intrinsic properties of FO membranes was also evaluated by conducting the experiments at temperatures of (20, 24, 30 °C). The highest temperature proved obtaining highest membrane permeability coefficients. At the highest tested temperature, coefficient A values are 3.419 and 0.256 $LMH.bar^{-1}$ and coefficient B values are 0.475 and 0.0581 LMH for NTU and TOYOBO membranes respectively. Despite the low permeability coefficients of TOYOBO when compared with NTU, normalizing the permeability coefficients by considering the area of each membrane discloses the higher amount of water permeation ($L.h^{-1}.bar^{-1}$) and salt permeation ($L.h^{-1}$) through TOYOBO membrane.

6.2. Future Prospects

Notwithstanding the successful operation of the OC pilot plant demonstrated for volume reduction of synthetic feed water mimicking real conditions, the investigation of OC pilot plant using the real produced and process water (PPW) effluent from Qatargas facilities will be executed in the future. Real PPW experimentation is intended to elucidate the pilot plant reliability in providing similar findings to the attained through this research study and demonstrate whether the PPW effluent characteristics diverge the OC process performance. A successful proof of concept for OC testing synthetic and real PPW effluents at pilot-scale will expedite the adoption of the technology at full-scale by relevant industries across the state of Qatar and will further spread it worldwide. Along with that, novel draw solutions can be developed as alternatives capable of producing convincing outcomes, providing that it should be of high osmotic pressure, cost effectiveness, environmental friendly materials and easy regeneration methods. For an improved and optimal performance of OC pilot plant, optimization of some defined operating parameters can be carried out. The FS and DS flowrates and osmotic driving force have a critical role on changing the feed recovery, water flux and reverse solute flux. Therefore, FS and DS flowrates along with DS concentration can be studied over specific ranges to determine the optimum values featured by providing the ideal responses of OC process. Nevertheless, the susceptibility of FO membrane to fouling can be examined via the addition of foulants to feed water. This allows evaluating the reduced water productivity and feed recovery of OC process along with determining the maximum foulants dosage that can be sustained by FO membrane without significant performance drop.

References

[1] R.L. McGinnis, M. Elimelech, Global Challenges in Energy and Water Supply: The Promise of Engineered Osmosis, Environ. Sci. Technol. (2008) 8625–8629. http://pubs.acs.org.ezproxy.nottingham.ac.uk/doi/full/10.1021/es800812m.

[2] B. Van Der Bruggen, P. Luis, Forward osmosis: Understanding the hype, Rev. Chem. Eng. 31 (2015) 1–12. https://doi.org/10.1515/revce-2014-0033.

[3] T.S. Chung, L. Luo, C.F. Wan, Y. Cui, G. Amy, What is next for forward osmosis (FO) and pressure retarded osmosis (PRO), Sep. Purif. Technol. 156 (2015) 856–860. https://doi.org/10.1016/j.seppur.2015.10.063.

[4] I.L. Alsvik, M.B. Hägg, Pressure retarded osmosis and forward osmosis membranes: Materials and methods, Polymers (Basel). 5 (2013) 303–327. https://doi.org/10.3390/polym5010303.

[5] A.M. Awad, R. Jalab, J. Minier-Matar, S. Adham, M.S. Nasser, S. Judd, The status of forward osmosis technology implementation, Desalination. 461 (2019) 10–21.

[6] W. Luo, F.I. Hai, W.E. Price, W. Guo, H.H. Ngo, K. Yamamoto, L.D. Nghiem, Phosphorus and water recovery by a novel osmotic membrane bioreactor-reverse osmosis system, Bioresour. Technol. 200 (2016) 297–304. https://doi.org/10.1016/j.biortech.2015.10.029.

[7] Q. Ge, M. Ling, T.S. Chung, Draw Solutions for forward osmosis processes: Developments, challenges, and prospects for the fututre, J. Memb. Sci. 442 (2013) 225–237. https://doi.org/10.1016/j.memsci.2013.03.046.

[8] N.C. Nguyen, H.T. Nguyen, S.S. Chen, H.H. Ngo, W. Guo, W.H. Chan, S.S. Ray, C.W. Li, H. Te Hsu, A novel osmosis membrane bioreactor-membrane distillation hybrid system for wastewater treatment and reuse, Bioresour. Technol. 209 (2016) 8–15. https://doi.org/10.1016/j.biortech.2016.02.102.

[9] B. Corzo, T. de la Torre, C. Sans, R. Escorihuela, S. Navea, J.J. Malfeito, Long-term evaluation of a forward osmosis-nanofiltration demonstration plant for wastewater reuse in agriculture, Chem. Eng. J. 338 (2018) 383–391. https://doi.org/10.1016/j.cej.2018.01.042.

[10] J.E. Kim, S. Phuntsho, L. Chekli, S. Hong, N. Ghaffour, T.O. Leiknes, J.Y. Choi, H.K. Shon, Environmental and economic impacts of fertilizer drawn forward osmosis and nanofiltration hybrid system, Desalination. 416 (2017) 76–85. https://doi.org/10.1016/j.desal.2017.05.001.

[11] Q. Wang, Z. Ma, J. Wang, Z. Sun, Y. Sun, Y. Jiang, X. Gao, Cost-oriented optimization of osmotic dilution based on concentration-dependent hydraulic pressure, Desalination. 467 (2019) 113–124. https://doi.org/10.1016/j.desal.2019.06.008.

[12] J.E. Kim, S. Phuntsho, F. Lotfi, H.K. Shon, Investigation of pilot-scale 8040 FO membrane module under different operating conditions for brackish water desalination, Desalin. Water Treat. 53 (2015) 2782–2791. https://doi.org/10.1080/19443994.2014.931528.

[13] L. Chekli, J. Eun, I. El, Y. Kim, S. Phuntsho, S. Li, N. Ghaffour, T. Leiknes, H. Kyong, Fertilizer drawn forward osmosis process for sustainable water reuse to

grow hydroponic lettuce using commercial nutrient solution, Sep. Purif. Technol. 181 (2017) 18–28. https://doi.org/10.1016/j.seppur.2017.03.008.

[14] S. Phuntsho, J. Eun, M.A.H. Johir, S. Hong, Z. Li, N. Ghaffour, T. Leiknes, H. Kyong, Fertiliser drawn forward osmosis process : Pilot-scale desalination of mine impaired water for fertigation, J. Memb. Sci. 508 (2016) 22–31. https://doi.org/10.1016/j.memsci.2016.02.024.

[15] T.Y. Cath, A.E. Childress, M. Elimelech, Forward osmosis: Principles, applications, and recent developments, J. Memb. Sci. 281 (2006) 70–87. https://doi.org/10.1016/j.memsci.2006.05.048.

[16] X. Bao, Q. Wu, J. Tian, W. Shi, W. Wang, Z. Zhang, R. Zhang, B. Zhang, Y. Guo, S. Shu, F. Cui, Fouling mechanism of forward osmosis membrane in domestic wastewater concentration: Role of substrate structures, Chem. Eng. J. 370 (2019) 262–273. https://doi.org/10.1016/j.cej.2019.03.174.

[17] W.C.L. Lay, T.H. Chong, C.Y. Tang, A.G. Fane, J. Zhang, Y. Liu, Fouling propensity of forward osmosis: Investigation of the slower flux decline phenomenon, Water Sci. Technol. 61 (2010) 927–936. https://doi.org/10.2166/wst.2010.835.

[18] S. Zhao, L. Zou, C.Y. Tang, D. Mulcahy, Recent developments in forward osmosis: Opportunities and challenges, J. Memb. Sci. 396 (2012) 1–21. https://doi.org/10.1016/j.memsci.2011.12.023.

[19] M. Perry, How forward osmosis (FO) performance is limited by concentration

polarization, ForwardOsmosisTech. (2013). https://www.forwardosmosistech.com/how-forward-osmosis-performance-is-limited-by-concentration-polarization/ (accessed August 20, 2019).

[20] A. Subramani, J.G. Jacangelo, Emerging desalination technologies for water treatment: A critical review, Water Res. 75 (2015) 164–187. https://doi.org/10.1016/j.watres.2015.02.032.

[21] E.M. Garcia-Castello, J.R. McCutcheon, M. Elimelech, Performance evaluation of sucrose concentration using forward osmosis, J. Memb. Sci. 338 (2009) 61–66. https://doi.org/10.1016/j.memsci.2009.04.011.

[22] N.A. Thompson, P.G. Nicoll, Forward osmosis desalination: a commercial reality, IDA World Congr. - Perth Conv. Exhib. Cent. (PCEC), Perth, West. Aust. Sept. 4-9, 2011. (2011) 16.

[23] N.R. Hutchings, E.W. Appleton, R.A. McGinnis, Making High Quality Frac Water out of Oilfield Waste, (2011) 19–22. https://doi.org/10.2118/135469-ms.

[24] A.M. Awad, R. Jalab, J. Minier-Matar, S. Adham, M.S. Nasser, S.J. Judd, The status of forward osmosis technology implementation, Desalination. (2019). https://doi.org/10.1016/j.desal.2019.03.013.

[25] R. Valladares Linares, Z. Li, S. Sarp, S.S. Bucs, G. Amy, J.S. Vrouwenvelder, Forward osmosis niches in seawater desalination and wastewater reuse, Water Res. 66 (2014) 122–139. https://doi.org/10.1016/j.watres.2014.08.021.

[26] P. Nasr, H. Sewilam, Forward osmosis: an alternative sustainable technology and

potential applications in water industry, Clean Technol. Environ. Policy. 17 (2015). https://doi.org/10.1007/s10098-015-0927-8.

[27] G. Blandin, A.R.D. Verliefde, J. Comas, I. Rodriguez-Roda, P. Le-Clech, Efficiently combining water reuse and desalination through forward osmosis-reverse osmosis (FO-RO) hybrids: A critical review, Membranes (Basel). 6 (2016). https://doi.org/10.3390/membranes6030037.

[28] B.D. Coday, T.Y. Cath, Forward osmosis: Novel desalination of produced water and fracturing flowback, J. Am. Water Works Assoc. 106 (2014) 37–38. https://doi.org/10.5942/jawwa.2014.106.0016.

[29] M. Qasim, N.A. Darwish, S. Sarp, N. Hilal, Water desalination by forward (direct) osmosis phenomenon: A comprehensive review, Desalination. 374 (2015) 47–69. https://doi.org/10.1016/j.desal.2015.07.016.

[30] Y.N. Wang, K. Goh, X. Li, L. Setiawan, R. Wang, Membranes and processes for forward osmosis-based desalination: Recent advances and future prospects, Desalination. 434 (2018) 81–99. https://doi.org/10.1016/j.desal.2017.10.028.

[31] K. Lutchmiah, A.R.D. Verliefde, K. Roest, L.C. Rietveld, E.R. Cornelissen, Forward osmosis for application in wastewater treatment: A review, Water Res. 58 (2014) 179–197. https://doi.org/10.1016/j.watres.2014.03.045.

[32] A.J. Ansari, F.I. Hai, W.E. Price, J.E. Drewes, L.D. Nghiem, Forward osmosis as a platform for resource recovery from municipal wastewater - A critical assessment of the literature, J. Memb. Sci. 529 (2017) 195–206.

https://doi.org/10.1016/j.memsci.2017.01.054.

[33] X. Wang, V.W.C. Chang, C.Y. Tang, Osmotic membrane bioreactor (OMBR) technology for wastewater treatment and reclamation: Advances, challenges, and prospects for the future, J. Memb. Sci. 504 (2016) 113–132. https://doi.org/10.1016/j.memsci.2016.01.010.

[34] Y. Cai, X.M. Hu, A critical review on draw solutes development for forward osmosis, Desalination. 391 (2016) 16–29. https://doi.org/10.1016/j.desal.2016.03.021.

[35] T. Alejo, M. Arruebo, V. Carcelen, V.M. Monsalvo, V. Sebastian, Advances in draw solutes for forward osmosis: Hybrid organic-inorganic nanoparticles and conventional solutes, Chem. Eng. J. 309 (2017) 738–752. https://doi.org/10.1016/j.cej.2016.10.079.

[36] S. Dutta, K. Nath, Prospect of ionic liquids and deep eutectic solvents as new generation draw solution in forward osmosis process, J. Water Process Eng. 21 (2018) 163–176. https://doi.org/10.1016/j.jwpe.2017.12.012.

[37] D. Zhao, S. Chen, C.X. Guo, Q. Zhao, X. Lu, Multi-functional forward osmosis draw solutes for seawater desalination, Chinese J. Chem. Eng. 24 (2016) 23–30. https://doi.org/10.1016/j.cjche.2015.06.018.

[38] D.J. Johnson, W.A. Suwaileh, A.W. Mohammed, N. Hilal, Osmotic's potential: An overview of draw solutes for forward osmosis, Desalination. 434 (2018) 100–120. https://doi.org/10.1016/j.desal.2017.09.017.

[39] A. Bogler, S. Lin, E. Bar-Zeev, Biofouling of membrane distillation, forward osmosis and pressure retarded osmosis: Principles, impacts and future directions, J. Memb. Sci. 542 (2017) 378–398. https://doi.org/10.1016/j.memsci.2017.08.001.

[40] Y. Chun, D. Mulcahy, L. Zou, I.S. Kim, A short review of membrane fouling in forward osmosis processes, Membranes (Basel). 7 (2017) 1–23. https://doi.org/10.3390/membranes7020030.

[41] Q. She, R. Wang, A.G. Fane, C.Y. Tang, Membrane fouling in osmotically driven membrane processes: A review, J. Memb. Sci. 87 (2016) 176–190. https://doi.org/10.1016/j.memsci.2015.10.040.

[42] W.A. Suwaileh, D.J. Johnson, S. Sarp, N. Hilal, Advances in forward osmosis membranes: Altering the sub-layer structure via recent fabrication and chemical modification approaches, Desalination. 436 (2018) 176–201. https://doi.org/10.1016/j.desal.2018.01.035.

[43] W. Xu, Q. Chen, Q. Ge, Recent advances in forward osmosis (FO) membrane: Chemical modifications on membranes for FO processes, Desalination. 419 (2017) 101–116. https://doi.org/10.1016/j.desal.2017.06.007.

[44] R.R. Said, Forward Osmosis Process for the Treatment Wastewater from Textile Industries, 19 (2011).

[45] R. Valladares Linares, Z. Li, M. Abu-Ghdaib, C.H. Wei, G. Amy, J.S. Vrouwenvelder, Water harvesting from municipal wastewater via osmotic gradient: An evaluation of process performance, J. Memb. Sci. 447 (2013) 50–56.

https://doi.org/10.1016/j.memsci.2013.07.018.

[46] S. Zhang, P. Wang, X. Fu, T.S. Chung, Sustainable water recovery from oily wastewater via forward osmosis-membrane distillation (FO-MD), Water Res. 52 (2014) 112–121. https://doi.org/10.1016/j.watres.2013.12.044.

[47] T.Y. Cath, N.T. Hancock, C.D. Lundin, C. Hoppe-jones, J.E. Drewes, A multi-barrier osmotic dilution process for simultaneous desalination and purification of impaired water, J. Memb. Sci. 362 (2010) 417–426. https://doi.org/10.1016/j.memsci.2010.06.056.

[48] N.T. Hancock, N.D. Black, T.Y. Cath, A comparative life cycle assessment of hybrid osmotic dilution desalination and established seawater desalination and wastewater reclamation processes, Water Res. 46 (2012) 1145–1154. https://doi.org/10.1016/j.watres.2011.12.004.

[49] Y. Choi, H. Cho, Y. Shin, Y. Jang, S. Lee, Economic evaluation of a hybrid desalination system combining forward and reverse osmosis, Membranes (Basel). 6 (2015) 3. https://doi.org/10.3390/membranes6010003.

[50] V. Yangali-Quintanilla, Z. Li, R. Valladares, Q. Li, G. Amy, Indirect desalination of Red Sea water with forward osmosis and low pressure reverse osmosis for water reuse, Desalination. 280 (2011) 160–166. https://doi.org/10.1016/j.desal.2011.06.066.

[51] C.F. Wan, T.S. Chung, Techno-economic evaluation of various RO+PRO and RO+FO integrated processes, Appl. Energy. 212 (2018) 1038–1050.

https://doi.org/10.1016/j.apenergy.2017.12.124.

[52] R. Jalab, A.M. Awad, M.S. Nasser, J. Minier-Matar, S. Adham, S.J. Judd, An empirical determination of the whole-life cost of FO-based open-loop wastewater reclamation technologies, Water Res. 163 (2019) 114879. https://doi.org/10.1016/j.watres.2019.114879.

[53] E.R. Cornelissen, D. Harmsen, E.F. Beerendonk, J.J. Qin, H. Oo, K.F. De Korte, J.W.M.N. Kappelhof, The innovative Osmotic Membrane Bioreactor (OMBR) for reuse of wastewater, Water Sci. Technol. 63 (2011) 1557–1565. https://doi.org/10.2166/wst.2011.206.

[54] D.L. Shaffer, L.H. Arias Chavez, M. Ben-Sasson, S. Romero-Vargas Castrillón, N.Y. Yip, M. Elimelech, Desalination and reuse of high-salinity shale gas produced water: Drivers, technologies, and future directions, Environ. Sci. Technol. 47 (2013) 9569–9583. https://doi.org/10.1021/es401966e.

[55] K.L. Hickenbottom, N.T. Hancock, N.R. Hutchings, E.W. Appleton, E.G. Beaudry, P. Xu, T.Y. Cath, Forward osmosis treatment of drilling mud and fracturing wastewater from oil and gas operations, Desalination. 312 (2013) 60–66. https://doi.org/10.1016/j.desal.2012.05.037.

[56] B.D. Coday, N. Almaraz, T.Y. Cath, Forward osmosis desalination of oil and gas wastewater: Impacts of membrane selection and operating conditions on process performance, J. Memb. Sci. 488 (2015) 40–55. https://doi.org/10.1016/j.memsci.2015.03.059.

[57] S. Adham, A. Hussain, J. Minier-Matar, A. Janson, R. Sharma, Membrane applications and opportunities for water management in the oil & gas industry, Desalination. 440 (2018) 2–17. https://doi.org/10.1016/j.desal.2018.01.030.

[58] B.D. Lutz, A.N. Lewis, M.W. Doyle, Generation, transport, and disposal of wastewater associated with Marcellus Shale gas development, Water Resour. Res. 49 (2013) 647–656. https://doi.org/10.1002/wrcr.20096.

[59] B.D. Coday, L. Miller-Robbie, E.G. Beaudry, J. Munakata-Marr, T.Y. Cath, Life cycle and economic assessments of engineered osmosis and osmotic dilution for desalination of Haynesville shale pit water, Desalination. 369 (2015) 188–200. https://doi.org/10.1016/j.desal.2015.04.028.

[60] R.L. McGinnis, N.T. Hancock, M.S. Nowosielski-Slepowron, G.D. McGurgan, Pilot demonstration of the NH3/CO2 forward osmosis desalination process on high salinity brines, Desalination. 312 (2013) 67–74. https://doi.org/10.1016/j.desal.2012.11.032.

[61] S. Lee, C. Boo, M. Elimelech, S. Hong, Comparison of fouling behavior in forward osmosis (FO) and reverse osmosis (RO), J. Memb. Sci. 365 (2010) 34–39. https://doi.org/10.1016/j.memsci.2010.08.036.

[62] B. Mi, M. Elimelech, Organic fouling of forward osmosis membranes: Fouling reversibility and cleaning without chemical reagents, J. Memb. Sci. 348 (2010) 337–345. https://doi.org/10.1016/j.memsci.2009.11.021.

[63] D. Li, Y. Yan, H. Wang, Recent advances in polymer and polymer composite

membranes for reverse and forward osmosis processes, Prog. Polym. Sci. 61 (2016) 104–155. https://doi.org/10.1016/j.progpolymsci.2016.03.003.

[64] B.D. Coday, P. Xu, E.G. Beaudry, J. Herron, K. Lampi, N.T. Hancock, T.Y. Cath, The sweet spot of forward osmosis: Treatment of produced water, drilling wastewater, and other complex and difficult liquid streams, Desalination. 333 (2014) 23–35. https://doi.org/10.1016/j.desal.2013.11.014.

[65] J. Minier-Matar, A. Santos, A. Hussain, A. Janson, R. Wang, A.G. Fane, S. Adham, Application of Hollow Fiber Forward Osmosis Membranes for Produced and Process Water Volume Reduction: An Osmotic Concentration Process, Environ. Sci. Technol. 50 (2016) 6044–6052. https://doi.org/10.1021/acs.est.5b04801.

[66] J.M. Sheikhan, I. Zainab, S. Janson, Arnold; Adham, Qatargas wastewater treatment plants : an advanced design for water, Int. Pet. Technol. Conf. Doha, Qatar. (2015).

[67] J. Su, T.S. Chung, B.J. Helmer, J.S. de Wit, Understanding of low osmotic efficiency in forward osmosis: Experiments and modeling, Desalination. 313 (2013) 156–165. https://doi.org/10.1016/j.desal.2012.12.022.

[68] S. Phuntsho, S. Sahebi, T. Majeed, F. Lotfi, J.E. Kim, H.K. Shon, Assessing the major factors affecting the performances of forward osmosis and its implications on the desalination process, Chem. Eng. J. 231 (2013) 484–496. https://doi.org/10.1016/j.cej.2013.07.058.

[69] X. Lu, C. Boo, J. Ma, M. Elimelech, Bidirectional diffusion of ammonium and sodium cations in forward osmosis: Role of membrane active layer surface chemistry and charge, Environ. Sci. Technol. 48 (2014) 14369–14376. https://doi.org/10.1021/es504162v.

[70] V. Sant'Anna, L.D.F. Marczak, I.C. Tessaro, Membrane concentration of liquid foods by forward osmosis: Process and quality view, J. Food Eng. 111 (2012) 483–489. https://doi.org/10.1016/j.jfoodeng.2012.01.032.

[71] B. Jiao, A. Cassano, E. Drioli, Recent advances on membrane processes for the concentration of fruit juices: A review, J. Food Eng. 63 (2004) 303–324. https://doi.org/10.1016/j.jfoodeng.2003.08.003.

[72] C.A. Nayak, S.S. Valluri, N.K. Rastogi, Effect of high or low molecular weight of components of feed on transmembrane flux during forward osmosis, J. Food Eng. 106 (2011) 48–52. https://doi.org/10.1016/j.jfoodeng.2011.04.006.

[73] K.B. Petrotos, P. Quantick, H. Petropakis, A study of the direct osmotic concentration of tomato juice in tubular membrane - Module configuration. I. The effect of certain basic process parameters on the process performance, J. Memb. Sci. 150 (1998) 99–110. https://doi.org/10.1016/S0376-7388(98)00216-6.

[74] E.M. Garcia-Castello, J.R. McCutcheon, Dewatering press liquor derived from orange production by forward osmosis, J. Memb. Sci. 372 (2011) 97–101. https://doi.org/10.1016/j.memsci.2011.01.048.

[75] L. Chekli, S. Phuntsho, J.E. Kim, J. Kim, J.Y. Choi, J.S. Choi, S. Kim, J.H. Kim,

S. Hong, J. Sohn, H.K. Shon, A comprehensive review of hybrid forward osmosis systems: Performance, applications and future prospects, J. Memb. Sci. 497 (2016) 430–449. https://doi.org/10.1016/j.memsci.2015.09.041.

[76] D.L. Shaffer, J.R. Werber, H. Jaramillo, S. Lin, M. Elimelech, Forward osmosis: Where are we now?, Desalination. 356 (2015) 271–284. https://doi.org/10.1016/j.desal.2014.10.031.

[77] R.K. McGovern, J.H. Lienhard V, On the potential of forward osmosis to energetically outperform reverse osmosis desalination, J. Memb. Sci. 469 (2014) 245–250. https://doi.org/10.1016/j.memsci.2014.05.061.

[78] G. Blandin, A.R.D. Verliefde, C.Y. Tang, P. Le-Clech, Opportunities to reach economic sustainability in forward osmosis-reverse osmosis hybrids for seawater desalination, Desalination. 363 (2015) 26–36. https://doi.org/10.1016/j.desal.2014.12.011.

[79] J.E. Kim, S. Phuntsho, S.M. Ali, J.Y. Choi, H.K. Shon, Forward osmosis membrane modular configurations for osmotic dilution of seawater by forward osmosis and reverse osmosis hybrid system, Water Res. 128 (2018) 183–192. https://doi.org/10.1016/j.watres.2017.10.042.

[80] J. Minier-Matar, A. Hussain, A.F. Janson, A.G. Fane, S. Adham, Application of Forward Osmosis to Reduce Produced Water Injection Volumes, in: Proc. 4th Int. Gas Process. Symp., 2015: pp. 309–316. https://doi.org/10.1016/b978-0-444-63461-0.50032-8.

[81] A. Achilli, T.Y. Cath, A.E. Childress, Selection of inorganic-based draw solutions for forward osmosis applications, J. Memb. Sci. 364 (2010) 233–241. https://doi.org/10.1016/j.memsci.2010.08.010.

[82] B. Corzo, T. de la Torre, C. Sans, E. Ferrero, J.J. Malfeito, Evaluation of draw solutions and commercially available forward osmosis membrane modules for wastewater reclamation at pilot scale, Chem. Eng. J. 326 (2017) 1–8. https://doi.org/10.1016/j.cej.2017.05.108.

[83] C. Klaysom, T.Y. Cath, T. Depuydt, I.F.J. Vankelecom, Forward and pressure retarded osmosis: Potential solutions for global challenges in energy and water supply, Chem. Soc. Rev. 42 (2013) 6959–6989. https://doi.org/10.1039/c3cs60051c.

[84] R.L. McGinnis, M. Elimelech, Energy requirements of ammonia-carbon dioxide forward osmosis desalination, Desalination. 207 (2007) 370–382. https://doi.org/10.1016/j.desal.2006.08.012.

[85] J.R. McCutcheon, R.L. McGinnis, M. Elimelech, Desalination by ammonia-carbon dioxide forward osmosis: Influence of draw and feed solution concentrations on process performance, J. Memb. Sci. 278 (2006) 114–123. https://doi.org/10.1016/j.memsci.2005.10.048.

[86] P. McCormick, J. Pellegrino, F. Mantovani, G. Sarti, Water, salt, and ethanol diffusion through membranes for water recovery by forward (direct) osmosis processes, J. Memb. Sci. 325 (2008) 467–478. https://doi.org/10.1016/j.memsci.2008.08.011.

[87] J. Su, T.S. Chung, B.J. Helmer, J.S. de Wit, Enhanced double-skinned FO membranes with inner dense layer for wastewater treatment and macromolecule recycle using Sucrose as draw solute, J. Memb. Sci. 396 (2012) 92–100. https://doi.org/10.1016/j.memsci.2012.01.001.

[88] K.S. Bowden, A. Achilli, A.E. Childress, Organic ionic salt draw solutions for osmotic membrane bioreactors, Bioresour. Technol. 122 (2012) 207–216. https://doi.org/10.1016/j.biortech.2012.06.026.

[89] S. Adham, J. Oppenheimer, L. Liu, M. Kumar, Dewatering Reverse Osmosis Concentrate from Water Reuse Applications Using Forward Osmosis, 2007.

[90] J. Kim, K. Jeong, M.J. Park, H.K. Shon, J.H. Kim, Recent advances in osmotic energy generation via pressure-retarded osmosis (PRO): A review, Energies. 8 (2015) 11821–11845. https://doi.org/10.3390/en81011821.

[91] M.M. Ling, T.S. Chung, Novel dual-stage FO system for sustainable protein enrichment using nanoparticles as intermediate draw solutes, J. Memb. Sci. 372 (2011) 201–209. https://doi.org/10.1016/j.memsci.2011.02.003.

[92] Q. Ge, J. Su, G.L. Amy, T.S. Chung, Exploration of polyelectrolytes as draw solutes in forward osmosis processes, Water Res. 46 (2012) 1318–1326. https://doi.org/10.1016/j.watres.2011.12.043.

[93] D. Li, X. Zhang, J. Yao, Y. Zeng, G.P. Simon, H. Wang, Composite polymer hydrogels as draw agents in forward osmosis and solar dewatering, Soft Matter. 7 (2011) 10048–10056. https://doi.org/10.1039/c1sm06043k.

[94] S. Phuntsho, H.K. Shon, T. Majeed, I. El Saliby, S. Vigneswaran, J. Kandasamy, S. Hong, S. Lee, Blended fertilizers as draw solutions for fertilizer-drawn forward osmosis desalination, Environ. Sci. Technol. 46 (2012) 4567–4575. https://doi.org/10.1021/es300002w.

[95] Hydration Technology Innovation (HTI), Forward Osmosis Solutions, (2010). http://www.htiwater.com/technology/forward_osmosis/index.html (accessed June 24, 2019).

[96] Oasys Water, (2019). http://oasyswater.com/solutions/technology/ (accessed June 24, 2019).

[97] Toyobo ’ s hollow fiber forward osmosis membrane adopted at Danish osmotic power plant Hollow fiber forward osmosis (FO) membranes manufactured by Toyobo Co ., Ltd ., (2018). https://www.toyobo-global.com/news/pdf/2018/12/press20181217.pdf.

[98] Membrane Modules, Porifera. (n.d.). https://www.porifera.com/modules (accessed June 25, 2019).

[99] Projects, Trevi Syst. (n.d.). https://www.trevisystems.com/projects (accessed June 25, 2019).

[100] AQUAPORIN INSIDE® FORWARD OSMOSIS MEMBRANE PRODUCTS, Aquaporin. (n.d.). https://aquaporin.com/fo/ (accessed June 25, 2019).

[101] A. Al-zuhairi, A.A. Merdaw, S. Al-aibi, M. Hamdan, P. Nicoll, A.A. Monjezi, S. Al-aswad, H.B. Mahood, M. Aryafar, A.O. Sharif, Forward Osmosis desalination

from labratory to market, Water Sci. Technol. (2015). https://doi.org/10.2166/ws.2015.038.

[102] Y. Chun, F. Zaviska, S.J. Kim, D. Mulcahy, E. Yang, I.S. Kim, L. Zou, Fouling characteristics and their implications on cleaning of a FO-RO pilot process for treating brackish surface water, Desalination. 394 (2016) 91–100. https://doi.org/10.1016/j.desal.2016.04.026.

[103] N.T. Hancock, P. Xu, M.J. Roby, J.D. Gomez, T.Y. Cath, Towards direct potable reuse with forward osmosis : Technical assessment of long-term process performance at the pilot scale, J. Memb. Sci. 445 (2013) 34–46. https://doi.org/10.1016/j.memsci.2013.04.056.

[104] R.W. Holloway, A.S. Wait, A. Fernandes da Silva, J. Herron, M.D. Schutter, K. Lampi, T.Y. Cath, Long-term pilot scale investigation of novel hybrid ultrafiltration-osmotic membrane bioreactors, Desalination. 363 (2015) 64–74. https://doi.org/10.1016/j.desal.2014.05.040.

[105] J.-J. Qin, G. Tao, C.L. Lay, E.R. Cornelissen, M.H. Oo, K.A. Kekre, C.J. Ruiken, C.H. Lew, Preliminary study of osmotic membrane bioreactor: effects of draw solution on water flux and air scouring on fouling, Water Sci. Technol. 62 (2010) 1353–1360. https://doi.org/10.2166/wst.2010.426.

[106] B.G. Choi, M. Zhan, K. Shin, S. Lee, S. Hong, Pilot-scale evaluation of FO-RO osmotic dilution process for treating wastewater from coal- fi red power plant integrated with seawater desalination, J. Memb. Sci. 540 (2017) 78–87. https://doi.org/10.1016/j.memsci.2017.06.036.

[107] R.A. Maltos, J. Regnery, N. Almaraz, S. Fox, M. Schutter, T.J. Cath, M. Veres, B.D. Coday, T.Y. Cath, Produced water impact on membrane integrity during extended pilot testing of forward osmosis – reverse osmosis treatment, Desalination. 440 (2018) 99–110. https://doi.org/10.1016/j.desal.2018.02.029.

[108] W.L. Ang, A. Wahab Mohammad, D. Johnson, N. Hilal, Forward osmosis research trends in desalination and wastewater treatment: A review of research trends over the past decade, J. Water Process Eng. 31 (2019) 100886. https://doi.org/10.1016/j.jwpe.2019.100886.

[109] S. Chakrabortty, M. Pal, M. Roy, P. Pal, Water treatment in a new flux-enhancing, continuous forward osmosis design: Transport modelling and economic evaluation towards scale up, Desalination. 365 (2015) 329–342. https://doi.org/10.1016/j.desal.2015.03.020.

[110] C.Y. Tang, Q. She, W.C.L. Lay, R. Wang, A.G. Fane, Coupled effects of internal concentration polarization and fouling on flux behavior of forward osmosis membranes during humic acid filtration, J. Memb. Sci. 354 (2010) 123–133. https://doi.org/10.1016/j.memsci.2010.02.059.

[111] J.R. McCutcheon, M. Elimelech, Influence of concentrative and dilutive internal concentration polarization on flux behavior in forward osmosis, J. Memb. Sci. 284 (2006) 237–247. https://doi.org/10.1016/j.memsci.2006.07.049.

[112] W.A. Phillip, J.S. Yong, M. Elimelech, Reverse draw solute permeation in forward osmosis: Modeling and experiments, Environ. Sci. Technol. 44 (2010) 5170–5176. https://doi.org/10.1021/es100901n.

[113] N. Akther, A. Sodiq, A. Giwa, S. Daer, H.A. Arafat, S.W. Hasan, Recent advancements in forward osmosis desalination: A review, Chem. Eng. J. 281 (2015) 502–522. https://doi.org/10.1016/j.cej.2015.05.080.

[114] S. Zhao, L. Zou, Relating solution physicochemical properties to internal concentration polarization in forward osmosis, J. Memb. Sci. 379 (2011) 459–467. https://doi.org/10.1016/j.memsci.2011.06.021.

[115] Y. Hartanto, S. Yun, B. Jin, S. Dai, Functionalized thermo-responsive microgels for high performance forward osmosis desalination, Water Res. 70 (2015) 385–393. https://doi.org/10.1016/j.watres.2014.12.023.

[116] Y. Lu, Z. He, Mitigation of Salinity Buildup and Recovery of Wasted Salts in a Hybrid Osmotic Membrane Bioreactor-Electrodialysis System, Environ. Sci. Technol. 49 (2015) 10529–10535. https://doi.org/10.1021/acs.est.5b01243.

[117] L. Huang, N.N. Bui, M.T. Meyering, T.J. Hamlin, J.R. McCutcheon, Novel hydrophilic nylon 6,6 microfiltration membrane supported thin film composite membranes for engineered osmosis, J. Memb. Sci. 437 (2013) 141–149. https://doi.org/10.1016/j.memsci.2013.01.046.

[118] M. Yasukawa, S. Mishima, M. Shibuya, D. Saeki, T. Takahashi, T. Miyoshi, H. Matsuyama, Preparation of a forward osmosis membrane using a highly porous polyketone microfiltration membrane as a novel support, J. Memb. Sci. 487 (2015) 51–59. https://doi.org/10.1016/j.memsci.2015.03.043.

[119] H. Guo, Z. Yao, J. Wang, Z. Yang, X. Ma, C.Y. Tang, Polydopamine coating on a

thin film composite forward osmosis membrane for enhanced mass transport and antifouling performance, J. Memb. Sci. 551 (2018) 234–242. https://doi.org/10.1016/j.memsci.2018.01.043.

[120] C. Boo, M. Elimelech, S. Hong, Fouling control in a forward osmosis process integrating seawater desalination and wastewater reclamation, J. Memb. Sci. 444 (2013) 148–156. https://doi.org/10.1016/j.memsci.2013.05.004.

[121] S. Kim, G.W. Go, A. Jang, Study of flux decline and solute diffusion on an osmotically driven membrane process potentially applied to municipal wastewater reclamation, J. Ind. Eng. Chem. 33 (2016) 255–261. https://doi.org/10.1016/j.jiec.2015.10.005.

[122] B. Mi, M. Elimelech, Chemical and physical aspects of organic fouling of forward osmosis membranes, J. Memb. Sci. 320 (2008) 292–302. https://doi.org/10.1016/j.memsci.2008.04.036.

[123] H.K. Shon, S. Vigneswaran, J. Cho, Comparison of physico-chemical pretreatment methods to seawater reverse osmosis: Detailed analyses of molecular weight distribution of organic matter in initial stage, J. Memb. Sci. 320 (2008) 151–158. https://doi.org/10.1016/j.memsci.2008.03.063.

[124] Y. Zhou, S. Yu, C. Gao, X. Feng, Surface modification of thin film composite polyamide membranes by electrostatic self deposition of polycations for improved fouling resistance, Sep. Purif. Technol. 66 (2009) 287–294. https://doi.org/10.1016/j.seppur.2008.12.021.

[125] A. Asatekin, A. Menniti, S. Kang, M. Elimelech, E. Morgenroth, A.M. Mayes, Antifouling nanofiltration membranes for membrane bioreactors from self-assembling graft copolymers, J. Memb. Sci. 285 (2006) 81–89. https://doi.org/10.1016/j.memsci.2006.07.042.

[126] A. Soroush, W. Ma, M. Cyr, M.S. Rahaman, B. Asadishad, N. Tufenkji, In Situ Silver Decoration on Graphene Oxide-Treated Thin Film Composite Forward Osmosis Membranes: Biocidal Properties and Regeneration Potential, Environ. Sci. Technol. Lett. 3 (2016) 13–18. https://doi.org/10.1021/acs.estlett.5b00304.

[127] A. Zirehpour, A. Rahimpour, M. Ulbricht, Nano-sized metal organic framework to improve the structural properties and desalination performance of thin film composite forward osmosis membrane, J. Memb. Sci. 531 (2017) 59–67. https://doi.org/10.1016/j.memsci.2017.02.049.

[128] R. Valladares Linares, Z. Li, V. Yangali-Quintanilla, N. Ghaffour, G. Amy, T. Leiknes, J.S. Vrouwenvelder, Life cycle cost of a hybrid forward osmosis - low pressure reverse osmosis system for seawater desalination and wastewater recovery, Water Res. 88 (2016) 225–234. https://doi.org/10.1016/j.watres.2015.10.017.

[129] A. Teusner, G. Blandin, P. Le-Clech, Augmenting water supply by combined desalination/water recycling methods: an economic assessment, Environ. Technol. (United Kingdom). 38 (2017) 257–265. https://doi.org/10.1080/09593330.2016.1189972.

[130] M.I. Baoxia, M. Elimelech, Gypsum scaling and cleaning in forward osmosis:

Measurements and mechanisms, Environ. Sci. Technol. 44 (2010) 2022–2028. https://doi.org/10.1021/es903623r.

[131] F. Votta, D.K. Anderson, Concentration of Dilute Industrial Wastes by Direct Osmosis, Rhode Isalnd, 1977.

[132] R.J. York, R.S. Thiel, E.G. Beaudry, Full-Scale Experience of Direct Osmosis Concentration Applied to Leachate Management, in: CISA (Ed.), 6th, Int. Waste Manag. Landfill Symp., Italy, 1999: pp. 359–366.

[133] T.Y. Cath, S. Gormly, E.G. Beaudry, M.T. Flynn, V.D. Adams, A.E. Childress, Membrane contactor processes for wastewater reclamation in space: Part I. Direct osmotic concentration as pretreatment for reverse osmosis, J. Memb. Sci. 257 (2005) 85–98. https://doi.org/10.1016/j.memsci.2004.08.039.

[134] T.Y. Cath, D. Adams, A.E. Childress, Membrane contactor processes for wastewater reclamation in space: II. Combined direct osmosis, osmotic distillation, and membrane distillation for treatment of metabolic wastewater, J. Memb. Sci. 257 (2005) 111–119. https://doi.org/10.1016/j.memsci.2004.07.039.

[135] J. Korenak, C. Hélix-Nielsen, H. Bukšek, I. Petrinić, Efficiency and economic feasibility of forward osmosis in textile wastewater treatment, J. Clean. Prod. 210 (2019) 1483–1495. https://doi.org/10.1016/j.jclepro.2018.11.130.

[136] E.A. Bell, T.E. Poynor, K.B. Newhart, J. Regnery, B.D. Coday, T.Y. Cath, Produced water treatment using forward osmosis membranes: Evaluation of extended-time performance and fouling, J. Memb. Sci. 525 (2017) 77–88.

https://doi.org/10.1016/j.memsci.2016.10.032.

[137] M. Raffin, E. Germain, S. Judd, Wastewater polishing using membrane technology: A review of existing installations, Environ. Technol. (United Kingdom). 34 (2013) 617–627. https://doi.org/10.1080/09593330.2012.710385.

[138] Q. Yang, J. Lei, D.D. Sun, D. Chen, Forward Osmosis Membranes for Water Reclamation, Sep. Purif. Rev. 45 (2016) 93–107. https://doi.org/10.1080/15422119.2014.973506.

[139] P. Côté, H. Buisson, C. Pound, G. Arakaki, Immersed membrane activated sludge for the reuse of municipal wastewater, Desalination. 113 (1997) 189–196.

[140] P. Lawrence, S. Adham, L. Barrott, Ensuring water re-use projects succeed - Institutional and technical issues for treated wastewater re-use, Desalination. 152 (2003) 291–298. https://doi.org/10.1016/S0011-9164(02)01076-7.

[141] E. Dialynas, E. Diamadopoulos, Integration of a membrane bioreactor coupled with reverse osmosis for advanced treatment of municipal wastewater, Desalination. 238 (2009) 302–311. https://doi.org/10.1016/j.desal.2008.01.046.

[142] D. De Jager, M.S. Sheldon, W. Edwards, Colour removal from textile wastewater using a pilot-scale dual-stage MBR and subsequent RO system, Sep. Purif. Technol. 135 (2014) 135–144. https://doi.org/10.1016/j.seppur.2014.08.008.

[143] E.L. Farias, K.J. Howe, B.M. Thomson, Effect of membrane bioreactor solids retention time on reverse osmosis membrane fouling for wastewater reuse, Water Res. 49 (2014) 53–61. https://doi.org/10.1016/j.watres.2013.11.006.

[144] L. Blanco, D. Hermosilla, Á. Blanco, N. Swinnen, D. Prieto, C. Negro, MBR+RO Combination for PVC Production Effluent Reclamation in the Resin Polymerization Step: A Case Study, Ind. Eng. Chem. Res. 55 (2016) 6250–6259.

[145] M. Gündoğdu, Y.A. Jarma, N. Kabay, T. Pek, M. Yüksel, Integration of MBR with NF/RO processes for industrial wastewater reclamation and water reuse-effect of membrane type on product water quality, J. Water Process Eng. (2018). https://doi.org/10.1016/j.jwpe.2018.02.009.

[146] S. Judd, Industrial MBRs, 1st ed., Judd and Judd Ltd, Cranfield, UK, 2014.

[147] B. Corzo, T. De, C. Sans, R. Escorihuela, S. Navea, J.J. Malfeito, Long-term evaluation of a forward osmosis-nano fi ltration demonstration plant for wastewater reuse in agriculture, Chem. Eng. J. 338 (2018) 383–391. https://doi.org/10.1016/j.cej.2018.01.042.

[148] R.W. Holloway, A.S. Wait, A. Fernandes, J. Herron, M.D. Schutter, K. Lampi, T.Y. Cath, Long-term pilot scale investigation of novel hybrid ultra fi ltration-osmotic membrane bioreactors, Desalination. 363 (2015) 64–74. https://doi.org/10.1016/j.desal.2014.05.040.

[149] A.A. Alturki, J.A. McDonald, S.J. Khan, W.E. Price, L.D. Nghiem, M. Elimelech, Removal of trace organic contaminants by the forward osmosis process, Sep. Purif. Technol. 103 (2013) 258–266. https://doi.org/10.1016/j.seppur.2012.10.036.

[150] R. Valladares Linares, V. Yangali-Quintanilla, Z. Li, G. Amy, Rejection of micropollutants by clean and fouled forward osmosis membrane, Water Res. 45

(2011) 6737–6744. https://doi.org/10.1016/j.watres.2011.10.037.

[151] Q. Yang, K.Y. Wang, T.S. Chung, Dual-layer hollow fibers with enhanced flux as novel forward osmosis membranes for water production, Environ. Sci. Technol. 43 (2009) 2800–2805. https://doi.org/10.1021/es803360t.

[152] R.B. Jackson, A. Vengosh, J.W. Carey, R.J. Davies, T.H. Darrah, F. O'Sullivan, G. Pétron, The Environmental Costs and Benefits of Fracking, Annu. Rev. Environ. Resour. 39 (2014) 327–362. https://doi.org/10.1146/annurev-environ-031113-144051.

[153] T.L.S. Silva, S. Morales-Torres, S. Castro-Silva, J.L. Figueiredo, A.M.T. Silva, An overview on exploration and environmental impact of unconventional gas sources and treatment options for produced water, J. Environ. Manage. 200 (2017) 511–529. https://doi.org/10.1016/j.jenvman.2017.06.002.

[154] T. Liden, D.D. Carlton, S. Miyazaki, T. Otoyo, K.A. Schug, Forward osmosis remediation of high salinity Permian Basin produced water from unconventional oil and gas development, Sci. Total Environ. 653 (2019) 82–90. https://doi.org/10.1016/j.scitotenv.2018.10.325.

[155] J. Veil, U.S Produced Water Volumes and Management Practices in 2012, (2015).

[156] R. Dores, A. Hussain, M. Katebah, S.S. Adham, Using Advanced Water Treatment Technologies To Treat Produced Water From The Petroleum Industry, (2012). https://doi.org/10.2118/157108-ms.

[157] J.A. Veil, M.G. Puder, D. Elcock, R.J. Redwick, A White Paper Describing

Produced Water From Production of Crude Oil, Natural Gas, and Coal Bed Methane, (2004).

[158] R.M. Abousnina, L.D. Nghiem, J. Bundschuh, Comparison between oily and coal seam gas produced water with respect to quantity, characteristics and treatment technologies: a review, Desalin. Water Treat. 54 (2015) 1793–1808. https://doi.org/10.1080/19443994.2014.893541.

[159] J. Veil, C. Clark, Produced Water Volume Estimates and Management Practices, SPE Prod. Oper. 26 (2011) 234–239. https://doi.org/10.2118/125999-pa.

[160] Z. Khatib, P. Verbeek, Water to Value – Produced Water Management for Sustainable Field Development of Mature and Green Fields, in: Heal. Saf. Environ. Oil Gas Explor. Prot., Malaysia, 2002: pp. 20–22.

[161] J.A. Veil, A.C. Rechner, T.A. Kimmell, Characteristics of Produced Water Discharged to the Gulf of Mexico Hypoxic Zone, (2005) 1–74. http://www.perf.org/images/Archive_Hypoxic_Report.pdf.

[162] L.G. Faksness, P.G. Grini, P.S. Daling, Partitioning of semi-soluble organic compounds between the water phase and oil droplets in produced water, Mar. Pollut. Bull. 48 (2004) 731–742. https://doi.org/10.1016/j.marpolbul.2003.10.018.

[163] M.A. Cluff, A. Hartsock, J.D. Macrae, K. Carter, P.J. Mouser, Temporal changes in microbial ecology and geochemistry in produced water from hydraulically fractured marcellus shale gas wells, Environ. Sci. Technol. 48 (2014) 6508–6517. https://doi.org/10.1021/es501173p.

[164] N.R. Warner, T.H. Darrah, R.B. Jackson, R. Millot, W. Kloppmann, A. Vengosh, New tracers identify hydraulic fracturing fluids and accidental releases from oil and gas operations, Environ. Sci. Technol. 48 (2014) 12552–12560. https://doi.org/10.1021/es5032135.

[165] K.L. Benko, J.E. Drewes, Produced Water in the Western United States: Geographical Distribution, Occurrence, and Composition, Environ. Eng. Sci. 25 (2008) 239–246. https://doi.org/10.1089/ees.2007.0026.

[166] E.A. Emam, T.M. Moawad, N.A. Aboul-Gheit, Evaluating the characteristics of offshore oilfield produced water, Petroelum Coal. 56 (2014) 363–372.

[167] M. Al-Kaabi, A. Ghazi, R. Qunnaby, F. Dawwas, H. Al-Hadrami, Z. Khatir, M. Yousif, T. Ahmed, M. Al-Ghouti, Enhancing the Quality of "Produced Water" by Activated Carbon, in: Qatar Found. Annu. Res. Conf. Proc., Hamad Bin Khalifa University Press, Qatar, 2016: pp. 16–17. https://doi.org/https://doi.org/10.5339/qfarc.2016.EEPP2459.

[168] A. Janson, A. Santos, M. Katebah, A. Hussain, J. Minier-Matar, S. Judd, S. Adham, Assessing the Biotreatability of Produced Water From a Qatari Gas Field, SPE J. 20 (2014) 1113–1119. https://doi.org/10.2118/173188-pa.

[169] K.B. Gregory, R.D. Vidic, D.A. Dzombak, Water management challenges associated with the production of shale gas by hydraulic fracturing, Elements. 7 (2011) 181–186. https://doi.org/10.2113/gselements.7.3.181.

[170] L.D. Nghiem, T. Ren, N. Aziz, I. Porter, G. Regmi, Treatment of coal seam gas

produced water for beneficial use in Australia: A review of best practices, Desalin. Water Treat. 32 (2011) 316–323. https://doi.org/10.5004/dwt.2011.2716.

[171] J. Welch, Reverse osmosis treatment of CBM produced water continues to evolv, Oil Gas J. 107 (2009) 45–50.

[172] B.M. Johnson, L.E. Kanagy, J.H. Rodgers, J.W. Castle, Chemical, physical, and risk characterization of natural gas storage produced waters, Water. Air. Soil Pollut. 191 (2008) 33–54. https://doi.org/10.1007/s11270-007-9605-8.

[173] P.J.C. Tibbetts, I.T. Buchanan, L.J. Gawel, R. Large, A Comprehensive Determination of Produced Water Composition, Prod. Water. (1992) 97–112. https://doi.org/10.1007/978-1-4615-2902-6_9.

[174] Z.L. Hildenbrand, D.D. Carlton, B.E. Fontenot, J.M. Meik, J.L. Walton, J.B. Thacker, S. Korlie, C.P. Shelor, A.F. Kadjo, A. Clark, S. Usenko, J.S. Hamilton, P.M. Mach, G.F. Verbeck, P. Hudak, K.A. Schug, Temporal variation in groundwater quality in the Permian Basin of Texas, a region of increasing unconventional oil and gas development, Sci. Total Environ. 562 (2016) 906–913. https://doi.org/10.1016/j.scitotenv.2016.04.144.

[175] Z.L. Hildenbrand, D.D. Carlton, B.E. Fontenot, J.M. Meik, J.L. Walton, J.T. Taylor, J.B. Thacker, S. Korlie, C.P. Shelor, D. Henderson, A.F. Kadjo, C.E. Roelke, P.F. Hudak, T. Burton, H.S. Rifai, K.A. Schug, A Comprehensive Analysis of Groundwater Quality in The Barnett Shale Region, Environ. Sci. Technol. 49 (2015) 8254–8262. https://doi.org/10.1021/acs.est.5b01526.

[176] A. Vengosh, R.B. Jackson, N. Warner, T.H. Darrah, A. Kondash, A critical review of the risks to water resources from unconventional shale gas development and hydraulic fracturing in the United States, Environ. Sci. Technol. 48 (2014) 8334–8348. https://doi.org/10.1021/es405118y.

[177] A. Fakhru'l-Razi, A. Pendashteh, L.C. Abdullah, D.R.A. Biak, S.S. Madaeni, Z.Z. Abidin, Review of technologies for oil and gas produced water treatment, J. Hazard. Mater. 170 (2009) 530–551. https://doi.org/10.1016/j.jhazmat.2009.05.044.

[178] J.-P. Nicot, B.R. Scanlon, R.C. Reedy, R.A. Costley, Source and Fate of Hydraulic Fracturing Water in the Barnett Shale: A Historical Perspective, Environ. Sci. Technol. 48 (2014) 2646–2471. https://doi.org/10.1201/ebk0824758325-c1.

[179] A.S. Abou-Sayed, Q. Guo, Drilling and Production Waste Injection in Subsea Operations - Challenges and Recommendations, (2008). https://doi.org/10.4043/14288-ms.

[180] D.B. Burnett, Potential for beneficial use of oil and gas produced water, Glob. Pet. Institute, Texas Water Resour. Inst. (2004) 1–11. http://www.circleofblue.org/waternews/wp-content/uploads/2010/08/beneficialuses-produced-water.pdf.

[181] P.J. van den Hoek, T. Matsuura, M. de Kroon, G. Gheissary, Simulation of Produced Water Reinjection Under Fracturing Conditions, SPE Prod. Facil. 14 (2007) 166–176. https://doi.org/10.2118/57385-pa.

[182] E.T. Igunnu, G.Z. Chen, Produced water treatment technologies, Int. J. Low-Carbon Technol. 9 (2014) 157–177. https://doi.org/10.1093/ijlct/cts049.

[183] J. Arthur, B. Langhus, C. Patel, Technical Summary of Oil & Gas Produced Water Treatment Technologies, Tulsa, Oklahoma, USA, ALL …. (2005) 1–53. http://w.all-llc.com/publicdownloads/ALLConsulting-WaterTreatmentOptionsReport.pdf.

[184] A. Hussain, J. Minier-Matar, A. Janson, S. Gharfeh, S. Adham, Advanced Technologies For Produced Water Treatment And Reuse, Int. Pet. Technol. Conf. (2014) 20–22. https://doi.org/10.2523/IPTC-17394-MS.

[185] C.T. Scurtu, Treatment of produced water : targeting dissolved compounds to meet a zero harmful dis- charge in oil and gas production, Norewgian University of Science and Technology, 2009.

[186] A.M.A. Tuwati, M. Fan, M.A. Bentley, Reaction kinetic model for a recent co-produced water treatment technology, J. Environ. Sci. 23 (2011) 360–365. https://doi.org/10.1016/S1001-0742(10)60463-9.

[187] Y. Lester, T. Yacob, I. Morrissey, K.G. Linden, Can We Treat Hydraulic Fracturing Flowback with a Conventional Biological Process? The Case of Guar Gum, Environ. Sci. Technol. Lett. 1 (2013) 133–136. https://doi.org/10.1021/ez4000115.

[188] J.M. Estrada, R. Bhamidimarri, A review of the issues and treatment options for wastewater from shale gas extraction by hydraulic fracturing, Fuel. 182 (2016)

292–303. https://doi.org/10.1016/j.fuel.2016.05.051.

[189] D.E. Freedman, S.M. Riley, Z.L. Jones, J.S. Rosenblum, J.O. Sharp, J.R. Spear, T.Y. Cath, Biologically active filtration for fracturing flowback and produced water treatment, J. Water Process Eng. 18 (2017) 29–40. https://doi.org/10.1016/j.jwpe.2017.05.008.

[190] M.K. Camarillo, J.K. Domen, W.T. Stringfellow, Physical-chemical evaluation of hydraulic fracturing chemicals in the context of produced water treatment, J. Environ. Manage. 183 (2016) 164–174. https://doi.org/10.1016/j.jenvman.2016.08.065.

[191] A. Altaee, N. Hilal, Dual-stage forward osmosis/pressure retarded osmosis process for hypersaline solutions and fracking wastewater treatment, Desalination. 350 (2014) 79–85. https://doi.org/10.1016/j.desal.2014.07.013.

[192] H. Chang, T. Li, B. Liu, R.D. Vidic, M. Elimelech, J.C. Crittenden, Potential and implemented membrane-based technologies for the treatment and reuse of flowback and produced water from shale gas and oil plays: A review, Desalination. 455 (2019) 34–57. https://doi.org/10.1016/j.desal.2019.01.001.

[193] R.K. McGovern, A.M. Weiner, L. Sun, C.G. Chambers, S.M. Zubair, J.H. Lienhard V, On the cost of electrodialysis for the desalination of high salinity feeds, Appl. Energy. 136 (2014) 649–661. https://doi.org/10.1016/j.apenergy.2014.09.050.

[194] T.D. Hayes, B.F. Severin, Electrodialysis of highly concentrated brines: Effects of

calcium, Sep. Purif. Technol. 175 (2017) 443–453. https://doi.org/10.1016/j.seppur.2016.10.035.

[195] T. Sirivedhin, J. McCue, L. Dallbauman, Reclaiming produced water for beneficial use: Salt removal by electrodialysis, J. Memb. Sci. 243 (2004) 335–343. https://doi.org/10.1016/j.memsci.2004.06.038.

[196] M. Peraki, E. Ghazanfari, Alternative method of flow-back water treatment in shale gas development for environmental protection, in: IFCEE 2015, ASCE, 2015: pp. 1816–1825. https://doi.org/10.1061/9780784479087.165.

[197] C. Ventresque, G. Turner, G. Bablon, Nanofiltration: From prototype to full scale, J. / Am. Water Work. Assoc. 89 (1997) 65–76. https://doi.org/10.1002/j.1551-8833.1997.tb08306.x.

[198] B.D. Coday, C. Hoppe-Jones, D. Wandera, J. Shethji, J. Herron, K. Lampi, S.A. Snyder, T.Y. Cath, Evaluation of the transport parameters and physiochemical properties of forward osmosis membranes after treatment of produced water, J. Memb. Sci. 499 (2016) 491–502. https://doi.org/10.1016/j.memsci.2015.09.031.

[199] J. Minier-Matar, A. Hussain, A. Santos, A. Janson, R. Wang, A.G. Fane, S. Adham, Advances in Application of Forward Osmosis Technology for Volume Reduction of Produced/Process Water from Gas-Field Operations, (2015) 1–15. https://doi.org/10.2523/iptc-18380-ms.

[200] I. Bawazir, M. Raja, I. Abdelmohsen, Q. Operating, C. Limited, Qatargas Flare Reduction Program, in: Int. Pet. Technol. Conf., 2014: pp. 20–22.

[201] Qatar Overview, (2017). https://www.theoilandgasyear.com/market/qatar/ (accessed August 29, 2019).

[202] J. Minier-Matar, A. Hussain, A. Janson, R. Wang, A.G. Fane, S. Adham, Application of forward osmosis for reducing volume of produced/Process water from oil and gas operations, Desalination. 376 (2015) 1–8. https://doi.org/10.1016/j.desal.2015.08.008.

[203] J. Ren, J.R. McCutcheon, A new commercial thin film composite membrane for forward osmosis, Desalination. 343 (2014) 187–193. https://doi.org/10.1016/j.desal.2013.11.026.

[204] R. Wang, L. Shi, C.Y. Tang, S. Chou, C. Qiu, A.G. Fane, Characterization of novel forward osmosis hollow fiber membranes, J. Memb. Sci. 355 (2010) 158–167. https://doi.org/10.1016/j.memsci.2010.03.017.

[205] S. Chou, L. Shi, R. Wang, C.Y. Tang, C. Qiu, A.G. Fane, Characteristics and potential applications of a novel forward osmosis hollow fiber membrane, Desalination. 261 (2010) 365–372. https://doi.org/10.1016/j.desal.2010.06.027.

[206] G. Tchobanoglous, F.L. Burton, H. David Stensel, Wastewater Engineering Treatment and Reuse, 4th ed., Metcalf & Eddy Inc., 2003.

[207] S. Loutatidou, B. Chalermthai, P.R. Marpu, H.A. Arafat, Capital cost estimation of RO plants: GCC countries versus southern Europe, Desalination. 347 (2014) 103–111. https://doi.org/10.1016/j.desal.2014.05.033.

[208] S. Judd, F. Turan, Sidestream vs immersed membrane bioreactors: A cost analysis,

in: WEFTEC, 2019: pp. 3722–3733.

[209] B. Verrecht, T. Maere, I. Nopens, C. Brepols, S. Judd, The cost of a large-scale hollow fibre MBR, Water Res. 44 (2010) 5274–5283. https://doi.org/10.1016/j.watres.2010.06.054.

[210] H. Itokawa, K. Tsuji, K. Yamashita, T. Hashimoto, Design and operating experiences of full-scale municipal membrane bioreactors in Japan, Water Sci. Technol. 69 (2014) 1088–1093. https://doi.org/10.2166/wst.2014.020.

[211] R. Iglesias, P. Simón, L. Moragas, A. Arce, I. Rodriguez-Roda, Cost comparison of full-scale water reclamation technologies with an emphasis on membrane bioreactors, Water Sci. Technol. 75 (2017) 2562–2570.

[212] S. Cashman, J. Mosely, Life cycle assessment and cost analysis of water and wastewater treatment options for sustainability: influence of scale on membrane bioreactor systems, 2016.

[213] C. Brepols, H. Schäfer, N. Engelhardt, Considerations on the design and financial feasibility of full-scale membrane bioreactors for municipal applications, Water Sci. Technol. 61 (2010) 2461–2468.

[214] J. DeCarolis, S. Adham, W.R. Pearce, Z. Hirani, S. Lacy, R. Stephenson, Cost Trends of Mbr Systems for Municipal Wastewater Treatment, Proc. Water Environ. Fed. (2007) 3407–3418. https://doi.org/10.2175/193864707787973734.

[215] E.J. Fleischer, A.D. Fonseca, G.T. Daigger, R.A. Canham, T.A. Broderick, N.A. Johnson, D.P. Lynch, Planning, Design, and Startup of a Large, Innovative

Membrane Bioreactor Facility, Water Pract. Technol. 5 (2010).

[216] T. Wozniak, Comparison of a conventional municipal plant, and an MBR plant with and without MPE: A comparison of the environmental and financial performance of a conventional activated sludge (CAS) plant, membrane bio-reactor (MBR), and MBR treated with Nalco Membran, Desalin. Water Treat. 47 (2012) 341–352. https://doi.org/10.1080/19443994.2012.672186.

[217] T. Young, S. Smoot, J. Peeters, P. Côté, When does building an MBR make sense? How variations of local construction and operating cost parameters impact overall project economics, Proc. Water Environ. Fed. 8 (2013) 6354–6365. https://doi.org/10.2175/193864713813716444.

[218] S.J. Judd, The status of industrial and municipal effluent treatment with membrane bioreactor technology, Chem. Eng. J. 305 (2016) 37–45. https://doi.org/10.1016/j.cej.2015.08.141.

[219] S.J. Judd, Membrane technology costs and me, Water Res. 122 (2017) 1–9. https://doi.org/10.1016/j.watres.2017.05.027.

[220] M.P. Shahabi, A. McHugh, G. Ho, Environmental and economic assessment of beach well intake versus open intake for seawater reverse osmosis desalination, Desalination. 357 (2015) 259–266. https://doi.org/10.1016/j.desal.2014.12.003.

[221] C. Fritzmann, J. Lowenberg, T. Wintgens, T. Melin, State-of-the-art of reverse osmosis desalination, Desalination. 216 (2007) 1–76. https://doi.org/10.1016/j.desal.2014.10.039.

[222] World Bank, The Role of Desalination in an Increasingly Water-Scarce World, Washington, 2019.

[223] S.J. Im, G.W. Go, S.H. Lee, G.H. Park, A. Jang, Performance evaluation of two-stage spiral wound forward osmosis elements at various operation conditions, Desalin. Water Treat. 57 (2016) 24583–24594. https://doi.org/10.1080/19443994.2016.1157989.

[224] A.H. Hawari, N. Kamal, A. Altaee, Combined influence of temperature and flow rate of feeds on the performance of forward osmosis, Desalination. 398 (2016) 98–105. https://doi.org/10.1016/j.desal.2016.07.023.

[225] M.A. Hafiz, A.H. Hawari, A. Altaee, A hybrid forward osmosis/reverse osmosis process for the supply of fertilizing solution from treated wastewater, J. Water Process Eng. 32 (2019). https://doi.org/10.1016/j.jwpe.2019.100975.

[226] P. Zhao, B. Gao, Q. Yue, S. Liu, H.K. Shon, Effect of high salinity on the performance of forward osmosis: Water flux, membrane scaling and removal efficiency, Desalination. 378 (2016) 67–73. https://doi.org/10.1016/j.desal.2015.09.028.

[227] M.S. Thabit, A.H. Hawari, M.H. Ammar, S. Zaidi, G. Zaragoza, A. Altaee, Evaluation of forward osmosis as a pretreatment process for multi stage flash seawater desalination, Desalination. 461 (2019) 22–29. https://doi.org/10.1016/j.desal.2019.03.015.

[228] Y.C. Kim, S.J. Park, Experimental study of a 4040 spiral-wound forward-osmosis

membrane module, Environ. Sci. Technol. 45 (2011) 7737–7745. https://doi.org/10.1021/es202175m.

[229] J. Heo, K.H. Chu, N. Her, J. Im, Y.G. Park, J. Cho, S. Sarp, A. Jang, M. Jang, Y. Yoon, Organic fouling and reverse solute selectivity in forward osmosis: Role of working temperature and inorganic draw solutions, Desalination. 389 (2016) 162–170. https://doi.org/10.1016/j.desal.2015.06.012.

[230] J. Ren, M.R. Chowdhury, J. Qi, L. Xia, B.D. Huey, J.R. McCutcheon, Relating osmotic performance of thin film composite hollow fiber membranes to support layer surface pore size, J. Memb. Sci. 540 (2017) 344–353. https://doi.org/10.1016/j.memsci.2017.06.024.

[231] V. Sanahuja-Embuena, G. Khensir, M. Yusuf, M.F. Andersen, X.T. Nguyen, K. Trzaskus, M. Pinelo, C. Helix-Nielsen, Role of operating conditions in a pilot scale investigation of hollow fiber forward osmosis membrane modules, Membranes (Basel). 9 (2019). https://doi.org/10.3390/membranes9060066.

[232] T.Y. Cath, M. Elimelech, J.R. McCutcheon, R.L. McGinnis, A. Achilli, D. Anastasio, A.R. Brady, A.E. Childress, I. V. Farr, N.T. Hancock, J. Lampi, L.D. Nghiem, M. Xie, N.Y. Yip, Standard Methodology for Evaluating Membrane Performance in Osmotically Driven Membrane Processes, Desalination. 312 (2013) 31–38. https://doi.org/10.1016/j.desal.2012.07.005.

[233] M. Xie, W.E. Price, L.D. Nghiem, M. Elimelech, Effects of feed and draw solution temperature and transmembrane temperature difference on the rejection of trace organic contaminants by forward osmosis, J. Memb. Sci. 438 (2013) 57–64.

https://doi.org/10.1016/j.memsci.2013.03.031.

[234] J.G. Lee, N. Ghaffour, Predicting the performance of large-scale forward osmosis module using spatial variation model: Effect of operating parameters including temperature, Desalination. 469 (2019). https://doi.org/10.1016/j.desal.2019.114095.

[235] Q. Wang, Z. Zhou, J. Li, Q. Tang, Y. Hu, Modeling and measurement of temperature and draw solution concentration induced water flux increment efficiencies in the forward osmosis membrane process, Desalination. 452 (2019) 75–86. https://doi.org/10.1016/j.desal.2018.11.001.

[236] L. Feng, L. Xie, G. Suo, X. Shao, T. Dong, Influence of Temperature on the Performance of Forward Osmosis Using Ammonium Bicarbonate as Draw Solute, Trans. Tianjin Univ. 24 (2018) 571–579. https://doi.org/10.1007/s12209-018-0159-1.

[237] S. Phuntsho, S. Vigneswaran, J. Kandasamy, S. Hong, S. Lee, H.K. Shon, Influence of temperature and temperature difference in the performance of forward osmosis desalination process, J. Memb. Sci. 415–416 (2012) 734–744. https://doi.org/10.1016/j.memsci.2012.05.065.

[238] S.J. You, X.H. Wang, M. Zhong, Y.J. Zhong, C. Yu, N.Q. Ren, Temperature as a factor affecting transmembrane water flux in forward osmosis: Steady-state modeling and experimental validation, Chem. Eng. J. 198–199 (2012) 52–60. https://doi.org/10.1016/j.cej.2012.05.087.

[239] M.R. Chowdhury, J.R. McCutcheon, Elucidating the impact of temperature gradients across membranes during forward osmosis: Coupling heat and mass transfer models for better prediction of real osmotic systems, J. Memb. Sci. 553 (2018) 189–199. https://doi.org/10.1016/j.memsci.2018.01.004.